Forschungszentrum Karlsruhe

Technik und Umwelt

Wissenschaftliche Berichte

FZKA 6506

Thermalhydraulic and Material Specific Investigations into the Realization of an Accelerator Driven System (ADS) to Transmute Minor Actinides

1999 Status Report

J. U. Knebel, X. Cheng, G. Müller, G. Schumacher,
J. Konys, O. Wedemeyer, G. Grötzbach, L. Carteciano

Institut für Kern- und Energietechnik
Institut für Hochleistungsimpuls- und Mikrowellentechnik
Institut für Materialforschung
Institut für Reaktorsicherheit
Programm Nukleare Sicherheitsforschung

Forschungszentrum Karlsruhe GmbH, Karlsruhe
2000

The co-authors and co-workers, who significantly contributed to this work, are listed together with the institute in alphabetical order:

Institut für Kern- und Energietechnik (IKET)
Institute for Nuclear and Energy Technologies

X. Cheng, F. Fellmoser, J.U. Knebel, V. Krieger, C.H. Lefhalm, K. Mack, P. Miodek, H.J. Neitzel, C. Pettan, H. Piecha, H. Schmidt, R. Vollmer

Institut für Hochleistungsimpuls- und Mikrowellentechnik (IHM)
Institute for Pulsed Power and Microwave Technology

A. Heinzel, R. Huber, G. Müller, G. Schumacher, F. Zimmermann

Institut für Materialforschung III (IMF III)
Institute for Materials Research III

H. Glasbrenner, J. Konys, H. Muscher, J. Novotny, Z. Voss, O. Wedemeyer

Institut für Reaktorsicherheit (IRS)
Institute for Reactor Safety

L. Carteciano, B. Dorr, G. Grötzbach

HGF Strategy Fund Project 99/16
Short Title: Innovative Technology to Reduce Radiotoxicity
Project within Section 3: Energy Research and Energy Technology

Thermalhydraulic and Material Specific Investigations into the Realization of an Accelerator Driven System (ADS) to Transmute Minor Actinides

1999 Status Report

Participating Research Center: Forschungszentrum Karlsruhe GmbH
Financial Support: 7.0 million DM
Time Period: July 1999 to September 2002

Dated July 09, 1999 the Senate of the Hermann von Helmholtz-Gemeinschaft Deutscher Forschungszentren (HGF) has decided to fund this Strategy Fund Project.

Dated October 18, 1999 the Bundesministerium für Bildung und Forschung (BMBF) has granted 7.0 million DM under the Förderkennzeichen 01SF9926/3.

Project Coordinator:

Dr.-Ing. Joachim U. Knebel
Forschungszentrum Karlsruhe GmbH
Institut für Kern- und Energietechnik (IKET)
Postfach 3640
D-76021 Karlsruhe

Tel.: (07247) 82-3451 oder 3585
Fax.: (07247) 82-4837
Email: joachim.knebel @ iket.fzk.de

Abstract

Thermalhydraulic and Material Specific Investigations into the Realization of an Accelerator Driven System (ADS) to Transmute Minor Actinides

1999 Status Report

At Forschungszentrum Karlsruhe an HGF Strategy Fund Project entitled "Thermalhydraulic and Material Specific Investigations into the Realization of an Accelerator-Driven System (ADS) to Transmute Minor Actinides" is performed which is funded by the Hermann von Helmholtz-Gemeinschaft Deutscher Forschungszentren (HGF) in the section "Energy Research and Energy Technology" over a time period from 07/1999 to 06/2002 with a financial support of 7.0 million DM (35 man years).

The objective of this HGF Strategy Fund Project is the development of new methods and technologies to design and manufacture thin-walled thermally highly-loaded surfaces (e.g. beam window) which are cooled by a corrosive heavy liquid metal (lead-bismuth eutectic). The beam window is a vital component of an ADS spallation target.
The results of this project will provide the scientific-technical basis which allows the conception and the design of an ADS spallation target and later on a European Demonstrator of an ADS system. The work performed at Forschungszentrum Karlsruhe is embedded in a broad European research and development programme on ADS systems.

The project is divided in three sub-projects:

Sub-Project SP1: Thermalhydraulic Investigations
In the field of experimental thermalhydraulics physical models are developped for conductive and convective heat transfer along thermally highly-loaded surfaces (e.g. beam window) in turbulent lead-bismuth flow. In parallel, a thermalhydraulic computer programme is validated for the low Prandtl number fluid lead-bismuth. Finally, a complete spallation target is numerically designed.

Sub-Project SP2: Material Specific Investigations
In the field of material science physical methods are developped to describe corrosion mechanisms and to solve the corrosion challenge for potential structure and window materials with and without surface treatment for flowing lead-bismuth.

Sub-Project SP3: Oxygen Control
In the field of reaction kinetics a physical / chemical method is developped to measure and control the oxygen potential in a lead-bismuth loop in order to prevent the corrosion of the materials used.

The experimental investigations are performed in the KArlsruhe Lead LAboratory KALLA.
The investigation of the complex system „heat transfer along thermally highly-loaded surfaces that are in contact with liquid corrosive lead-bismuth under well-defined chemical and material specific boundary conditions" has not been performed up to now. It will be done within this project and directly applied to the design of a spallation target, one key component of an ADS.
This report gives the results achieved during the year 1999.

Kurzfassung

Thermohydraulische und materialspezifische Untersuchungen zur Realisierung einer Beschleuniger getriebenen Anordnung (ADS) zur Transmutation von Aktiniden

1999 Status Report

Am Forschungszentrum Karlsruhe wird ein HGF-Strategiefonds Projekt mit dem Titel „Thermohydraulische und materialspezifische Untersuchungen zur Realisierung einer Beschleuniger getriebenen Anordnung (ADS) zur Transmutation von Aktiniden“ durchgeführt, das von der Hermann von Helmholtz-Gemeinschaft Deutscher Forschungszentren (HGF) in der Sektion 3 „Energieforschung und Energietechnologie“ für den Zeitraum 07/1999 bis 06/2002 mit einem Finanzvolumen von 7.0 Millionen DM (35 Personenjahre) gefördert wird.
Ziel dieses HGF-Strategiefondsprojektes ist es, neue Methoden und Technologien zur Auslegung und Herstellung dünnwandiger, thermisch hochbelasteter Oberflächen (z.B. Strahlfenster), die von einem korrosiven schweren Flüssigmetall (eutektisches Blei-Wismut) gekühlt werden, zu entwickeln. Das Strahlfenster ist eine entscheidende Komponente eines Spallationstargets für einen ADS.
Das Ergebnis dieses Projektes ist ein wissenschaftlich-technisches Instrumentarium zur Konzeption und zur detaillierten Auslegung zunächst eines Spallationstargets und später einer Europäischen Demonstrationsanlage eines ADS. Die Arbeiten am Forschungszentrum sind in ein breites europäisches Forschungs- und Entwicklungs-programm zu Beschleuniger getriebenen Anordnungen (ADS) eingebunden.

Das Projekt gliedert sich in drei Teilprojekte:
Teilprojekt 1: Thermohydraulische Untersuchungen
Im Bereich der *Thermohydraulik* werden für das Fluid Blei-Wismut physikalische Gesetzmäßigkeiten zum konduktiven und konvektiven Wärmeübergang für die turbulente Umströmung einer thermisch hochbelasteten Oberfläche (z.B. Strahlfenster) entwickelt. Parallel dazu wird ein thermohydraulisches Rechenprogramm für ein Fluid kleiner molekularer Prandtl-Zahl (Blei-Wismut) validiert. Abschließend wird ein komplettes Spallationstarget numerisch ausgelegt.
Teilprojekt 2: Materialspezifische Untersuchungen
Im Bereich der *Materialforschung* werden physikalische Methoden zur Beschreibung der Korrosionsmechanismen und zur Lösung der Korrosionsproblematik für potenzielle Struktur- und Fensterwerkstoffe, mit und ohne Schutzschichten, in strömendem Blei-Wismut entwickelt.
Teilprojekt 3: Sauerstoffkontrolle
Im Bereich der *Reaktionskinetik* wird auf der Basis von physikalisch / chemischen Überlegungen ein Verfahren zur Messung und Regelung des Sauerstoffpotenzials in Blei-Wismut und somit zur Kontrolle der Korrosion der eingesetzten Werkstoffe entwickelt.

Die experimentellen Untersuchungen werden im Flüssigmetalllabor KALLA (KArlsruhe Lead LAboratory) durchgeführt. Eine Betrachtung des komplexen Gesamtsystems „Wärmeübertragung an thermisch hochbelasteten Oberflächen in flüssigem, korrosivem Blei-Wismut unter Berücksichtigung von reaktionskinetisch kontrollierten und materialspezifisch definierten Randbedingungen“ ist bisher noch nicht erfolgt. Dies wird mit dieser Arbeit geleistet und direkt für die Auslegung eines Spallationstargets, das eine wesentliche Komponente eines ADS ist, eingesetzt.
Dieser Bericht gibt die im Jahr 1999 erzielten Ergebnisse wieder.

CONTENTS

Thermalhydraulic and Material Specific Investigations into the Realization of an Accelerator Driven System (ADS) to Transmute Minor Actinides

1999 Status Report

Thermalhydraulic and Material Specific Investigations into the Realization of an Accelerator Driven System (ADS) to Transmute Minor Actinides

1999 Status Report

1. Research Programme

1.1 Description ot the Project and Envisaged Objectives

1.1.1 Concrete Objectives of the Project

The objective of this HGF Strategy Fund Project is the development of new methods and technologies to design and manufacture thermally highly-loaded surfaces (e.g. beam window) which are cooled by a corrosive heavy liquid metal (lead-bismuth eutectic). The beam window is a vital component of an ADS spallation target.

The project is divided in three sub-projects:

Sub-Project 1: Thermalhydraulic Investigations
In the field of experimental thermalhydraulics physical models are developped for conductive and convective heat transfer along thin-walled thermally highly-loaded surfaces (e.g. beam window) in turbulent lead-bismuth flow. In parallel, a thermalhydraulic computer programme is validated for the low Prandtl number fluid lead-bismuth. Finally, a complete spallation target is numerically designed.

Sub-Project 2: Material Specific Investigations
In the field of material science physical methods are developped to describe corrosion mechanisms and to solve the corrosion challenge for potential structure and window materials with and without surface treatment for flowing lead-bismuth.

Sub-Project 3: Oxygen Control
In the field of reaction kinetics a physical / chemical method is developped to measure and control the oxygen potential in a lead-bismuth loop in order to prevent the corrosion of the materials used.

The strategy of the project is based both on a theoretical / numerical approach and on an experimental approach. The results of both approaches are tightly linked within all sub-projects. The sub-projects are complementing one another.
The investigation of a complex integral system is still lacking today in the fields of heat transfer along corroded surfaces and heat transport within lead-bismuth, which has well-defined chemical and material specific boundary conditions.

The summary of the results of the three sub-projects contributes to the method and technology to realize critical and system-relevant components of an Accelerator Driven System (ADS), such as the beam window and the spallation target. The safe design of these components relative to heat transfer, material selection and corrosion control is a basic requirement to guarantee the integral funtionality of an ADS.

The methods and technologies resulting from this project are regularly discussed and harmonized with our European partners during various working group meetings, e.g. TECLA Project of the 5th EU-Framework Programme (Benamati, Latge, Knebel (2000)), MEGAPIE Initiative (Bauer, Salvatores, Heusener (1999)), Wissenschaftlich-Technische Zusammenarbeit (BMBF (1998)), European Benchmark Working Group (Buono et al. (1999)). The most important partners are: CEA, CNRS and SUBATECH France, ENEA, CRS4 and ANSALDO Italy, PSI Switzerland, CIEMAT and LAESA Spain, RIT Sweden, SCK/CEN Belgium, IPPE and PROMETEY Russian Federation. The methods and technologies are essential steps towards the concept of a common European Experimental Demonstrator of an ADS, Technical Working Group (1998, 1999). An ADS has the potential and the strategic objective to transmute minor actinides and long-lived fission products. Thus an ADS is essentially participating in closing the fuel cycle now including minor actinides, Heusener (1999, 2000).
The research work of this HGF strategy fund project is of international actuality and of engineering and scientific importance.

1.1.2 Long-Term and Strategic Objectives

The overall and long-term objective of the project is – on the basis of the newly developped methods and technologies – to provide the scientific-technical tool which allows, now, the conceptual design and, at a later stage, the detailed design of a European Experimental Demonstrator of an ADS.
The tools comprise of a thermalhydraulic and material specific data base resulting from fundamental and application-oriented experiments, a computational fluid dynamics (CFD) code validated for lead-bismuth, an identification of beam window and structure materials, and an instruction for corrosion control, material conditioning and oxygen control in lead-bismuth loops.
The Experimental Demonstrator with a thermal power of about 100 MW(th) is a milestone towards the long-term realization of a prototypical ADS with a thermal power of about 1500 MW(th).

An accelerator driven system (ADS) consists of three main parts: an accelerator for primary particles (protons), a spallation target (or target module) in which the protons produce free nucleons (neutrons) in a spallation reaction (external neutron source), and a subcritical blanket in which, first, the fission reaction, producing fission neutrons (internal neutron source) and thermal energy, and second, the transmutation reaction occur, Bowman (1992). The protons are injected into the spallation target through a vacuum beam pipe, the beam pipe being closed by a window at the end. The target is a heavy liquid metal (e.g. lead Pb or eutectic lead-bismuth Pb-Bi). The spallation neutrons produced in the spallation target are completely independent of the subcritical blanket. A shut-down of the accelerator or an interruption of the proton beam immediately stops the fission reaction. Safety aspects of such a subcritical system are discussed in Wider (1998), Maschek, Thiem, Heusener (1999), Klügel et. al. (1999). A sketch of an ADS is given in figure 1.

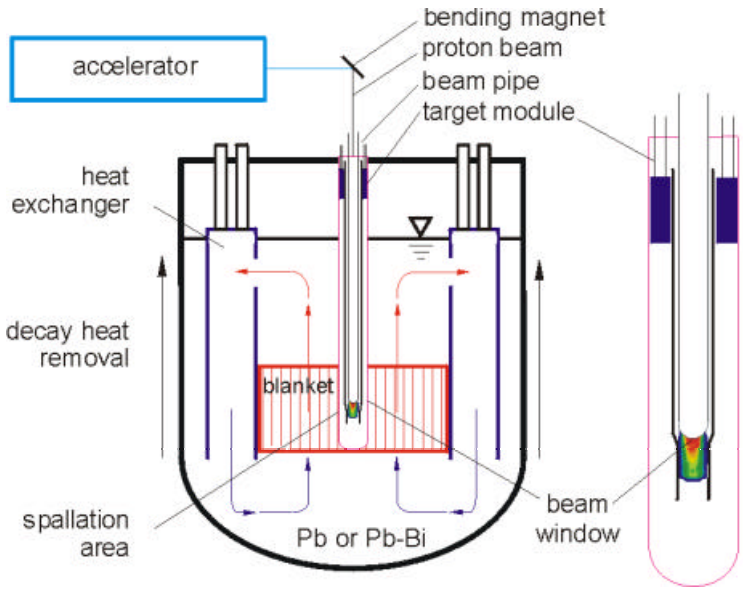

Figure 1: Sketch of an accelerator driven system (ADS).

The strategic objective of an ADS is to transmute long-lived radioactive waste and, thus, to close the fuel cycle including minor actinides, (Heusener und Salvatores (1998), Carminati et al. (1993), Rubbia et al. (1995), Takizuka et al. (1998)). The waste which is treated in an ADS can be divided into two parts: the minor actinides such as Neptunium, Americium und Curium and some long-lived fission products such as technetium 99 and iodine 129. The two latter species can diffuse in the biosphere in the long run where they can be selectively incorporated by organisms.
The ADS technology is a natural extention to the existing park of light water reactors (LWR). The use of ADS reduces the amount and the radiotoxicity of radioactive waste which has to be transported and stored in a final repository, US-DOE (1999).

The evaluation commission of the Bundesministerium für Wirtschaft (BMWi) considers the strategic work on transmutation a priority task. The evaluation commission considers it as required to fundamentally investigate the physical and technical conditions for the technological realization of the ADS technology, Evaluierungskommission (2000).

The objective of the Experimental Demonstrator is to provide experimental data and to obtain practical experience in the field of nuclear technology and energy technology. In the field of nuclear technology there is a need to improve the accuracy and reliability of nuclear cross-section data, to amend data for missing elements or isotopes, and to extend the high energy range of existing evaluations for those nuclei relevant for ADS concepts. On the basis of updated data libraries, the calculation methods have to be benchmarked to assess their capability for predicting the interaction of highly energetic protons and neutrons with the materials of a spallation target and a subcritical blanket.
In the field of energy technology there is a need to establish a broader basis of understanding, knowledge and experience related to heavy liquid metal coolant technology and to gain experience in the field of thermalhydraulics (experiment, physical model development, numerics) of the beam window, the spallation target and the primary circuit, as well as detailed knowledge about the corrosion mechanisms and the long-term behaviour of materials used for the beam window, the target module and the primary system under realistic conditions. In addition, methods

to measure, control and remove impurities, caused by proton and neutron induced particle reactions and by liquid metal corrosion within the cooling loops, have to be developped.
This HGF Strategy Fund Project provides an essential scientific contribution to the application-oriented fundamental research work within the energy technology of an ADS as mentioned above.
The strategic objective of the Experimental Demonstrator is to prove the safe and continuous coupling of an accelerator, a spallation target and a subcritical blanket in order to finally transmute minor actinides and long-lived fission products.

The work within the field of nuclear technology is not part of this project.
The neutronic boundary conditions which are needed to run this project are defined and elaborated in cooperation with other groups at Forschungszentrum Karlsruhe and the European partners.

1.2 Positioning within the Activities of the HGF

The HGF Strategy Fund Project is part of the main research area „Energy research and energy technology“. About 40% of the total budget of Forschungszentrums Karlsruhe is in the research field „energy“ which is sub-divided into nuclear research and decommissioning, fusion technology, superconductivity. This Project is related to a comprehensive study on actinide transmutation that is comparing a critical with a sub-critical system in respect to the following topics: system design, neutronics, transmutation, safety, thermalhydraulics, materials and corrosion, Projekt Nukleare Sicherheitsforschung (1999, 2000).

To-date, Forschungszentrum Karlsruhe is the only institution in Germany which has the scientific competence and the infrastructure in order to immediately start on a larger scale with ADS-relevant, experimental and theoretical work in the field of liquid metal technology, thermalhydraulics and material science.

The long-term fundamental work to this international and highly innovative research area and the preparatory work at Forschungszentrum Karlsruhe were performed with intensive support of PhD students and Young Generation scientists. The preparatory work for this project is embedded in the long-term research and development programme of Forschungszentrum Karlsruhe.
Another important aspect of the project is to further develop the scientific skills within liquid metal technology resulting from the breeder programme and to hand it on to a newly growing generation of young scientists.

By intensively incorporating university students, PhD students, Young Generation scientists and guest scientists from other national and international research institutions in the work, the requirement of the HGF is fulfilled to educate young people, to keep competence in nuclear energy technology and to cooperate with universities and research institutions.

1.3 Other Applications

The objective of this HGF project is the design of a spallation target. In general, the aim of a spallation target is the production of a high neutron flux which is produced in a spallation reaction caused by protons hitting a heavy metal target. Such a spallation neutron source can be operated in two modes: pulse mode which is primarily used for neutron scattering experiments, and continuous mode which is used for large-scale isotope production or transmutation of nuclear waste.
The neutron scattering technique is one of the most effective ways to obtain information on the arrangement, the motion and the interaction of atoms in materials and on the excitations of materials. A wide area of problems which range from fundamental physics to solid state physics and chemistry and from materials science to biology, medicine and environmental science can be investigated with this technique. Using the neutron scattering technique one can obtain more information in comparison to other techniques such as optical spectroscopy and x-ray diffraction.
Some typical research areas are: improvement of materials for high-temperature superconductors, powerful lightweight magnets, aluminium bridge decks and stronger lighter plastic products, SNS Project Office, (2000).

In table 1 a list of today's operating spallation neutron sources is given. Currently, an upgrade of existing facilities or plans for new facilities are being made (table 2). The intention is to increase the neutron pulse intensity, which is equivalent to a higher energy per pulse. Having a more intense spallation neutron source, the neutron scattering experiments will allow a better resolution, shorter exposure times for data collection and the use of smaller material samples.

Table 1: Existing spallation neutron source facilities, Cappiello (1999).

Facility	Energy (MeV)	Average current (μA)	Pulse frequency (Hz)	Energy per pulse (kJ)	Target material
ISIS / UK	800	200	50	3.2	Tantalum plates
IPNS / US	500	15	30	0.25	Depleted uranium plates
SINQ / CH	590	850	contin.	contin.	Zirconium rods
Lujan / US	800	100	20	4.0	Tungsten plates
KENS / JAP	500	5	20	0.125	Depleted uranium plates

Table 2: Planned upgrades or new spallation neutron source facilities, Cappiello (1999).

Facility	Energy (MeV)	Average current (μA)	Pulse frequency (Hz)	Energy per pulse (kJ)	Target material
ISIS / UK	800	300	50	4.8	Tungsten plates
Lujan / US	800	200	30	5.3	Tungsten plates
Meson / RUS	502	70	100	0.35	Unknown
SNS / US	1000	2000	60	33.3	Mercury
JSNS / JAP	3000	333	25	40.0	Tungsten / mercury
Austron / A	1600	312	50	10.0	Tungsten
ESS / Europe	1334	3750	50	100.0	Mercury

An example of an existing spallation neutron source is SINQ at Paul Scherrer Institute (PSI), Switzerland (PSI (1997)): The spallation neutron source SINQ is a continuous source -the first of its kind in the world- with a flux of about 10^{14} n $s^{-1}cm^{-2}$. Beside thermal neutrons that are moderated by heavy water (D_2O), a cold moderator of liquid deuterium (D2 at 25 K) slows neutrons down and shifts the neutron spectrum to the desired lower energies. These neutrons have proved to be particularly valuable in materials research and in the investigation of biological substances.

Within the MEGAPIE Initiative (Bauer et al. (1999)) the neutron flux of the presently installed solid lead target (MARK III) shall be increased by a factor of 1.6 by substituting it by a liquid lead-bismuth target. MEGAPIE (MEGAwatt Pilot Experiment) is a joint initiative by Commissariat à l'Energie Atomique (CEA), France, Forschungszentrum Karlsruhe, Germany, and Paul Scherrer Institute (PSI), Switzerland, to design, build, operate, explore and decommission a liquid lead-bismuth spallation target for 1 MW of beam power. A sketch of the MEGAPIE spallation target for SINQ is given in figure 2.

Within the MEGAPIE Initiative, this HGF Strategy Fund Project will provide valuable results based on experimental and numerical investigations in the following areas:

- thermalhydraulic design,
- liquid metal technology,
- material specification and selection,
- corrosion and surface protection,
- cooling of the beam window.

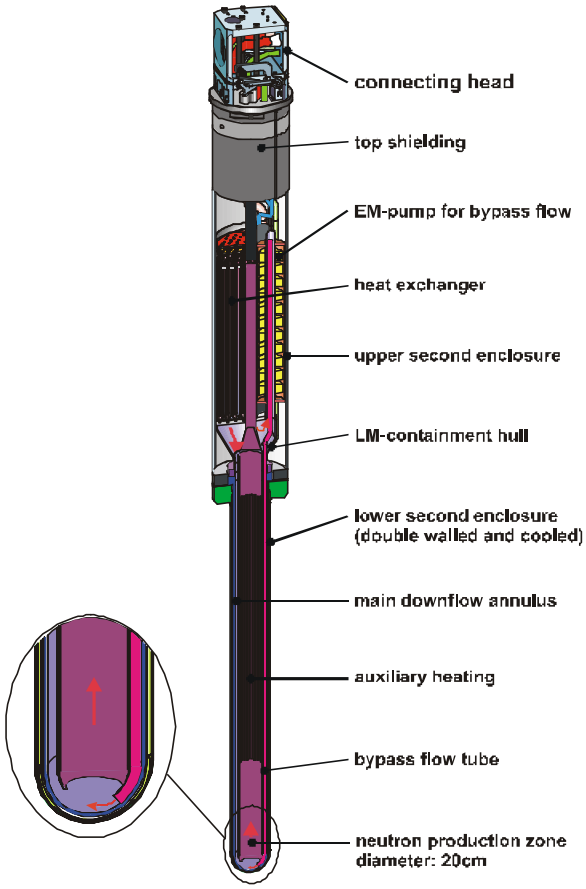

Figure 2: Sketch of the MEGAPIE (MEGAwatt Pilot Experiment) spallation target for SINQ at Paul Scherrer Institute (PSI) Switzerland.

1.4 Scientific Approach

The scientific approach is governed by three critical technical questions to an ADS, which need further research and development efforts and the answer to which is a basic requirement to successfully operate an ADS. The three questions are basically worked upon in the following three sub-projects:

- SP1: Thermalhydraulic investigations
  Thermalhydraulic investigations of thin-walled, thermally highly-loaded surfaces (beam window and spallation target module) with lead-bismuth as coolant,
- SP2: Material specific investigations
  Investigation of corrosion mechanisms and development of an instruction to condition metals in flowing lead-bismuth,
- SP3: Oxygen control
  Oxygen concentration measurement and oxygen control in lead-bismuth loops.

The three sub-projects are supporting each other by methodological findings and immediate technology transfer. Considering industrial and licensing aspects, the safe and long-term operation of an ADS requires, among others, the following three issues: description and control of liquid metal corrosion for the materials used, knowledge of the thermalhydraulics of the integral ADS system, description of the interaction between corrosion and thermalhydraulics which results, for example, in a deterioration of the heat transfer characteristics due to a corrosion related change in surface topology or composition.
These three selected questions are internationally ranked to be scientifically very acute issues, for which, however, there is no technically feasible and applicable solution available today. Considering the focussing withing the three sub-projects, the requirement of the HGF is fulfilled to combine long-term innovative research strategies with available research potential and to develop this potential to a new quality level. The solution methods are developped and exchanged with the international partners. An important partner is the Russian Federation which has a large know-how in liquid lead-bismuth technology. However, this technology is difficult to access up to now.

The scientific approach within the HGF Strategy Fund Project in order to reach the objectives is schematically given in figure 3.

The funding of the work is divided: The cost-intensive construction and running of the test loops within the KArlsruhe Lead LAboratoy KALLA, the test sections together with the measurement techniques, and the data acquisition and control system are financed out of the basic research and development funding of Forschungszentrum Karlsruhe. The HGF funding is taken to account for personal costs that are needed to scientifically perform, interprete and document the experiments and the numerical calculations.

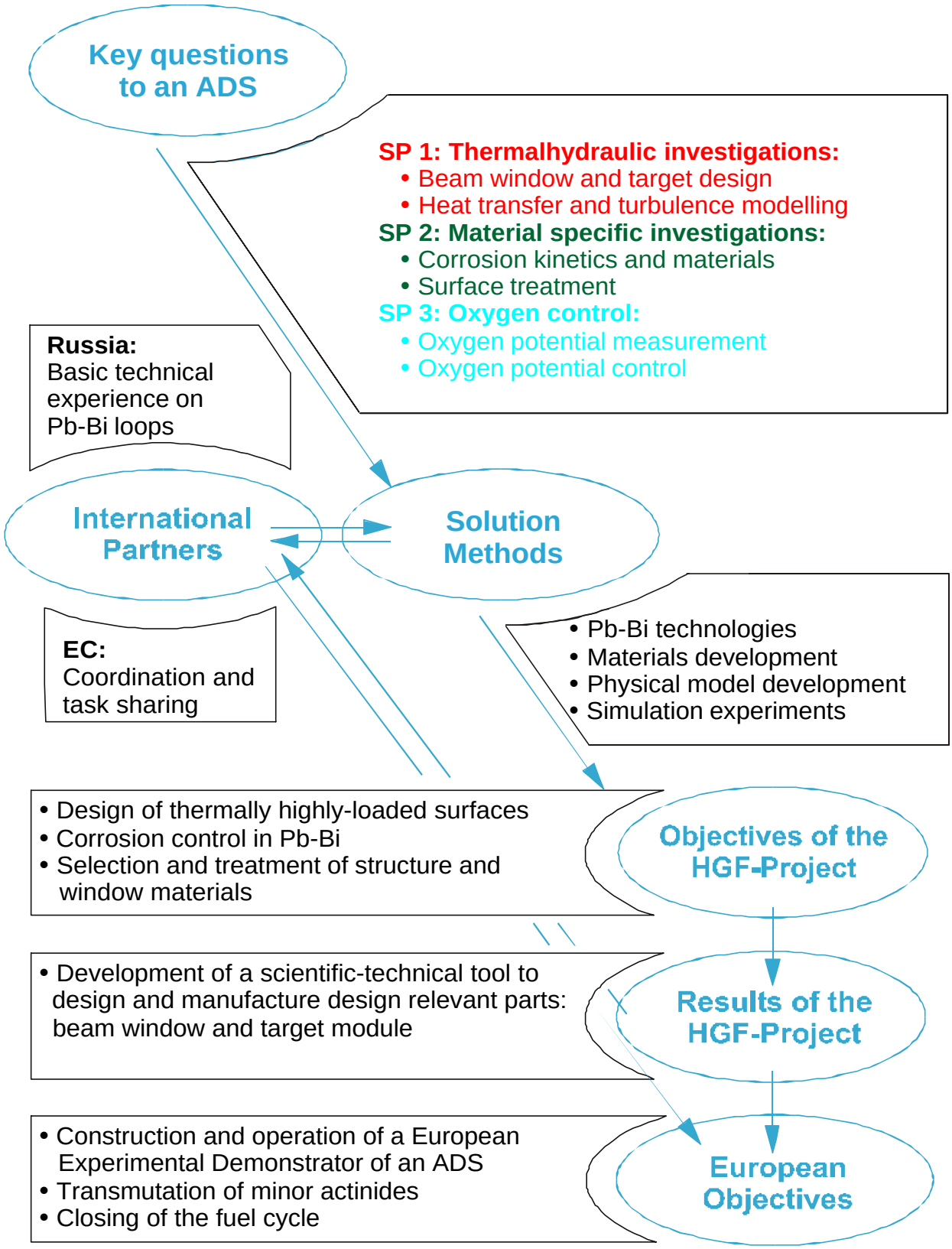

Figure 3: Scientific approach within the HGF Strategy Fund Project to reach the objectives.

2. Positioning within the International Research Activities

The research ministers from France, Italy and Spain have nominated a Technical Working Group TWG in order to develop a common European research and development programme for an accelerator driven system, Technical Working Group (1998, 1999). Since 1999 Germany is a member of the TWG.

The basic opinion and the most important suggestions from the TWG are:

- The concept of an ADS has the potential to transmute minor actinides and long-lived fission products,
- Performance of a well-coordinated European research and development programme that is carried out by research institutions and industry, the duration is limited to 10 years at the present state,
- Invitation to the Russian Federation to join the programme due to their large experience in using lead-bismuth as coolant in nuclear submarine reactors.
- Development and construction of an Experimental Demonstrator with a thermal power of about 100 MW(th) in order to, first, demonstrate the operability of the system as a whole, comprising of an accelerator, a spallation target and a subcritical blanket and, second, prove the feasibility of the system to transmute minor actinides and long-lived fission products,

The following critical technical issues that do need further extensive research and development work are identified by the TWG:

- Technology of accelerators,
- Technology of the beam window and of the spallation target,
- Technology of heavy liquid metals as spallation material and as coolant,
- Material development,
- Fuel, fuel cycle and reproccessing,
- Safety analysis and licensing.

Similar conclusions are drawn by the United States Department of Energy, US-DOE (1999). Both the TWG and the US-DOE could identify no serious show-stoppers that could bring the ADS technology to an early end.

On the basis of the suggestions of the TWG several proposals were handed in for funding within the 5th European Framework Programme (1999 to 2002) by the European research institutions and industries, Technical Working Group (1998). Ten proposals are funded now. The objectives of the proposals is given below:

Chemical Separation (Partitioning):

- PYROREP: Pyrometallurgical Processing Research Programme,
- PARTNEW: Partitioning: New Solvent Extraction Processes for Minor Actinides,
- CALIXPART: Selective Extraction of Long Life Nuclides from High Activity Liquid Waste by Organized Matrices: Removal of Minor Actinides and a Process for Cesium Extraction,

Transmutation (Technology):

- CONFIRM: Uranium Free Fuels for ADS: Collaboration on Oxide and Nitride Fuel Irradiation and Modelling,

- SPIRE: Irradiation Effects in Martensitic Steels under Neutron and Proton Mixed Spectrum,
- TECLA: Technologies, Materials and Thermalhydraulics for Lead Alloys.

Transmutation (Basic Studies):

- MUSE: The MUSE Experiment for Sub-Critical Neutronic Validation,
- HINDAS: High and Intermediate Energy Nuclear Data for ADS,
- N-TOF-ADS: ADS Nuclear Data,
- N-TOF-TH: Thorium Nuclear Data,
- NEDUFPA: Neutron Cross Section Data for Unstable Fission Products and Actinides.

The research institutions and industries that are working on ADS within Europe and the areas of activity are given in figure 4. Some of the larger activities are divided into smaller working packages. Forschungszentrum Karlsruhe is present in most of the activities. The HGF Strategy Fund Project is linked to the TECLA (TEChnologies, Materials and Thermalhydraulics for Lead Alloys) Programme.

The investigations of this HGF Strategy Fund Project are in line with a pre-selection of five design options of an ADS.

- 2 coolants (lead-bismuth and gas),
- 2 powers (80-100 MW(th) and 600-800 MW(th)),
- Molten salt system.

All design options have one common feature: a spallation target with liquid lead-bismuth as spallation material and coolant. The safe control of the corrosion issue, the know-how about lead-bismuth technology and the selection of suitable structure and window materials is an indispensible requirement. In addition, all design options are equipped with a beam window that separates the evacuated beam pipe from the spallation area within the liquid metal. The safe cooling and the safe long-term operation of the beam window have to be demonstrated for all operational conditions. This makes the beam window per se an essential research and development element in the field of thermalhydraulics of a thin-walled thermally highly-loaded surface in a corrosive environment. The same holds for the heat transport within the target module itself.

The results of this project are directly linked to the MEGAPIE Initiative, (Bauer, Salvatores, Heusener (1999)). Within the MEGAPIE Initiative the three founder members PSI Switzerland, CEA France and Forschungszentrum Karlsruhe Germany together with CNRS France, ENEA Italy, JAERI Japan and SCK-CEN Belgium are designing, constructing and running a liquid lead-bismuth cooled spallation target of 1 MW beam power within the SINQ facility at PSI. Operation is scheduled in 2004. The successful operation of MEGAPIE is an important milestone towards an Experimental Demonstrator of an ADS.

The Technical Working Group proposes to establish only a few larger laboratories for experimental investigations in liquid lead-bismuth within the European Union. With the KArlsruhe Lead LAboratory KALLA at Forschungszentrum Karlsruhe there will be a strategic focal point in the field of lead-bismuth technologies in Germany.

Due to the international and transdisciplinary cooperations which promote and coordinate technology transfer, the requirement of the HGF is fulfilled to implement young scientists in a long-term and innovative project in cooperation with other scientific institutions and industry.

The positive assessment of ADS by both the French government and the French and Italien industries will promote a new rating of the treatment of long-lived and highly radioactive waste and the closing of the fuel cycle. According to the requirement of the HGF, this can lead to long-term technological innovations in the area of energy research.

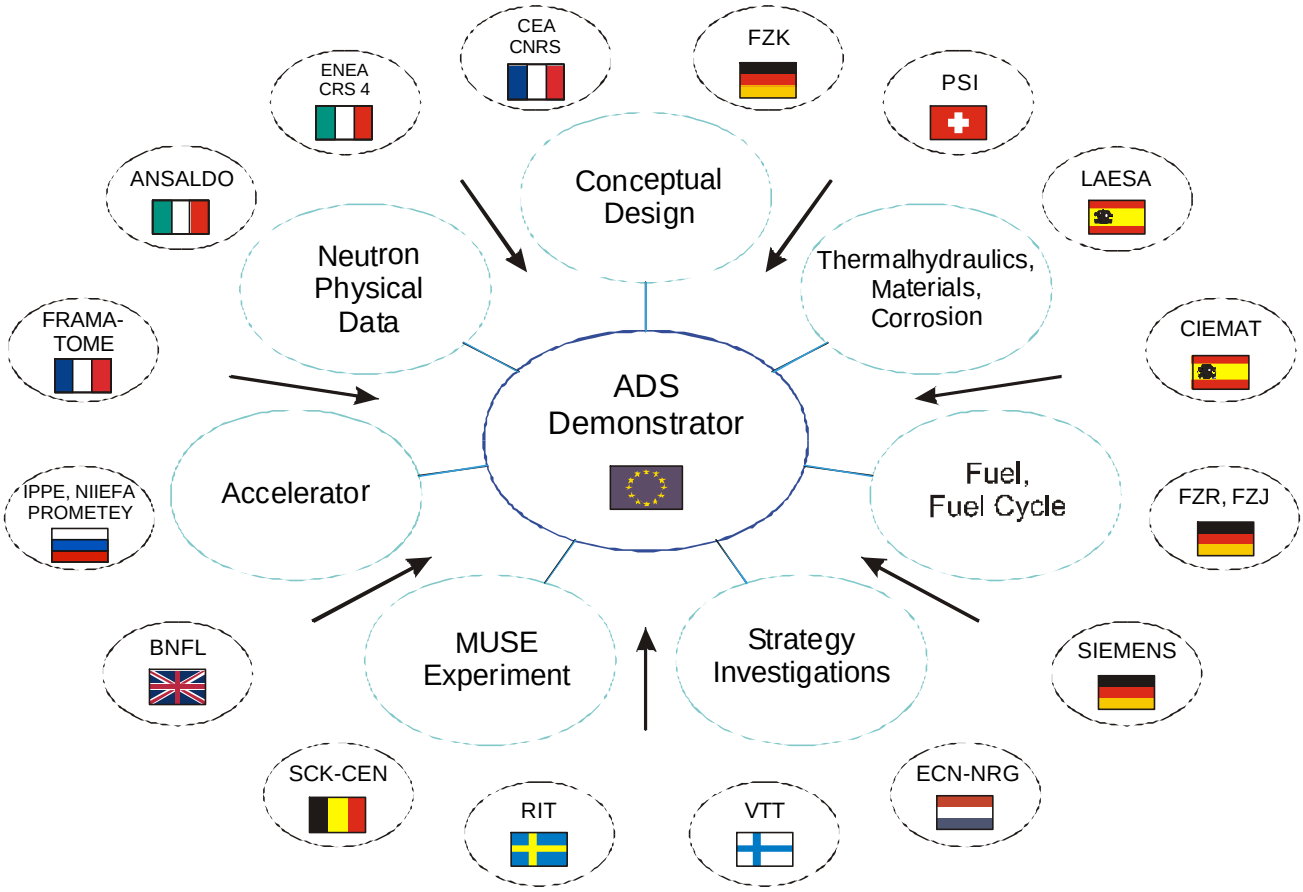

Figure 4: The research institutions and industries that are working on ADS within Europe and the areas of activity.

3. Project Time Table and Project Cost Plan

Table 3: Project time table.

period / Sub-Projects		2000				2001				2002		
	IV	I	II	III	IV	I	II	III	IV	I	II	III
Sub-Project 1: *WP1.* Design of beam window, Model experiment in water *WP2.* Basic experiment in Pb-Bi and physical model development *WP3.* Experiment and modelling of beam window in Pb-Bi *WP1.-WP3.* Validation of thermalhydraulic computer code												
Sub-Project 2: *WP1. – WP3.* Orientation experiments in stagnant Pb-Bi Performance of corrosion experiments Data / probe evaluation and material specific interpretation												
Sub-Project 3: *WP1.* Development of oxygen probe, oxygen measurement, long-term investigations *WP2.* Oxygen Control System OCS												
Final report												

Table 4: Project cost plan.

Period	Person years			Sum
	SP1	*SP2*	*SP3*	
10/1999 – 12/1999	2	0.5	1	0.7 million DM
01/2000 – 12/2000	7	2	2	2.2 million DM
01/2001 – 12/2001	8	2	2	2.4 million DM
01/2002 – 09/2002	6	1.5	1	1.7 million DM
	23	6	6	**7.0 million DM**

4. Scientific Procedure within the Project

4.1 Project Plan

The project plan (figure 5) schematically illustrates the division of the project into three sub-projects. The sub-projects are separated into theoretical (physical model development and numerical calculations) and experimental work packages.
The research work already done both at Forschungszentrum Karlsruhe and at other research institutions that is relevant for this HGF Strategy Fund Project, are equally given in the project plan.

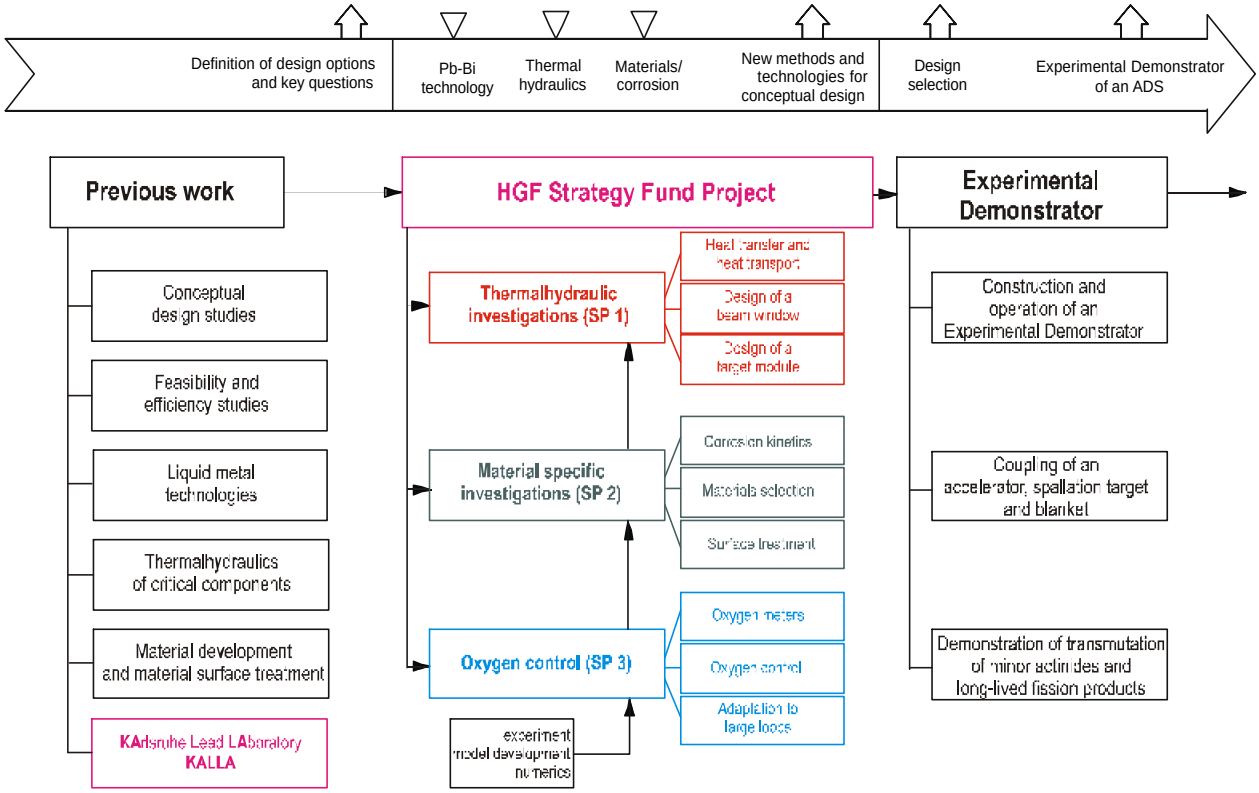

Figure 5: Project plan.

4.2 Scientific Programme

The engineering-scientific programme of each sub-project is described separately, following the headings:

- Overview and short description
- Problem, objectives and working strategy
- Working programme
- Milestones
- Sub-project time plan

The state of the art, previous work at Forschungszentrum Karlsruhe and relevant literature is given in the porposal for this HGF Project, Knebel (1999). Any literature references are omitted in chapter 4. Cross-links between the sub-projects are individually referred to.

4.3 KArlsruhe Lead LAboratory KALLA

Currently, at the Forschungszentrum Karlsruhe the KArlsruhe Lead LAboratory KALLA is being planned and constructed. A sketch of KALLA is given in figure 6. KALLA comprises three different experimental loops, each emphasizing on different specific objectives, briefly summarised in table 5 together with the main data.

The *Technology Loop* concentrates on fundamental lead-bismuth technologies, e.g. the establishment of an oxygen measurement and control technique, the most important prerequisite to safely operate a Pb or Pb-Bi loop. Thermalhydraulic measurement techniques are adapted to or specially developed for Pb and Pb-Bi (temperature: thermocouples and PT100-thermometers; pressure: pressure gauges with coupling fluid; velocity: miniature permanent magnet flowmeter probe, ultrasonic Doppler technique; wall heat flux: heat emitting temperature sensing surface). Basic heat transfer and turbulence experiments will be performed. In addition, high performance inconel heaters are developped.

The *Thermalhydraulic Loop*, first, is designed for single-effect investigations of the thermally highly-loaded beam window and the heat removal from a complete closed target module. Furtheron, detailed experiments can be done for a fuel element and a steam generator. Second, integral real-height investigations into the heat removal from the blanket and spallation target under normal and decay heat removal conditions can be performed.

The *Corrosion Loop* allows for fundamental investigations of corrosion mechanisms of low-activation steels and structural materials, the formation and the stability of protection layers and the performance of mechanical tests. The final aim is the development of a structure and a beam window material that can withstand corrosion.

The automization scheme of KALLA, e.g. control and monitoring processes, safety instrumentation, data acquisition, is based on Siemens S5 technology and National Instruments BridgeView and LabView architecture.

Parallel to the lead-bismuth experiments in KALLA, model experiments with water as fluid are performed in the test facility HYTAS (HYdraulic behaviour in spallation TArget Systems). HYTAS allows for hydraulic and heated experiments in various lucid test sections, the measurement techniques being a 4-beam 2-component fiber optical Laser Doppler Anemometer (LDA) and Laser light sheet for the velocity field and thermocouples and shadow graph for temperature field. The application of particle image velocimetry (PIV) is envisaged.

Table 5: KArlsruhe Lead LAboratory KALLA: Investigations.

Technology Loop	Thermalhydraulic Loop Investigations:	Corrosion Loop
	Single-effect investigations:	Corrosion mechanisms
Oxygen measurement	Beam window	Protection layers
Oxygen control	Closed Target module	Mechanical tests
Measurement techniques	Fuel element	
Heat transfer	Steam generator	
Turbulence	Heat exchanger	
High-performance heaters	*Integral investigations:*	
	Heat removal	
	Decay heat removal	
Fluid volume: 0.1 m³	Fluid volume: 0.5 - 4.0 m³	Fluid volume: 0.1 m³
Temperature: max 550°C	Temperatur: max 550°C	Temperature: max 550°C
	Power: 0.3 - 4.0 MW	
Flow rate: max 5 m³/h	Flow rate: max 100 m³/h	Flow rate: max 3.5 m³/h

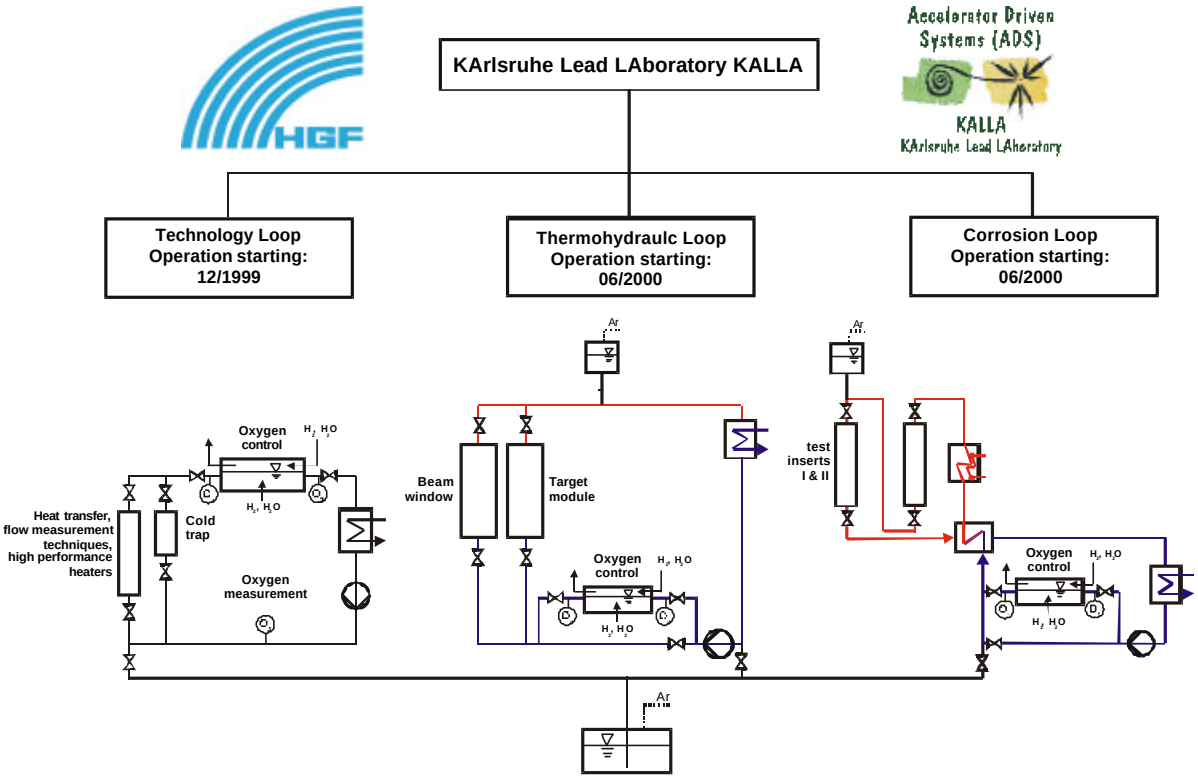

Figure 6: KArlsruhe Lead LAboratory KALLA: Sketch of the loops.

4.4 Sub-Project SP1: Thermalhydraulic Investigations
Thermalhydraulic Investigations of Thermally Highly-Loaded Surfaces with Lead-Bismuth as Coolant

4.4.1 Overview and Short Description

This sub-project elaborates the scientific-technical basis to describe the heat transfer along thermally highly-loaded surfaces with lead-bismuth as coolant. Such a thermally highly-loaded surface is the beam window. The character of the flow can be laminar or turbulent, the flow can be forced convection or natural circulation. Here, the setting-up of a data base for heat transfer along simple model geometries and their theoretical description using physical models is the primary task. For these investigations a change in structure and morphology of the surface due to corrosion and erosion effects and thus a change in heat transfer is considered. Existing physical models such as turbulence models or wall functions will be adapted to lead-bismuth and validated. Lead-bismuth has a molecular Prandtl number of 0.045 at a temperature of 400°C. The turbulent heat transfer and turbulent transport mechanisms of momentum and heat under natural circulation and forced convection are fundamentally different from what holds for fluids with Prandtl numbers around 1, for which a great number of physical models is implemented in computer codes and validated. In the appendix (chapter 8) the most important physical properties of lead-bismuth are given togeher with the properties of water, sodium and lead.
The elaborated and validated basics for the coolant lead-bismuth are, at a later stage, used for the design, the experimental investigation and the numerical simulation of the beam window and the complete spallation target module of an ADS.

The experimental work is partly embedded in the COULI Project at CEA France and the MEGAPIE Initiative, the numerical work is partly embedded in the European Benchmark Working Group EBWG, the ISTC 559 Project and the MEGAPIE Initiative.

Due to its strategic importance this work is partly supported within the 5th European Framework Programme TECLA „Technologies, Materials and Thermalhydraulics for Lead Alloys“ over a period from 2000 to 2002. Here, the major European partners are ANSALDO, CEA, CIEMAT, CNRS, ENEA, PSI, RIT, SCK/CEN. The work is done in such a way that the most effective interaction and work sharing is achieved between the partners.

4.4.2 Problem, Objectives and Working Strategy

Problem:

The Technical Working Group TWG that develops a common European research and development programme on accelerator driven systems (ADS), proposes liquid lead or lead-bismuth as suitable spallation material and coolant. The main reason for this are the neutron-physical characteristics of lead alloys, such as for example the low absoption cross sections both for thermal and for fast neutrons and the high neutron gain of the spallation reaction. Due to the very low molecular Prandtl number of lead alloys that is two orders of magnitude smaller compared to water, lead alloys show excellent heat transport capacities which allows their applicability as coolant even

with high surface heat fluxes present. The shielding characteristics of lead alloys in comparison to for example sodium are simplifying the construction of an ADS significantly.
In comparison to other liquid metals such as sodium lead alloys show great advantages in the area of system safety as highly exothermic reactions such as burning in contact with ambient, humid air or water can be excluded. The thermodynamic properties of lead alloys such as vaporization point, evaporation rate and saturation pressure at prototypic temperatures are much more favourable in comparison to sodium.
Disadvantages when using lead alloys are the high density that results in high dynamic pressure losses and that requires a more robust construction. The strong corrosion characteristics of lead alloys are discussed in sub-project 2. Another disadvantage is the production of polonium during the spallation reaction, especially in the presence of bismuth.
Among the various lead-alloys the lead-bismuth eutectic with about 55 wt-% bismuth is of prior importance due to its low melting point of about 123°C. Pure lead has a melting point of 327°C. The low melting point of the eutectic composition facilitates the handling and pumping of the melt in technical loops compared to pure lead.
In accordance with the European partners it was decided to perform all experimental investigations in lead-bismuth.
At present, there is no freely available experience in handling of lead or lead-bismuth in technical systems in Europe, nor is there experience in special measurement techniques such as ultrasonic Doppler technique to measure velocity at elevated temperatures. Similarly, there are no detailed measurements of temperature or velocity fields in lead-bismuth for simple geometrical configurations with heat transfer that could be used both for physical model development and model validation and for the thermalhydraulic design of ADS components. The investigation of a windowless target design for the spallation neutron source SNQ in the late seventies was limited to the level of a simple study. However, a comprehensive experimental data base and application-oriented know-how on handling lead or lead-bismuth is available in the Russian Federation. As the data orients from former USSR military research and application (coolant for nuclear propelled alpha-class submarines) and therefore has a safety classification, this data can hardly be accessed and used.

Objectives:

The objective of the research work is the setting up of a detailed thermalhydraulic data base, the improvement of existing or the development of new physical models to describe the heat transfer along thermally highly-loaded surfaces (beam window) and the development of a validated CFD computer code for flow simulation. On this fundamental basis the design and the performance of a solid beam window will be developped. Finally, there is the design of a closed spallation target module with this CFD computer programme.

Working Strategy:

Experimental thermalhydraulic investigations in liquid lead-bismuth require a complex measurement technique even if the investigated geometry is very simple. Lead-bismuth is opaque, a test loop has to be operated at elevated temperatures above the melting point and lead-bismuth is very corrosive in respect to steels as structure material.

A thermalhydraulic instrumentation consisting of NiCr-Ni-thermocouples or PT100-resistivity thermometers for temperature measurement, differential or absolute pressure transducers with coupling fluid for pressure measurement have to be adapted and tested before being used in lead-bismuth. Most velocity measurement techniques known from water and air cannot be used with lead-bismuth. Permanent magnet flowmeter probes that are based on Faraday's induction law and that show a good performance in sodium, have to be modified and tested before being used in lead-bismuth. The performance of ultrasonic Doppler probes, up to now, are limited due to the temperature limitation of the signal transducers, a significant effort has to be done here. Wall heat flux sensors have to be adapted to the elevated temperatures as well.
Within the project of the Sodium Cooled Fast Breeder Reactor several CFD computer codes (FLUTAN as FZK development) were developped and validated for sodium as coolant for laminar or turbulent flow in the primary system, the flow being driven by natural circulation and/or forced convection. What has to be done within this Project is to consequently transfer the code to lead-bismuth as coolant and to validate it using the detailed single effect experiments described before.

Within sub-project SP1 three consecutive work packages WP1 to WP3 are executed. A detailed description of the working programme is given in chapter 4.4.3.

(WP1.) Design of a beam window based on numerical simulations and model experiments with water as fluid
(WP2.) Fundamental experiments in liquid lead-bismuth on heat transfer and model development / model validation
(WP3.) Simulation experiments for the optimized beam window in lead-bismuth and numerical simulation

Within this first yearly progress report, the results obtained until December 1999 are presented in chapter 5.

4.4.3 Working Programme

The simulation experiments and accompanying numerical simulations in lead-bismuth are preceded, first, by design experiments and accompanying numerical simulations in water as model fluid and, second, by fundamental investigations on heat transfer and heat transport in lead-bismuth. The model experiments using the model fluid water allow for direct flow visualization around the beam window. This cannot be done with lead-bismuth.

(WP1.) Design of a beam window based on numerical simulations and model experiments with water as fluid

According to the recommendations of the Technical Working Group TWG and the coordinated projects for the 5th European Framework Programme, a solid beam window is chosen for all further investigations. The geometry (half sphere at the lower end of the beam pipe), the diameter and the power distribution within the window itself and in the spallation area are given.
Due to the half-sphere design of the beam window the flow of the coolant around the window results in a stagnation point flow where the stagnation point is located at the

point of highest power deposited by the proton beam. This is for a symmetric beam that is alligned with the beam pipe axis. Numerical simulations for a spallation target that were performed at Forschungszentrum Karlsruhe in the framework of the International Science and Technology Center ISTC 559 Projects have shown that a 1 MW(th) spallation target without intelligent flow guides or adapted window design exhibits extremely high excess temperatures close to the stagnation point. By introducing a perforated plate close to the beam window, the numerical calculation shows a significantly improved cooling of the beam window close to the stagnation point.
Within the MEGAPIE Initiative the cooling of the beam window is improved by introducing a forced cross-flow over the beam window surface. This cross-flow results in a strong convective cooling, there is no more stagnation point any more.
Another possibility to reduce the thermal load on the beam window is by changing the general design of an ADS: The multiple-beam concept realizes three separate closed spallation target modules that are located in the outer part of the blanket. With this Thre-Beam Concept the proton beam power for each of the three beam windows is reduced by a factor of about 2 relative to a single-beam concept.
Another innovative approach is a non-spherical beam window: By optimizing a cylindrical geometry that is cut at an angle (resulting in an ellipsoidal surface), a stagnation point flow can be omitted as well. However, the resulting stresses in the window material and the problem of manufacturing have to be considered.
These concepts with an improved beam window cooling have not yet been applied to a European Demonstrator (thermal power of about 100 MW_{th}) or a prototypical ADS (thermal power of about 1500 MW(th).
Within Work Package WP1 the beam window geometry, the perforated plate and the flow configuration are designed and optimized. This is done both for 1 MW beam power as used for the ISTC 559 and the MEGAPIE beam window, and for a maximum of 4 MW as used for the Three-Beam Concept with a thermal power of 1500 MW(th) or the European Demonstrator. This results in a maximum mean wall heat flux of about 100 W/cm².

The first iteration step to design the beam window is done by using the CFD computer code CFX, alternatively FLUTAN. The experience and the numerical results gained from the ISTC 559 Project and the MEGAPIE Initiative are used. Then, before starting a difficult and expensive experiment using lead-bismuth as fluid a hydraulic model experiment with water as fluid is performed in a geometrically similar scaled model geometry. The velocity field (mean value, fluctuations and correlations) is measured using a 4-beam 2-component fiber optical Laser Doppler Anemometer (LDA).
The water experiment is done in the test facility HYTAS (HYdraulic behaviour in spallation TArget Systems). The boundary conditions for the hydraulic experiment are: geometrical scaling of 1:2, beam window diameter 0.1 m, volume flow rate maximum 100 m³/h. Possibly, the heating of the beam window is considered using a heat emitting temperature sensing surface (HETSS) in order to qualitatively investigate the influence of various flow configurations on the local heat transfer characteristics.
The CFD codes and the numerical methods are validated with the data from the model experiment. Possibly, a second iteration step has to be done to optimize the geometry and the flow configuration. The results are compared with the outcomings of the COULI Programme at CEA in the framework of which a similar experiment and accompagnying numerical investigations on an ADS beam window are performed.

Then, the velocity field is transferred to lead-bismuth by using similarity scaling laws. This procedure is verified by various investigations in water and their transferability to sodium.

The result from work package WP1 is the definition of the beam window geometry and flow configuration that is optimized using a scaled model experiment with water as fluid and numerical simulations.

(WP2.) Fundamental experiments in liquid lead-bismuth on heat transfer and model development / model validation

A transfer of the temperature field from scaled model experiments in water to the situation in lead-bismuth cannot be done directly. The molecular Prandtl number of both fluids differs by a factor of 100. In addition, the turbulent heat fluxes, the intensity of the temperature fluctuations and its dissipation rate cannot be directly transferred from water to a liquid metal such as lead-bismuth. The physical description of these quantities by using a turbulence model has been extensively investigated and validated for sodium at Forschungszentrum Karlsruhe. In order to validate these physical models for lead-bismuth, a number of fundamental experiments on heat transfer along a flat heated plate and a heated cylinder in laminar and turbulent forced convection flow will be performed in the Technology Loop of the KArlsruhe Lead LAboratory KALLA.
The experimentally achievable wall heat flux is at maximum 120 W/cm² so that the heat flux formulated in WP1 which is expected for the Experimental Demonstrator and the Three-Beam Concept can be achieved in the experiment. The heating is done either by high-performance inconel coil heaters developped at Forschungszentrum Karlsruhe or by using a CO_2 laser with a net power of about 20 kW. The morphology of the heat-transferring surface is of major interest with the experiments. The influence of the surface structure and morphology is investigated in detail. The surface structure is characterised by the surface roughness, the heat transfer is, among others, determined by the chemical composition and the thickness of the corrosion and protection layers and their thermal conductivities.
The heat transfer measurements within the Technology Loop are performed in a pipe test insert of 60 mm inner diameter and a total length of 60 hydraulic diameters. This allows for thermalhydraulic developped conditions. The temperature and the velocity field are measured using traversable thermocouples and a traversable Miniature Permanent-Magnet Flowmeter Probe. The Flowmeter Probes are adapted to lead-bismuth and are calibrated in well defined flow conditions. In addition, ultrasonic Doppler technique will be applied.
Using the data base of mean and fluctuating values of temperature and velocity, the physical model developped at Forschungszentrum Karlsruhe (turbulence models, wall functions, heat transfer) are modified for use with lead-bismuth if necessary, implemented in the CFD computer codes FLUTAN and CFX and validated.
The commissioning tests for the Technology Loop are planned for early 2000.

The result of work package WP2 is a CFD computer code that is validated for the heat transfer along a thermally highly-loaded surface of simple geometry (heated flat plate, heated cylinder) that is cooled by lead-bismuth.

(WP3.) Simulation experiments for the optimized beam window in lead-bismuth and numerical simulation

A further step is the commissioning of the Thermalhydraulic Loop and the performance of a semiscale simulation experiment of the optimized beam window geometry. The optimized geometry is achieve by an iteration between the numerical simulation and the model experiment in water from work package WP1 and an optimization procedure with the COULI Programme.
The boundary conditions for the lead-bismuth experiment are: geometrical scaling at a scale of 1:1, beam window diameter of 0.2 m, inlet flow temperature 200-300°C, volume flow rate 10-70 m^3/h, wall heat flux at window surface 0-100 W/cm^2.
The heating of the beam window will be done by the inconel coil heater or the CO_2 laser, developped in work package WP2. The beam window test insert is intensively instrumented with thermocouples, velocity technique and pressure transducers, so that a data base of mean amd fluctuating temperature and velocity data together with the relevant boundary conditions can be set up. Special care is taken to measure the maximum surface temperature of the beam window.
The first experiments are performed without heating of the beam window. The measured flow field of the model experiment in water from work package WP1 will be compared with the measured velocity field in lead-bismuth in order to allow for a transferability criteria of the velocity data from water to lead-bismuth and thus for a scaling law.
In further experiments the thermal loading of the beam window under relevant boundary conditions and the corresponding temperature and velocity fields are investigated and measured.
The experiments in lead-bismuth are now simulated using the validated computer codes from work package WP2. The experimental data are compared with the numerical results. The computer codes are critically evaluated according to their performance and their grade of validation.

In a final step a numerical pre-calculation of a complete closed target module is performed. Using the validated computer code from work packages WP1 and WP2, the complete target module of an Experimental Demonstrator or of a prototypical ADS that is of the type Three-Beam Concept is calculated, taking into account the beam window, the riser, the heat exchanger, the downcomer and the spallation area. The heat transfer correlations are taken from work package WP2. The calculation allows for the dimensioning of the heat exchanger.

The result of work package WP3 is the experimental design of the beam window of an Experimental Demonstrator and the provision of a thermalhydraulic computer code that is validated for this geometry and boundary conditions. Using this computer code a pre-calculation for a complete target module is performed.

4.4.4 Milestones

03/2000: Definition of the optimized beam window geometry that is to be investigated in lead-bismuth;
06/2000: Commissioning tests of the Thermalhydraulic Loop;
03/2001: Validation of the thermalhydraulic computer code using fundamental heat transfer and heat transport experiments in lead-bismuth, documentation;
03/2002: End of beam window simulation experiment, end of thermalhydraulic computer programme validation in lead-bismuth, documentation;
06/2002: End of pre-calculation of a closed spallation target module, documentation;
09/2002: Final report.

4.4.5 Sub-Project Time Table

Table 6: Time table of sub-project SP1.

period / Work package		2000				2001				2002		
	IV	I	II	III	IV	I	II	III	IV	I	II	III
WP1. Design of beam window, Model experiment in water												
WP2. Basic experiment in Pb-Bi, Physical model development and validation												
WP3. Beam window experiment in Pb-Bi, Physical model development and validation, Pre-calculation of a target module												
Final report												

4.5 Sub-Project SP2: Material Specific Investigations Investigation of Corrosion Mechanisms and Development of an Instruction to Condition Metals in Flowing Lead-Bismuth

4.5.1 Overview and Short Description

The objective of this sub-project is to elaborate the scientific-technical fundamentals of the corrosion / erosion behaviour of metallic structure and window materials that are in contact with eutectic lead-bismuth. Here, the main interest is on the chemical-physical interaction between the solid and the liquid metal.
Due to its strategic importance this work is partly supported within the 5th European Framework Programme TECLA „Technologies, Materials and Thermalhydraulics for Lead Alloys“ over a period from 2000 to 2002.

4.5.2 Problem, Objectives and Working Strategy

Problem:

Liquid eutectic lead-bismuth is generally considered to be an adequate spallation material for an ADS. A description of some specific advantages and disadvantages of lead or lead-bismuth is given in chapter 4.4.2.
Besides the well known advantages lead and lead-bismuth have a high corrosion potential relative to metals. The fundamental mechanism of this physical-chemical interaction that is called liquid metal corrosion is characterised by the following points:

- Solution of some metal components of the structure material in the liquid metal,
- Mass transport of structure material within the loop due to temperature gradients, e.g. dissolution in the hot part and precipitation in the cold part of the loop,
- Compatibility and long-term stability of the oxygen probes, the flow instrumentation and other components that are in contact with lead-bismuth,
- Change in the structure and the morphology of the surface,
- Influence on the mechanical characteristics of the structure material,
- Reaction of the structure material with non-metals that are dissolved in the liquid metal, e.g. oxygen.

The isotopes that are produced in the presence of high energy protons and neutrons during the spallation and fission reaction of heavy elements, are phenomena specific for a spallation neutron source. These isotopes can change the physical-chemical characteristics of the liquid metal and thus the corrosivity considerably. As for possible window materals this chemical attack is combined with the thermal load due to the internal heating by the high energy proton beam.
It is know that austenitic steels with a high amount of nickel are severely corroded as long as they are unprotected. Ferritic, low-alloyed and non-alloyed steels, however, show a better corrosion resistance. Although there are no corrosion data available in the literature for tungsten and tungsten-rhenium, only little corrosion is expected due to their low solubility in lead and lead-bismuth.

Objectives:

The objective of this sub-project is to elaborate the scientific-technical fundamentals of the corrosion / erosion behaviour of metallic structure and window materials that are in contact with flowing eutectic lead-bismuth. The main interest is in nickel-free, ferritic-martensitic chromium-steels and, due to the high temperature stability, in high chromium and high-nickel austenitic steels. In order to guarentee little corrosion of structure materials the following scientific fundamentals are elaborated:

- Chemical-physical effect of corrosion inhibitors in lead-bismuth,
- Long-term stability of scales on the structure material that are formed by a pre-oxidation under air atmosphere,
- Application of aluminium hot dipping plus oxidation as a measure of surface treatment (hot dipping facility available at Forschungszentrum Karlsruhe),
- Application of GESA-surface treatment, e.g. surface improvement by remelting, restructuring and aluminum alloying of a thin surface layer using a pulsed electron beam (GESA test facility in operation at Forschungszentrum Karlsruhe).

This work includes all technologies necessary to handle and to operate a lead-bismuth loop safely and without interruption.

Working Strategy:

The basic approaches to improve the corrosion resistance of potential structure and window materials are to coat the surface with a tight and liquid metal resistant scale of aluminium oxide by surface alloying of aluminium through hot dipping or GESA treatment, see pulsed electron beam test facility GESA in chapter 4.5.3.
Another possibility is to improve the corrosion resistivity by setting and controlling the oxygen concentration in the liquid metal within a small range. The oxygen concentration has to be set in such a way that a stable Fe-Cr-Mn-Oxid scale is formed on the metal surface. This approach is considered in sub-project SP3, chapter 4.6.3.

Within sub-project SP2 three work packages are considered.

(WP1.) Investigation of the corrosion and erosion of structure and window materials in flowing lead-bismuth
(WP2.) Improvement of the corrosion resistivity using surface protection
(WP3.) Surface modification using the pulsed electron beam facility (GESA)

The experiments are performed in the corrosion loop of the KArlsruhe Lead LAboratory KALLA. The corrosion loop will be equipped with the oxygen control system of sub-project SP3 as soon as available.
A description and a schematic diagramme of the KArlsruhe Lead LAboratory KALLA is given in chapter 4.3.

4.5.3 Working Programme

(WP1.) Investigation of the corrosion and erosion of structure and window materials in flowing lead-bismuth

In a first step experiments in stagnant lead-bismuth are performed. The oxygen control is done via the gas atmosphere. Corrosion investigations in stagnant liquid metal can only give a rough estimation for a material selection, as the corrosion kinetics are influenced by fluiddynamic parameters such as the flow velocity. Thus, exposure tests in flowing lead-bismuth are indispensible. These experiments are performed in the Corrosion Loop of the KArlsruhe Lead LAboratory KALLA, fig. 6. The important data of the corrosion loop are as follows:

- Piping and components: Austenitic high temperature steel
- Total volume of the liquid metal: 0.03 m^3
- Maximum temperature: 550°C
- Reynolds number within test section: > 2300 (turbulent flow)
- Flow velocity within test section: 2.0 m/s
- Number of test sections: 2
- Probe geometry: Cylindrical probes
- Oxygen measurement: oxygen meter (development in WP3)
- Oxygen control: via gas phase (development in WP3)
- Mode of operation: continuous

The design and construction of the corrosion loop was done in 1999, the construction will be finished in the middle of 2000. The experimental programme investigates the following materials:

Structure materials:

- Ferritic-martensitic steels (no nickel): Low-activation 10% chromium-steels of types Optifer (FZK-development and T91) X 20 CrMoV 12 1 (1.4922)
- Austenitic high temperature steels: X 10 NiCrMoTiB 15 15 (1.4970) X 6 CrNi 18 11 (1.4948) X 7 CrNi 23 14 (1.4833), equivalent to Russian steel used for lead-bismuth loops

Window materials:

- High melting metals: Thungsten und W-26Re-alloy
- Steels as above

The reliable investigation of the corrosion attack kinetics requires a minimum of 1 year experimental time (approximately 8000 h). In order to develop time dependent physical relationships, probes are withdrawn from the test sections after 1000, 3000 and 5000 hours. The specimen are micro-analytically investigated, using metallography, SEM, AES and microprobe.

The result of work package WP1 is the metallurgical description of the corrosion mechanism for various materials as a function of thermodynamic / thermalhydraulic parameters.

(WP2.) Improvement of the corrosion resistivity using surface protection

The practical experience in the Russian Federation clearly demonstrates that materials without a proper coating and especially those with a high content of nickel have no sufficient corrosion resistance in flowing lead or lead-bismuth. A solution of this corrosion problem can be expected by applying a protection layer on the material surface that is resistant to lead-bismuth. Within this work package three different coating methods and their influence on improving corrosion resistivity are investigated. These methods can be easily applied to large components of an ADS.

Pre-oxidation in air:

After a specific heat treatment in air all materials have a very thin natural passivation layer that sometimes has only a few micrometers in thickness. Depending on the steel used this layer consists of a mixture of Fe-Cr-Mn-oxides. Corrosion investigations at Forschungszentrum Karlsruhe clearly demonstrate that such a natural oxide layer does not give a long-term protection against lead-lithium.
Thus, this work package develops and defines the optimal process parameters that allow the growth of a thick (10-20 µm), tight and well-adhesive oxide protection layer during pre-oxidation in air. For these investigations one species of each steel type (ferritic-martensitic and austenitic) is chosen. The pre-oxidation time is at a maximum of 100 hours in order to simulate production-relevant conditions.

Hot-dip aluminizing:

Another method to form a protective surface layer is the hot-dip aluminizing. This method was developped at Forschungszentrum Karlsruhe in the framework of manufacturing tritium permeation barriors on ferritic-martensitic steels. Here, the steel specimens are dipped into a liquid aluminium bath of about 700°C for a few minutes. Due to a solution-diffusion-reaction an iron-aluminium oxide layer is formed on the specimen surfaces. This layer is very brittle and has to be transformed into more ductile phases by adapting a heat-treatment, known from ordinary hardening of steels. If this heat-treatment is done in an oxygen rich environment, an aluminium oxide layer of a few micrometers in thickness is formed on the material surface.
Within this sub-project the scientific-technical fundamentals to transfer this process to austenitic steels is elaborated. The influence of nickel on the formation of an Fe-Al-layer after the hot dipping and on the homogeneity of the Al_2O_3-layer is of special importance.

In situ formation of a protective oxide layer:

From work performed in the Russian Federation it is well known that an improved corrosion resistivity of high-nickel steels can only be achieved, if the oxygen concentration within the liquid lead-bismuth is kept between well defined limits. The task, now, is to define this „concentration window“ and to develop a method that allows to keep the oxygen concentration within this window during normal operation. All activities dealing with oxygen measurement and oxygen control are discussed in detail in sub-project SP3.

The result of work package WP2 is the development of a corrosion protection method for structure and window materials in lead-bismuth by applying suitable surface treatment technologies or materials.

(WP3.) Surface modification using the pulsed electron beam facility (GESA)

The surface treatment of the steel is carried out with the GESA facility (gepulste Elektronenstrahlanlage), Müller et al. (1996). GESA is a pulsed electron beam facility that consists of a high voltage generator with a pulse duration control unit, a multipoint explosive emission cathode, a controlling grid and an anode which form a triode system. A sketch of the facility is given in figure 7. The electron kinetic energy can be varied in the range of 50 to–150 keV with an energy density up to 50 J/cm² at the target. This is sufficient to melt metallic materials adiabatically up to a depth of 10 to 50 µm. The beam diameter is 6 to 10 cm and this is the area of surface melting by applying one single pulse. Due to the high cooling rate in the order of 10^7 K/s very fine grained or even amorphous structures develop during solidification of the molten surface layer.
The following steels are chosen for GESA treatment: ferritic steels such as Optifer, T91 and austenitic steels such as 1.4970, 316LN and 1.4948. The most simple method to form a protective oxide layer is the in situ oxidation within the loop itself. To apply this method, the oxygen concentration within the lead-bismuth has to be controlled via the gas phase, cf. sub-project SP3.

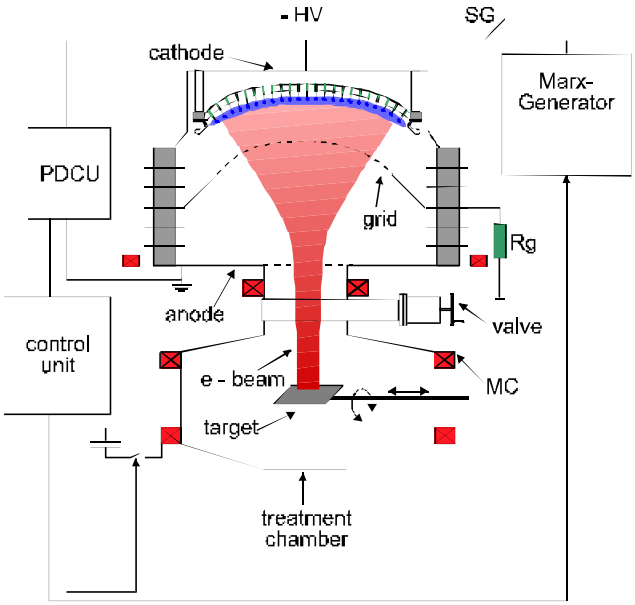

Figure 7: GESA facility, sketch.

In experiments on surface treatment by the GESA installation, it was observed that formation of protective oxide scales can be improved by such treatment Müller et al. (1998). By the same process a metal that is precipitated on the surface can be alloyed into the molten layer (e.g. Al or Si). Both methods, restructuring and surface alloying, will be applied in this work to examine, whether the corrosion resistance of steels in liquid lead and lead/bismuth could be improved.
Surface modification using the GESA facility is a promising technique to treat small but thermally highly loaded surfaces, such as the beam window, heat exchanger tubes or claddings. Here, peak temperatures are expected that are beyond the 150 K temperature span allowed within a loop, so that a special surface protection is needed for these components.

The result of work package WP3 is the statement whether the surface modification of structure and window materials by using the pulsed electron beam of the GESA facility can improve the corrosion resistivity.

4.5.4 Milestones

03/2000: Commissioning of the Corrosion Loop;
04/2002: Corrosion kinetics and life cycle expectations for selected structure and window materials, documentation;
06/2002: Selection of suitable materials for use in lead-bismuth, documentation;
08/2002: Evaluation of the results, final report.

4.5.5 Sub-Project Time Table

Table 7: Time table of sub-project SP2.

period / Work package		2000				2001				2002		
	IV	I	II	III	IV	I	II	III	IV	I	II	III
WP1.-WP3. Orientation experiments in stagnant Pb-Bi, Performance of corrosion experiments in flowing Pb-Bi, Microanalytical post-examination of the corrosion specimen, Description of corrosion kinetics, Evaluation of results												
Final report												

4.6 Sub-Project SP3: Oxygen Control
Oxygen Concentration Measurement and Oxygen Control in Lead-Bismuth Loops

4.6.1 Overview and Short Description

The objectives of the sub-project are to work out the scientific-technical fundamentals to measure and to control the oxygen concentration in flowing lead-bismuth and to provide an instruction on how to improve the corrosion resistance of structure materials.
The control of the oxygen concentration is of major importance for the long-term operation of a lead-bismuth loop. The measurement of the oxygen potential is done with an electro-chemical oxygen probe. The oxygen probe and the reference system are adapted to lead-bismuth, this is for the long-term stability of the probe ceramics and the sensitivity towards strong temperature fluctuations. The oxygen control itself is done via the gas phase above the liquid lead-bismuth by controlling the hydrogen/steam-ratio in the gas phase. The cover gas is argon. Finally, the transferability of the oxygen control system to large lead-bismuth loops, e.g. the spallation target module or the primary system of an Experimental Demonstrator of an ADS, is investigated.
Due to its strategic importance this work is partly supported within the 5th European Framework Programme TECLA „Technologies, Materials and Thermalhydraulics for Lead Alloys“ over a period from 2000 to 2002.

4.6.2 Problem, Objectives and Working Strategy

Liquid eutectic lead-bismuth is worldwide considered to be a suitable spallation target material for an ADS. As described in sub-project SP2, the combination of steel as structure material and liquid lead-bismuth as spallation material and coolant results in considerable corrosion problems. In order to technically realize an ADS this corrosion mechanism has to be described in a physical-chemical way. Liquid metal corrosion is the partial solution of metallic components out of the structural material into the liquid metal. A possible solution is the use of metals that have a very low solubility, such as tungsten. From the technical point of view tungsten cannot be realized as structure material on a large scale, its use as beam window material however can be considered. A technically more feasible way is to form an oxidic protection layer on the steel structure surface. This can be done by formation of an oxide layer on the steel surface by reaction of steel elements with gaseous oxygen. Another possibility is to alloy the steel surface with reactive elements as is described in sub-project SP2.
Oxidic protection layers can so effectively slow down the corrosion attack of the liquid metal that corrosion is considerably suppressed and that the structure material reaches an acceptable life time. The requirement for the protective effect of the oxidic layer is both the tightness towards metal ion and oxygen diffusion and the mechanical stability and the adhesive strength towards the steel surface. This has to hold under thermal cycling conditions as well. These requirements are essentially defined by the chemical composition of the active surface layer. The concentration and the distribution of the alloying constituants, which are forming the effective oxidic protection layer, is of prior importance. The long-term stability of the oxide layer can only be guaranteed, if two boundary conditions for the oxygen potential within the liquid lead-bismuth are fulfilled: the oxygen potential has to be high enough in order

to prevent the dissolution of the oxides from the steel surface, and the oxygen potential has to be low enough to prevent the formation of lead oxide. This requires the continuous measurement and control of the oxygen concentration in a lead-bismuth loop.

Within sub-project SP3 there are two work packages that are dealing with instructions for the oxygen measurement using electro-chemical probes and for the oxygen control in a lead-bismuth loop.

4.6.3 Working Programme

(WP1.) Oxygen measurement in flowing lead-bismuth

Within this work package the oxygen probes that are well known from sodium and lead-lithium technology, are adapted to be used in liquid lead-bismuth. Thermodynamic calculations that give the theoretical correlation between the electromotorive force EMF and the temperature for non-saturated and saturated oxygen in lead-bismuth, form the physical-chemical basis for the evaluation of the probe signals.

Three reference systems are chosen for the use in lead-bismuth:

- Platinum/air,
- Bi/Bi_2O_3,
- In/In_2O_3.

First, the experiments are performed with stagnant liquid lead or lead-bismuth in crucibles that are part of the technology loop of KALLA, see figure 6. The calibration of the oxygen probe and of the reference system and thus a criterion for a successful application in flowing lead, is achieved by comparing the theoretical EMF with the experimental data. A positive evaluation of the oxygen probe is done, if the experimetally found temperature dependency is equal to the calculated one. This is a proof that similar thermally-activated processes are both measured and theoretically assumed. Then, a reliable calibration curve can be set up.
Besides the selection of an adequate reference system the long-term stability and the resistivity to thermal cycling of the oxygen probe has to be investigated. Here, the aging of the ceramics and of the reference material is of major importance. The physical-chemical effects that can limit the long-term application, are defined and possible counter-measures are described.
The implementation of the oxygen probes in the corosion loop and the thermalhydraulic loop of KALLA is done after this selection process.

The result of work-package WP1 is the development of a long-term stable, electro-chemical oxygen probe with reference system for continuous use in flowing lead-bismuth.

(WP2.) Oxygen control in flowing lead-bismuth

In a first step, a gas-phase oxygen control system has to be developped for the corrosion loop and the thermalhydraulic loop of KALLA with 0.1 m³ and 4 m³ lead-bismuth inventory, respectively. The main requirement of the oxygen control system is to establish a stable oxygen potential for a given temperature gradient over the loop (this holds for steady-state and transient operational conditions). From a theoretical point of view, the reaction kinetics has to be described for the transition of the oxygen from the gas phase into the liquid metal over the free surface. In a second step, an oxygen control system for a complete closed spallation target module with heat removal system (e.g. Integral Experiment K4T, Karlsruhe 4 MW Target) and for the primary loop of a European ADS Demonstrator is designed. The overall design of the closed spallation target module is done in sub-project SP1.
The maximum permissible temperature difference within a loop is given by the technically tolerable PbO-sedimentations, the technical features of the loop (additional purification loop or cold trap) and thermodynamic considerations. Thermodynamic calculations result in a maximum temperature difference of 150 K within a closed loop. The gas-phase oxygen control is done at a location of constant and high temperature in the loop in order to set well defined thermodynamic equilibrium conditions. The same holds for the oxygen probes: Due to kinetic reasons the oxygen probes accuracy increases with increasing temperature. In addition, the influence of the oxygen potential and of the maximum temperature difference within the loop on the PbO-sedimentation and on the protection effect of the oxidic layer is investigated.
The physical description and the technological understanding of the transition of oxygen from the gas phase into the liquid metal is important for the description of the time scales that are characteristic to reach thermodynamic equilibrium conditions in a loop system. These time scales automatically determine the liquid metal inventory of an ADS that can be controlled via the gas phase in a fast and technically feasible way. The physical exchange and diffusion processes for the gas-phase oxygen control are essentially determined by the temperature, the free surface area between gas phase and liquid metal and by the partial pressures of steam and hydrogen in the gas phase.
With the technology loop two techniques of oxygen control are investigated:

- The mixture of cover gas (argon) and hydrogen/steam flows *over* the free surface of the lead-bismuth,
- The mixture of cover gas (argon) and hydrogen/steam is injected *into* the lead-bismuth as a dispersed bubbly flow.

The fundamental difference between both techniques is in the interfacial area that is relevant for the exchange processes. The second technique offers a large interfacial area within a small construction volume. The injection can be done using porous media or nozzles. The design is done with the help of an analytical approach from two-phase flow. The design objective is to determine the void fraction, the bubble size and the interfacial area concentration.

The result of work package WP2 is an engineering-technical instruction to continuously control the oxygen potential in a lead-bismuth loop.

4.6.4 Milestones

06/2000: Selection of an oxygen probe with reference system suitable for implementation in the lead-bismuth loops of KALLA, documentation;
12/2000: Determination of oxygen concentration and temperature gradients for the loops;
02/2002: Determination of the size of loops / systems that can be controlled via the gas phase;
08/2002: Evaluation of the results, final report.

4.6.5 Sub-Project Time Table

Table 8: Time table of sub-project SP3.

period / Work package		2000				2001				2002		
	IV	I	II	III	IV	I	II	III	IV	I	II	III
WP1. Thermodynamic calculation for the reference systems, Tests to select reference system, Long-term investigation of the oxygen probes												
WP2. Formation of protection layers and PbO layers depending on ΔT und p_{O2} , Investigations to achieve equilibrium conditions via the gas phase, Adaptation of oxygen control system to large loops												
Final report												

5. Results during 1999

Within this chapter the results achieved during 1999 are collected. The results are classed with the respective sub-projects and work packages. Cross-links between the sub-projects are outlined. Milestones are addressed when achieved. If a milestone could not be achieved or if a work is running behind schedule an appropriate explanation is given.
As the project was approved by the HGF Council dated July 09, 1999 and as the funding was granted by BMBF dated October 18, 1999, Forschungszentrum Karlsruhe could employ most of the staff for this project after this date. This resulted in a general delay of some tasks.
Before the 1999 results of the three sub-projects are presented and discussed in detail, a short description of KALLA (loops and automization scheme) is given.

5.1 KArlsruhe Lead LAboratory KALLA

At Forschungszentrum Karlsruhe the KArlsruhe Lead LAboratory KALLA is being designed and built up. Commissioning will be in 2000. KALLA comprises three different experimental loops (see figure 6), each emphasizing on different specific objectives, briefly summarized in table 5 together with the main data.
All three loops are manufactured out of stainless steel 1.4571 (X6CrNiMoTi17-12-2). Due to the high temperature and pressure levels, the loops are treated as pressure containers. All materials (piping, bends, flanges) and components (valves, vessels, gas system, instrumentation) require a licensing according to VdTÜV (1986). All weldings have to be according to VdTÜV (1996). This results in time-consuming checking procedures of all used materials, components and all weldings.
In the future, KALLA shall be developped into a user-laboratory for ADS relevant experiments.

5.1.1 Technology Loop

The technology loop consists of an electromagnetic pump, a flowmeter, a cold-trap, an oxygen control system (OCS) and a heat exchanger. The test section is circular in cross-section, the diameter is 60 mm, the length-to-diameter ratio is 60.
A picture of the technology loop is given in figure 8. The piping and instrumentation scheme is given in figure 9.
In preparation of the heat transfer experiments a high performance heater rod is being developped. It is a mono-heater rod with a helical inconel heater core. A sketch together with the main dimensions and data are given in table 9, a photo during the heating process in air and a cut after the tests is given in figure 10. One can clearly see the helical heater core and the connectors at the left and right end. Both the heater and the instrumentation (thermocouple and/or MPP probe, cf. figure 29) can be moved using stepping motors.
First heating tests in air resulted in a linear heat flux rating of 70.6 W/cm that could be removed without damaging the heater. The heat flux that has to be generated and removed in Pb-Bi, is 357 W/cm at an electrical resistivity of 0.978 Ω/m. This will be demonstrated directly after the commissioning tests of the technology loop.
In order to prevent the thin sheath of the heater from corrosion attack, it will be thermally treated in the GESA facility, cf. Chapter 5.3.3. As described in Müller (2000) aluminium will be alloyed into the steel surface to increase corrosion protection.

a) thermohydraulic test section

b) oxygen control system (OCS)

c) high temperature cone valve

Figure 8: Picture of the technology loop with main components: .

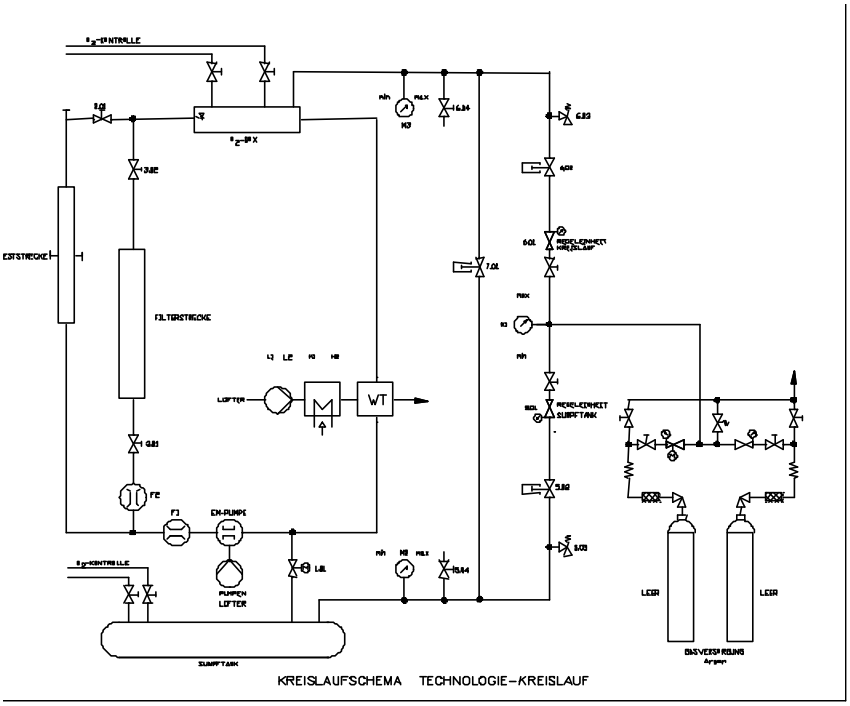

Figure 9: Piping and instrumentation scheme of the technology loop.

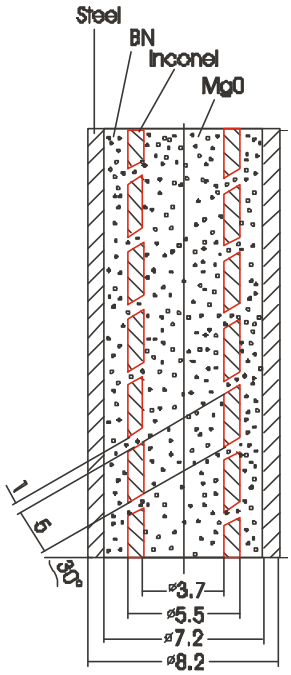

Table 9: High performance heater: dimensions and data.

Heater coil material:	Inconel
Heated length:	0.2 m
Electrical resistivity (cold):	384 mΩ / 0.2 m
Electrical resistivity (hot):	205 mΩ / 0.2 m
Current:	83 A
Voltage:	17 V
Specific power (in air):	70.6 W/cm
Surface temperature (in air):	1100°C

a) heated condition in air

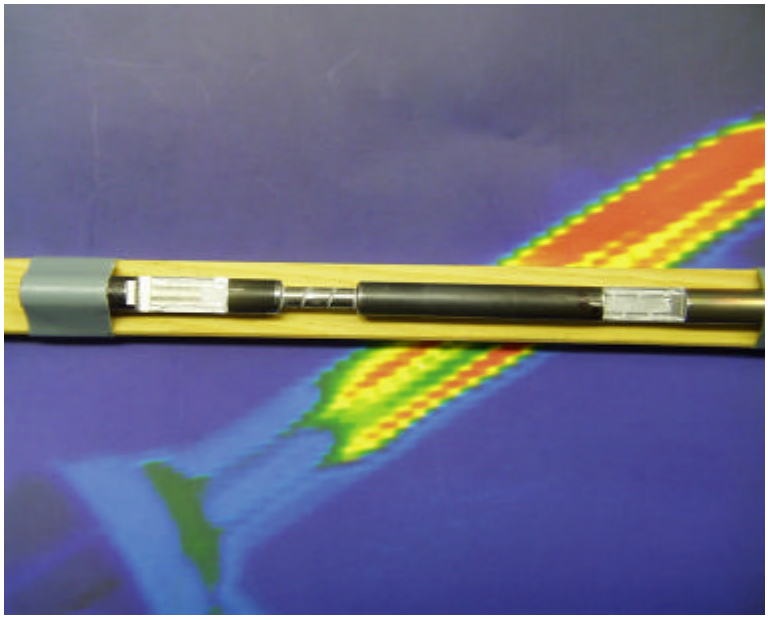

b) post-heated condition (cut)

Figure 10: High performance heater.

5.1.2 Thermalhydraulic Loop

The thermalhydraulic loop consists of

- mechanical immersion pump,
- test section positions (3 maximum),
- heat exchanger,
- cold trap,
- oxygen control system (OCS),
- expansion volume,
- gas system,
- sump tank.

The main data of the components is summarized in table 10. The piping and instrumentation scheme is given in figure 11. In position B8 a test section for a windowless target, having a falling free surface, is foreseen. This test section will be provided by SCK-CEN, Mol Belgium.

Table 10: Main data of components of thermalhydraulic loop.

Mechanical immersion pump: B5		**Cold trap: B7**	
Electr. Supply:	P(el) = 22 kW	Flow rate:	V_{CT} = 0.1 V_{tot}
Flow rate:	V_{tot} = 50 m³/h	Diameter:	450 mm
	at Δp = 5 bar	Height:	470 mm
Vessel diameter:	750 mm	Volume:	60 l
Vessel height:	1200 mm	Material:	steel meshing
Test sections: B2, B3, B9		**Oxygen control system (OCS): B6**	
Max vert. height:	3400 mm	Flow rate:	V_{OCS} = 0.1 V_{tot}
Rad. dimension:	variable	Height:	1300 mm
		Diameter:	750 mm
		Volume:	490 l
Heat exchanger: W1		**Expansion volume: B4**	
Pipes:	ϕ 13.5x1.6, n = 387	Height:	1300 mm
Height:	1490 mm	Diameter:	750 mm
Diameter:	1035 mm	Volume:	490 l
Sump tank: B1		**Gas system:**	
Diameter:	1100 mm	Gas:	Argon
Length:	6500 mm	Pressure:	1.2 bar
Volume:	5800 l	**Piping:**	
Inventory:	4000 l	DN 100 / DN 50 / DN 25	

5.1.3 Corrosion Loop

The corrosion loop is designed as an 8-shaped loop and consists of

- electromagnetic pump,
- heat exchanger,
- heater,
- oxygen control system (OCS),
- test sections (2 maximum),
- expansion volume,
- cold trap,
- gas system,
- sump tank.

The main data of the components is summarized in table 11. The piping and instrumentation scheme is given in figure 12.

Table 11: Main data of the components of the corrosion loop.

Electromagnetic pump: P1	**Cold trap:**
Voltage, current: 340 V, 480 A	Principle: magnetic trap
Channel: cross-section 160 x 16 mm²	**Heater: E1, E2**
Length 1255 mm	Power: 28 kW each
	Length: 1400 mm
Test sections: B5, B6	**Oxygen control system (OCS):**
Length: 450 to 500 mm	Position: horizontal
Inner diameter: ϕ 20 mm	Length: 1100 mm
	Diameter: 324 mm
Heat exchanger: W2	**Expansion volume: B2, B3**
Pipes: ϕ 12.0x2.0, n = 151	Not yet defined
Length: 1050 mm	
Diameter: 220 mm	
Height: 1300 mm	
Sump tank: B1	**Gas system:**
Diameter: 800 mm	Gas: Argon
Height: 1170 mm	Pressure: 1.2 bar
Volume: 320 l	**Piping:**
Inventory: 200 l	DN 25

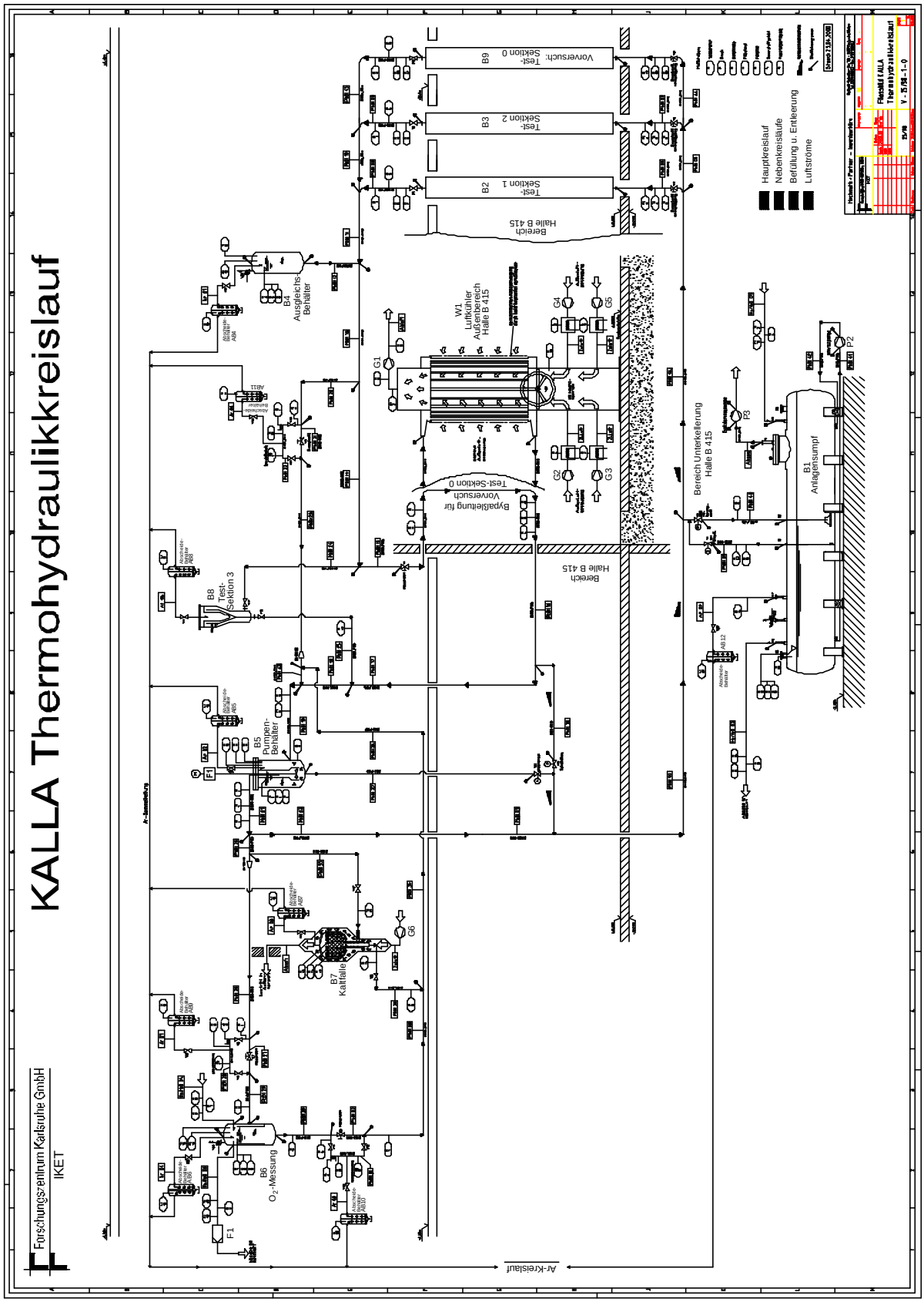

Figure 11: Piping and instrumentation scheme of the thermalhydraulic loop.

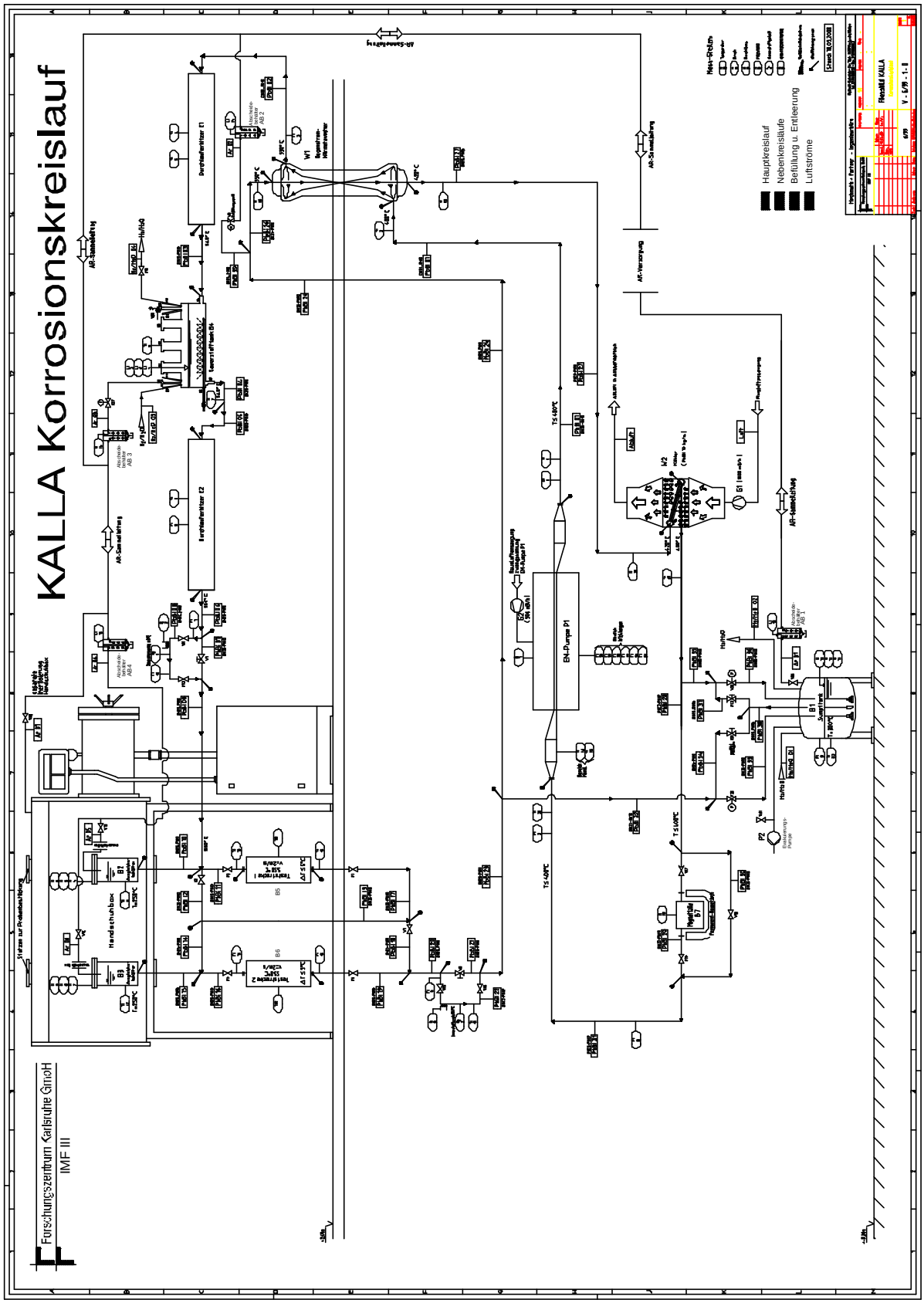

Figure 12: Piping and instrumentation scheme of the corrosion loop.

5.1.4 Automization Scheme

The automization scheme of KALLA, e.g. control and monitoring processes, safety instrumentation, data acquisition, is based on Siemens S5 technology and National Instruments BridgeView and LabView architecture. All data are logged on a server.

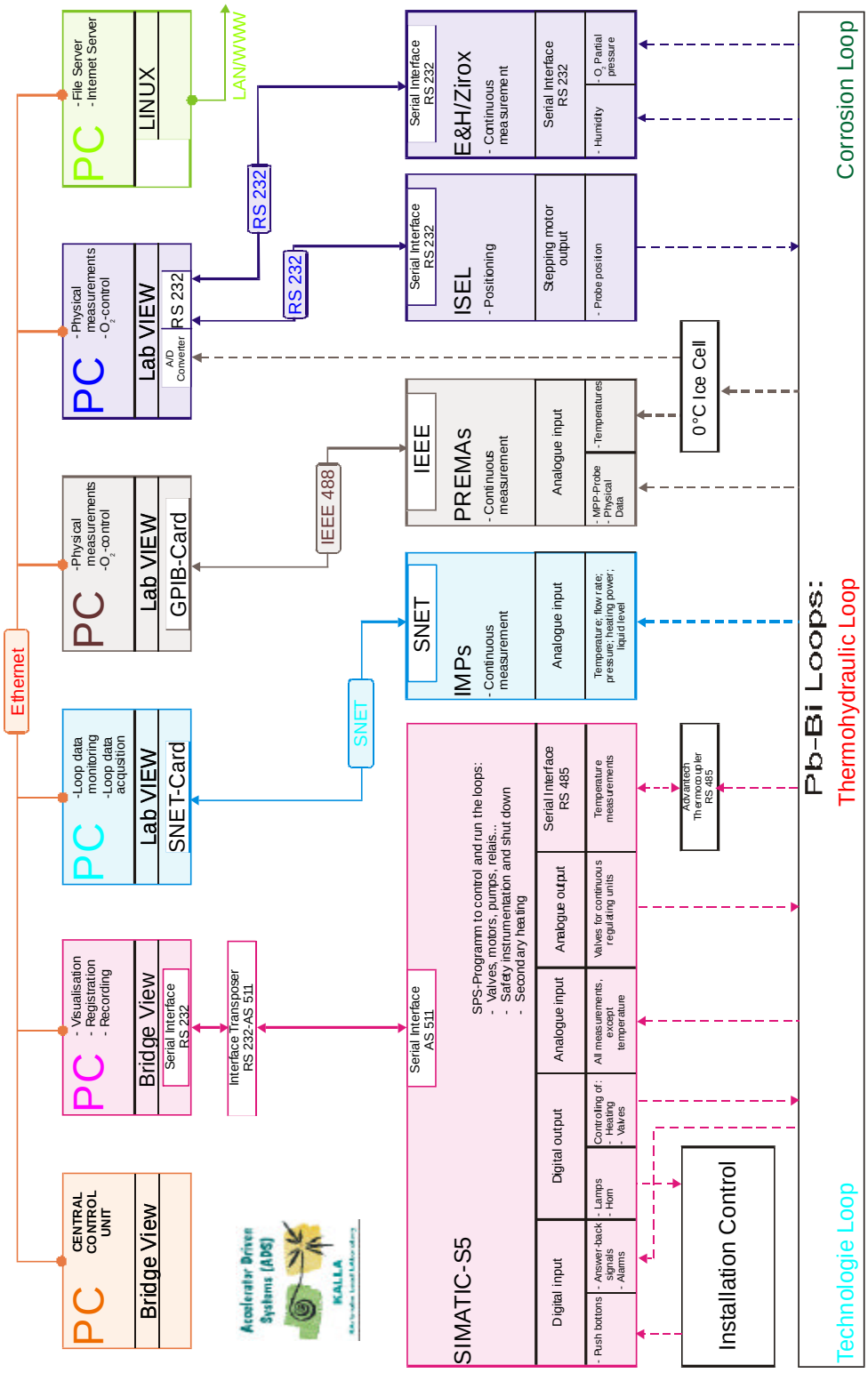

Figure 13: Automization scheme of KALLA.

5.2 Sub-Project SP1: Thermalhydraulic Investigations of Thermally Highly-Loaded Surfaces with Lead-Bismuth as Coolant

A three steps strategy has been proposed for the research activities accompanying the spallation target design. In the *first step* a numerical analysis is carried out with available CFD codes (CFX (CFX Int. Services (1995)), FIDAP (Fluid Dynamics International (1993)) and FLUTAN (Willerding and Baumann (1996)), to provide the first knowledge about the thermalhydraulic behaviour in a target. In the *second step* model experiments are performed, to provide informations for the spallation target design and to provide an experimental data base for model development and code validation. It is well agreed that at the present stage where a large deficiency in practical Pb-Bi experience exists, experimental investigations with a model fluid, e.g. water, are recommended. Such a model experiment enables a systematical study into the physical phenomena involved and much more sophisticated measurement techniques than is the case with the prototypical fluid. To this purpose the HYTAS test facility has been set up at IKET with water as the working fluid. However, the results obtained in a model experiment can not be directly transferred to the prototype, as far as heat transfer is concerned. Therefore, as the *third step* experimental studies in liquid Pb-Bi will be untertaken for the final design of a beam window and a spallation target.

5.2.1 Work Package WP1: Design of a Beam Window Based on Numerical Simulations and Model Experiments with Water as Fluid

5.2.1.1 Experimental Apparatus

HYTAS Test Facility:

Figure 14 shows schematically the HYTAS test facility. The water loop is capable of circulating a maximun volumetric flow rate of 100 m^3/h with a maximum pressure drop of 0.4 MPa. Test sections with a length of up to 3.5 m can be integrated in the test facility.

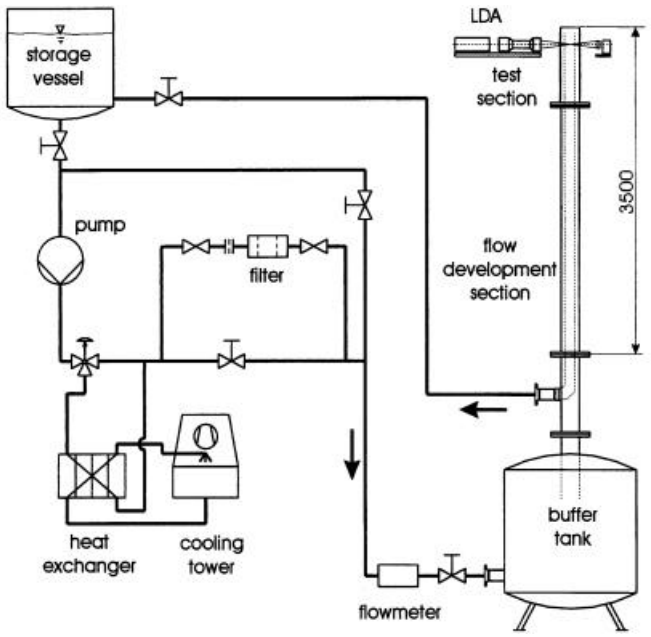

Figure 14: The HYTAS test facility at IKET, sketch.

The main purpose of the HYTAS experiment is to study the hydraulic behaviour in a spallation target. It is well known that the hydraulic behaviour can be exactly simulated in the model experiment, if the Reynolds number in both the prototype (liquid metal flow) and the model experiment (water flow) is identical, Ishii and Kataoka (1984), Knebel (1993).

Test Sections:

During the time period of this report experiments have been carried out for the ISTC 559 target. More details about the ISTC 559 project can be found in Takizuka (1998) and Cheng et al. (1999). The main technical data of the target are summarized in table :

Table 12: Main technical data of the ISTC 559 target.

• proton-energy:	0.8 GeV	• target material & coolant:	Pb-Bi
• beam current:	1.25 mA	• window material:	steel
• beam power:	1.0 MW	• coolant flow rate:	15 m³/h
• beam diameter:	6.5 cm	• coolant inlet temperature:	220°C
• window thickness:	1.0 – 1.5 mm	• perforated plate:	yes

The design of the active part (beam window and spallation area) is one of the main tasks in the target design. For the ISTC 559 different designs have been proposed. Figures 15 and 16 show schematically two examples. The first one (figure 15) has a semi-spheric window surface, the diameter being 110 mm. The active part consists of two coaxial cylinders with inner diameters of 130 mm and 185 mm, respectively. The coolant flows into the annular gap between the cylinders, makes a U-turn at the top, cools the window surface, and then exits the active part via the central cylinder. To reduce the flow stagnation zone near the window center, a perforated plate made of steel with distributed holes is installed near the window. The porosity is highest on the centerline and decreases with increasing distance from the center. In this way, the coolant flow and the heat transfer near the window center will significantly be enhanced.
The second design (figure 16) is similar to the first one and consists of two coaxial cylinders with the same diameter as the first proposal. The beam window is a surface of two different curvature radii, i.e. 80 mm for the center part and 37 mm for the outer part. The main advantage of the second proposal is the short height of the beam window and the U-turn part. For both proposals the window thickness is about 1.0 - 1.5 mm. The location of the perforated plate, the size and the distribution of the holes on the plate should be optimized referring to the thermalhydraulic performance. The experimental studies at the HYTAS test facility concentrated on the first design proposal (figure 15).
Two different test sections were designed and used in the experiments: a 2-D and a 3-D test section. The 2-D test section, shown in figure 17, is made of a 130×128 mm rectangular central channel, with the beam window mounted near the top, and two 130×25 mm peripheral rectangular channels at each side. The total height of the 2-D test section is 860 mm. Although the 2-D test section is not geometrically similar to the prototypic target, it is useful for a qualitative visualization and understanding of the fundamental flow behavior and for pointing out critical issues, e.g. stagnation point, flow recirculation, flow separation. These issues might deteriorate the cooling of the beam window.

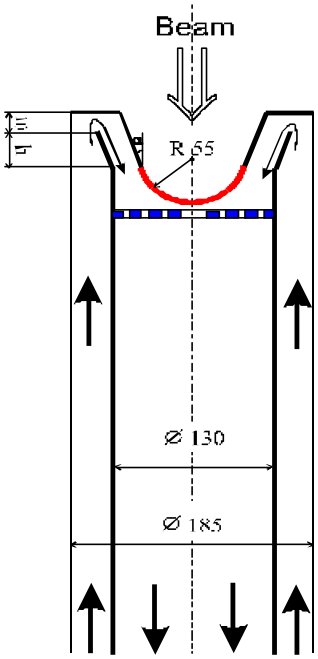

Figure 15: ISTC target design: proposal I.

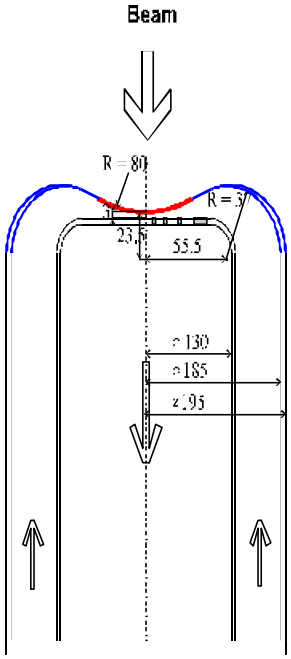

Figure 16: ISTC target design: proposal II.

The 3-D test section, shown in figure 18, is geometrically similar to the first design proposal. It is made of a square channel 200×200 mm. It has a central circular channel, 130 mm of I.D., with the beam window mounted near the top, and peripheral channels 25 mm wide surrounding the central channel. The total height of the test section is the same as that of the 2-D test section (860 mm).
For both test sections, the flow can be bi-directional, i.e. either flowing upwards through the peripheral channels and downwards through the central channel, or upwards through the central channel and downwards through the peripheral channels. This is done by exchanging the connector between the outlet of buffer tank and the flow development section.

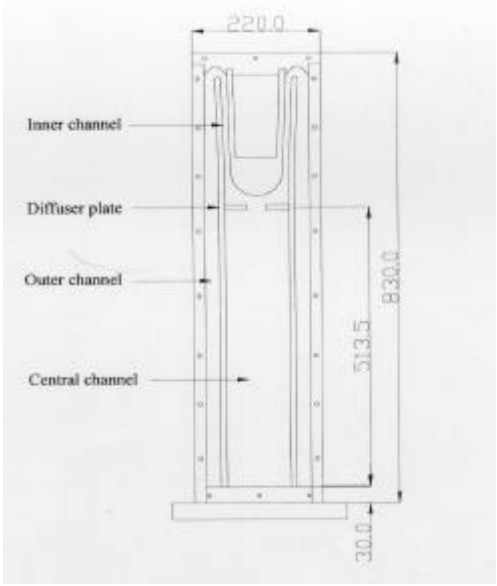

Figure 17: The 2-D test section.

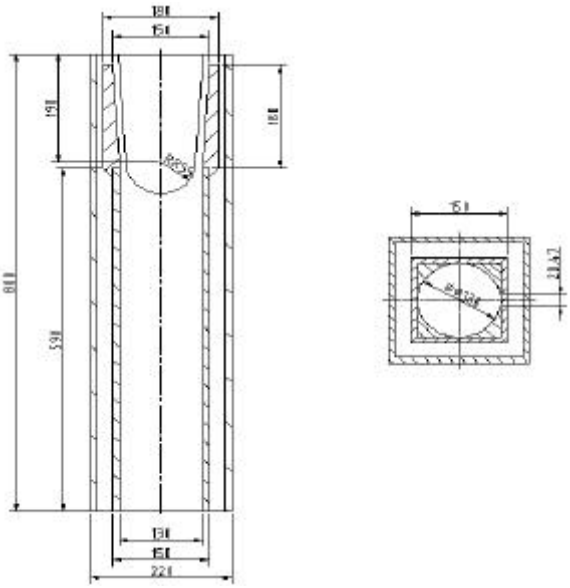

Figure 18: The 3-D test section.

Measurement Techniques:

The flow behaviour around the beam window was visualized for both test sections by using the laser light sheet technique, indicated in figure 19. Polystyrene spherical particles of 0.5 mm in diameter were added to the loop via the water storage tank. The states of fluid flow in the test section were revealed by the paths of the tracer particles, and filmed by both a Sony video camera and a KAPPA CCD camera which offers a real-time digitization and image display with a resolution of up to 768 $\times$ 576.

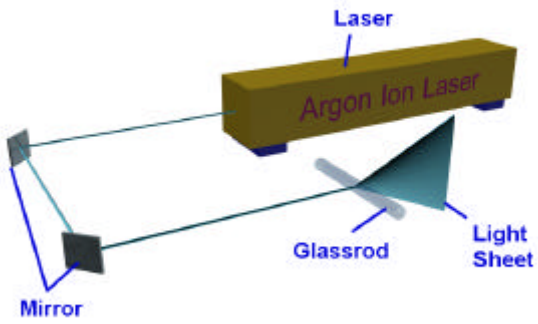

Figure 19: Laser light sheet technique.

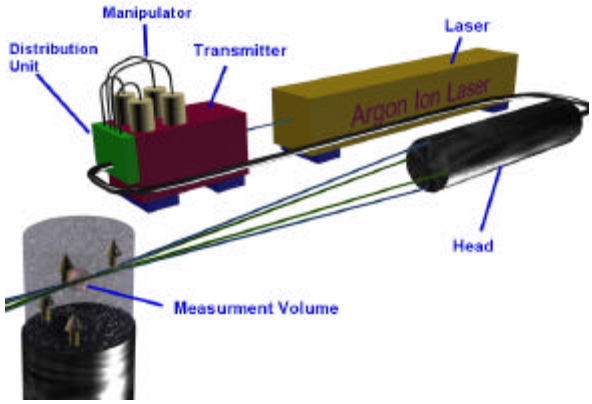

Figure 20: 2-D LDA system.

The local velocities were measured with a 2-D Laser-Doppler Anemometer (LDA), as indicated in figure 20. The traversing system that controls the 2-D movement of the probe, is controlled using the software MEMESS, Lefhalm et al. (1998). Due to the refractive index difference between air and water, changes in the position of the measurement volume occur. The displacement of the measurement volume was computed using the law of refraction in conjunction with the geometrical relationships:

$$dx_1 = dx_0 \tan a_1 \cot\left[\arcsin\left(\frac{n_1}{n_5}\sin a_1\right)\right] \quad . \tag{1}$$

The explanation of the letters in equation (1) is indicated in figure 21.

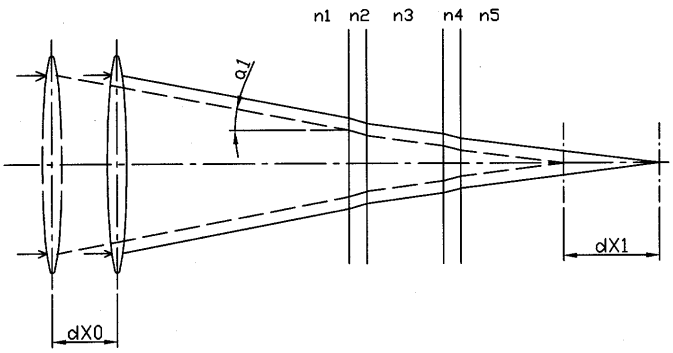

Figure 21: Displacement of the measurement volume in the fluid.

5.2.1.2 RESULTS

Flow Visualization in the 2-D Test Section:

Figure 22 shows the streamline pattern around the beam window of the 2-D test section for water flowing upwards through the central channel. The water flows upwards in the central channel, diverges in the vicinity of the beam window, and is carried to both sides. In the laser light sheet a zero velocity point, which is consequently known as the flow stagnation point, could be seen at the central surface of the beam window.

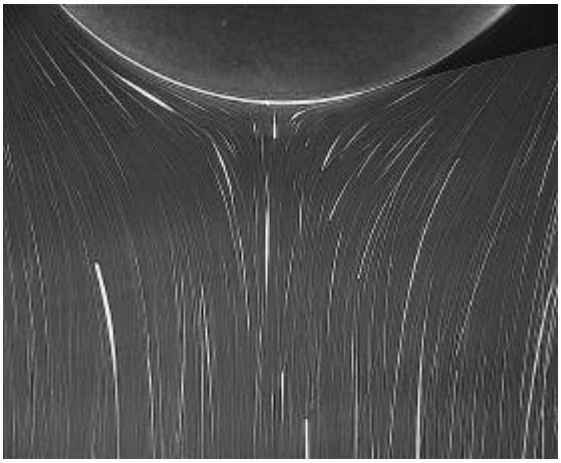

Figure 22: Flow pattern near the beam window for upward flow.

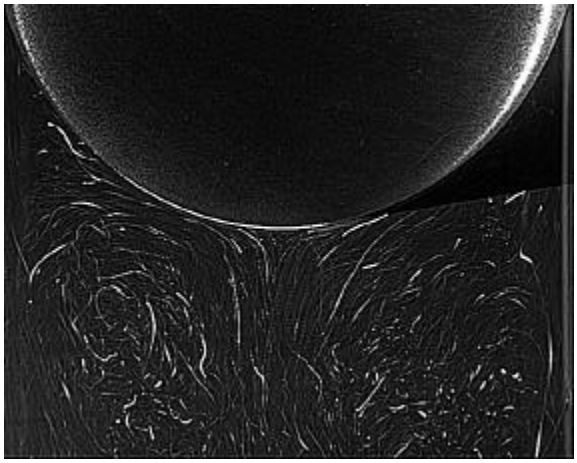

Figure 23: Flow pattern near the beam window for downward flow.

Figure 23 shows an example of the flow pattern around the beam window for water flowing downwards through the central channel. It can be seen that the flow pattern in a downward flow is much more complicated than in an upward flow. The water flows nearly vertically downwards along the wall after entering the central channel from the top. The flow separates from the beam window surface. After travelling a certain distance downstream from the window, some amount of water reverses its direction and flows upwards in the central region of the central channel towards the stagnation point. It follows the window profile and, then, is carried down the central channel again, entraining into the faster outer downward flow. Two large vortices (recirculation zones) are symmetrically formed downstream of the beam window.

Figure 24 shows the general flow patterns which were sketched according to the flow visualization for water flowing downwards through the central channel of the 2-D test section.

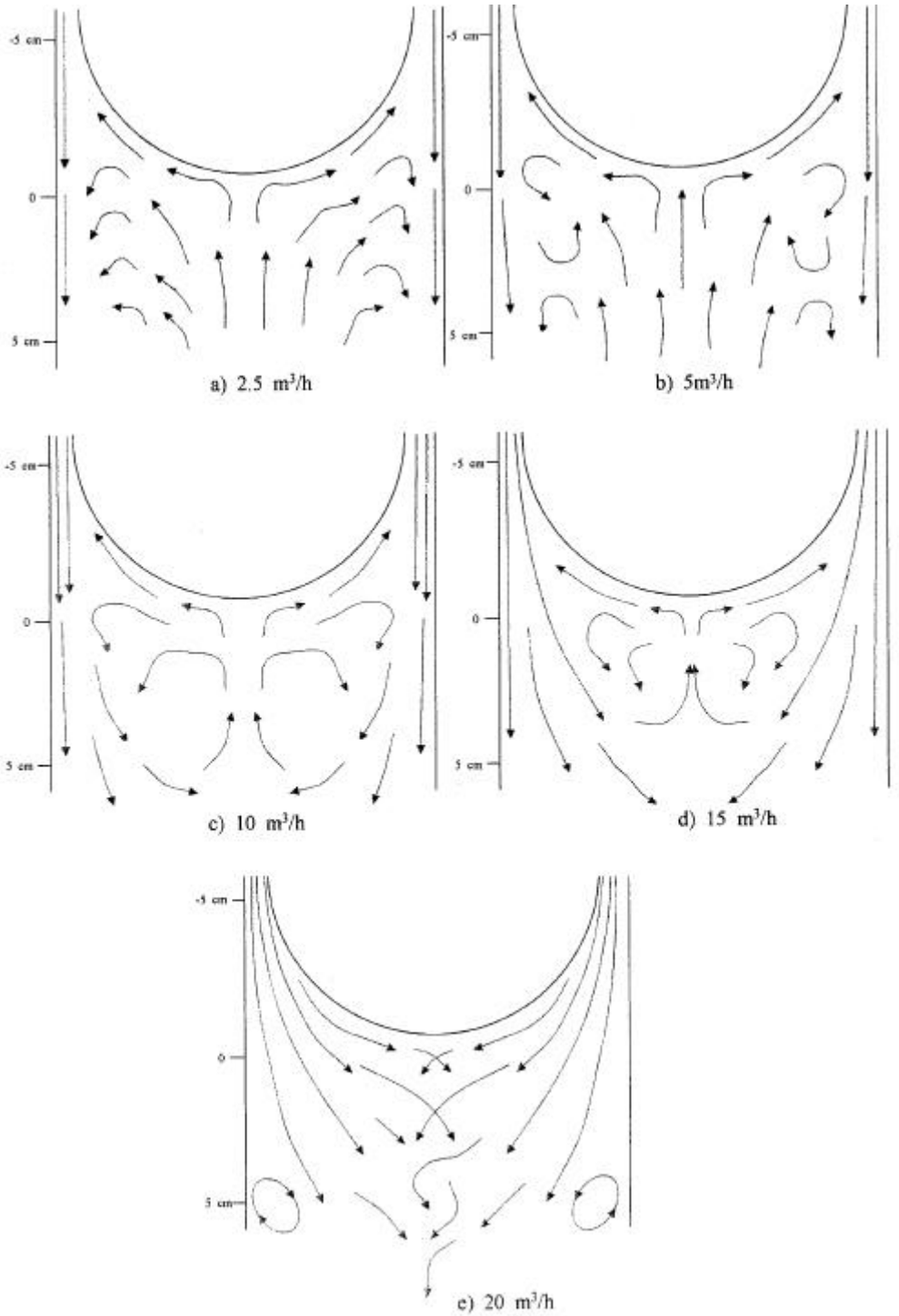

Figure 24: Flow patterns for a downward flow around the beam window at different volumetric flow rates.

Velocity Measurements in the 3-D Test Section:

Velocity measurements were made in the 3-D test section. To present the results, a coordinate system is chosen, the origin of which is located on the center of the window surface. The x-axis is in the horizontal direction. The positive y-axis is in (vertical) upward direction. Figure 25 shows the velocity distribution along the x-axis on the x-y plane at different y-elevations for water flowing downwards through the central channel at a volumetric flow rate of 10 m^3/h. The velocity u is positive in

positive y-direction. As expected, the plotted data show two distinct flow regions below the beam window: the downward flow close to the wall and the upward flow in the central region of the channel. A fast downward flow can be seen at x≈ 60 mm. Fluid flowing in the central region turns its flow direction from upward to downward at a certain distance below the window. Below y = -150 mm, the flow is fully developed, and the velocity distribution is relatively flat except for the boundary region near the wall. At y = 10 mm, the velocity is positive near the surface of window, indicating that above y = 0 mm the upward flow follows the profile of the beam window. Qualitatively, the velocity measurements show a good agreement with the flow visualizations.

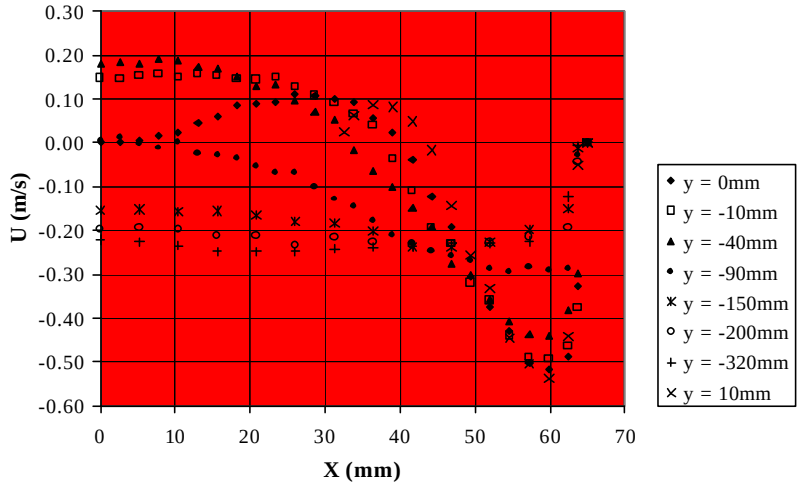

Figure 25: Velocity distribution for downward flow.

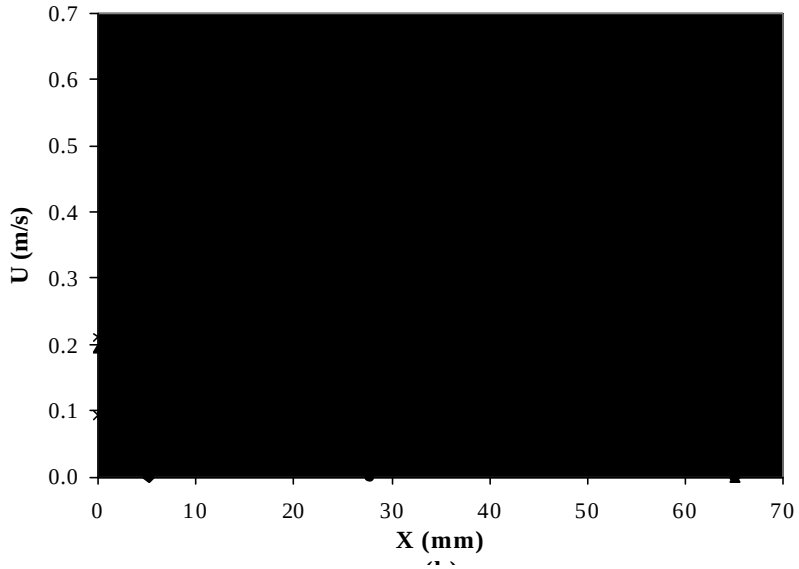

Figure 26: Velocity distribution for upward flow.

Figure 26 shows the velocity distributions along the x-axis on the x-y plane at different y-elevations for water flowing upwards through the central channel at a volumetric flow rate of 10 m^3/h. As seen, below y = -50 mm, the velocity field is fully developed in the channel. Due to the reduction of flow area above y = 0 mm, the fluid slows down in the central region and accelerates near the wall as it approaches the bottom-center of the window. For y = 10 mm, the velocity reaches a maximum at x ≈ 62.3 mm.

5.2.1.3 Comparison Experiment / Calculations

For the numerical calculations the CFD codes FIDAP and CFX-4.3 have been applied. For turbulence modelling, the standard *k-e* model with wall functions has been used. Special attention has been paid to the mesh size near the walls, so that the first mesh will fulfil the condition:

$$30 \leq y^{+} \leq 300 \quad . \tag{2}$$

Figure 27 compares the measured velocity distribution with the numerical results for the downward flow at a volumetric flow rate of 10 m³/h. A good agreement is obtained between the numerical results and the experimental data. The flow recirculation zone downstream of the beam window and the separation of the boundary from the window surface can be well reproduced by the codes.

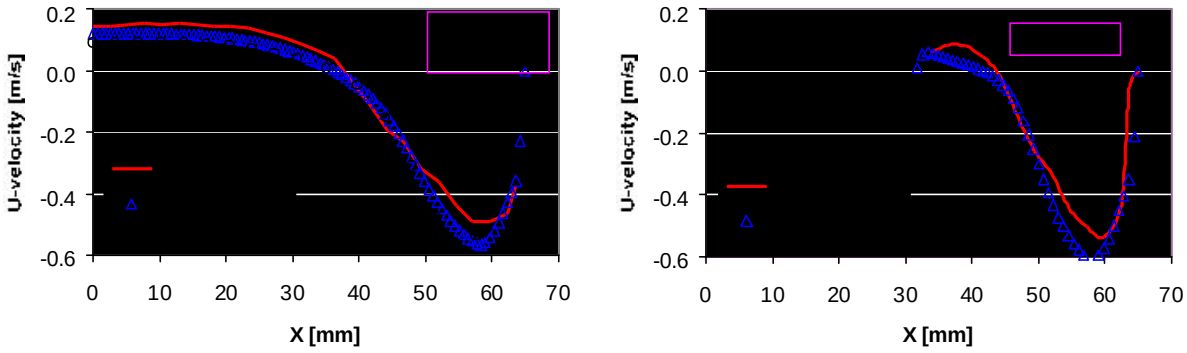

(a) y = -10 mm (b) y = +10 mm

Figure 27: Velocity distribution for downward flow:
comparison of numerical results with experimental data.

5.2.1.4 Conclusions

In the HYTAS test facility both qualitative measurements (Laser light sheet) and quantitative measurements (Laser Doppler Anemometry) can be performed to investigate the flow field of small to medium scale test inserts, e.g. beam window, with water as model fluid. Experimental results were achieved for the beam window of the ISTC 559 Project, doing various parameter variations. The experiments were simulated using the two CFD codes CFX and FIDAP. A good agreement between experiment and calculation could be achieved.

5.2.2 Work Package WP2: Fundamental Experiments in Liquid Lead-Bismuth on Heat Transfer and Model Development / Model Validation

5.2.2.1 Experiments in Lead-Bismuth

In the technology loop an experiment to fundamentally study heat transfer and turbulence quantities along a heated cylinder is being designed, figure 29. The pipe diameter is D = 60 mm, the heater diameter is d = 8.2 mm, the maximum power is 357 W/cm. The heater diameter corresponds with the fuel pin diameter of the Three-Beam Concept of an ADS proposed in Knebel et al. (1999).
As a heater either the heater rod described in figure 10 or a cylinder equipped with CHETSS (Cylindrical Heat Emitting Temperature Sensing Surface) can be applied, figure 28. The CHETSS are developped in cooperation with the University of Riga, Latvia, Platnieks et al. (1998). A HETSS module consists of many temperature-sensitive resistors (minimum surface area 5 x 5 mm^2) which are adapted to high temperatures. Parallel to the temperature measurement over one module, a defined heat flux can be released by the resistors. Knowing the heat flux and the temperatures of both the wall (HETSS module) and the bulk fluid, the heat transfer coefficient can be determined.
The following measurement techniques are planned to be applied:

- Thermocouples (temperature),
- Miniature Permanentmagnet Flowmeter Probes (velocity), Knebel et al. (1998),
- Heat Emitting Temperature Sensors (heat flux),
- Ultrasonic Measurement Technique (velocity), Takeda and Kikura (1997).

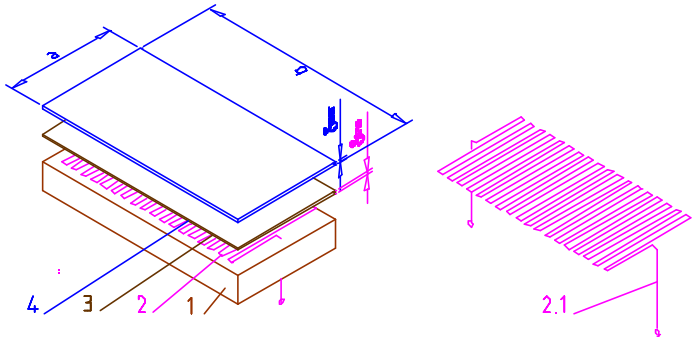

Figure 28: Scheme of HETSS:
1 – substrate,
2 – heater-sensor,
2.1 – current leads,
3 – electrical insulation,
4 – stainless steel screen,
(private communication
S. Dementjev, Riga).

The heater and the probes / sensors can be traversed in x and r direction, respectively, using stepping motors. Experiments are scheduled for 2000.

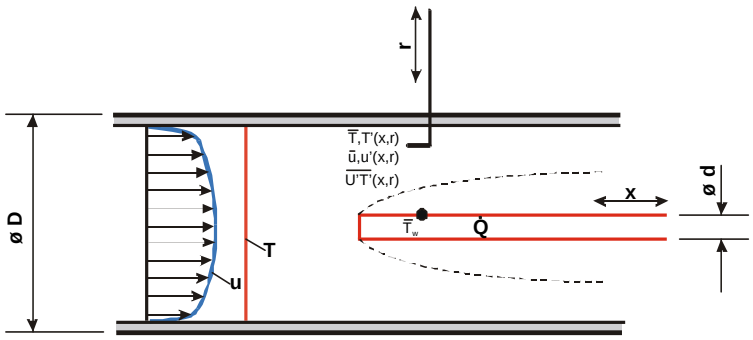

Figure 29: Model experiment on heat transfer and turbulence in Technology Loop.

5.2.2.2 Turbulence Modeling in the FLUTAN-Computer Code and Related Direct Numerical Simulations

Introduction:

The numerical simulation of turbulent flow fields with heat transfer in complex geometries is an important prerequisite in order to design, in a first step, a beam window and, in a second step, a spallation model. Having a liquid metal such as lead-bismuth with a low molecular Prandtl number requires additional modelling and validation efforts, as for turbulence, wall functions, free surface phenomena, two-phase flow. In chapter 5.2.1 two commercial CFD codes, CFX and FIDAP, were applied to model a beam window water experiment. Here, the capabilities and some applicabilities of the code FLUTAN, developped and validated at Forschungszentrum (Willerding and Baumann (1996), will be discussed.

Turbulence Modelling Approach:

The temperatures in the structures of a spallation target will reach critical values at the beam window. To determine these structure temperatures accurate turbulence models are required to predict the temperatures in the cooling fluid. Standard turbulence models, which are used in commercial codes, are not suitable for the proper simulation of heavy liquid metal flows: the models using a turbulent Prandtl number to describe the turbulent heat transport assume the Reynolds analogy between the turbulent transport of momentum and heat. This assumption is not valid for liquid metals because the momentum field is mainly turbulence dominated and has only thin wall layers dominated by molecular viscous forces, whereas the temperature field is less turbulence dominated and has thick wall layers governed by molecular conduction. Liquid metals are characterised by a small molecular Prandtl number.

The turbulence models having a distinct description of the turbulent heat transport contain many parameters. Their values, which are determined through both dimensional and empirical analysis, depend on the type of fluid and on the type of flow. Standard values of these parameters are available for common fluids like gases and water but not for Heavy Liquid Metals (HLMs). Moreover, new model relationships are necessary to extend the validity of the modeled equations to low Peclet-numbers. Preliminary benchmarks on experiments using liquid metals show that the turbulent parameters contained in CFD codes could be unsuitable for liquid metals, Baumann et al. (1997). Therefore, measurements of the turbulent quantities in liquid metal flows are needed in order to validate the turbulence models, cf. figure 29. And, as a data base coming from liquid metal experiments does usually not give results on turbulent velocity fluctuations and cross correlations between velocity and temperature fluctuations which are sufficiently detailed for turbulence model development, but of course for validation purposes, additional direct numerical simulation data are required to extend the models in an adequate manner and to 'tune' the new parameters.

The TMBF Model:

At Forschungszentrum Karlsruhe, a Turbulence Model for Buoyant Flows (TMBF) has been developed, Carteciano et al. (1997). The TMBF is a combination of a first-order 2-equation model for the turbulent transport of momentum and of a second-order 5-equation model for the turbulent transport of heat. Thus, the turbulent stresses are calculated assuming an isotropic eddy viscosity and solving the

transport equations for turbulent kinetic energy k and for its dissipation rate ε. The three turbulent heat fluxes $\overline{U_i'T'}$ are determined by means of the corresponding transport equations. Moreover, transport equations for the variance of temperature $\overline{T'^2}$ and its dissipation rate ε_T are used in the description of the turbulent transport of heat.

The TMBF does not introduce six additional transport equations for the turbulent stresses and thus differs from the so-called Reynolds stress model. However, the calculated turbulent stresses and heat fluxes are no longer related through a fixed turbulent Prandtl number σ_t. The TMBF represents a compromise between the classical k-ε-σ_t model and a full Reynolds stress model, but it is clearly an improvement of the k-ε-σ_t model for turbulent flows where the turbulent transport of heat is complex, such as for buoyant flows, and the Reynolds analogy is not valid, such as for liquid metals. The TMBF has been implemented in the FLUTAN computer code, Willerding and Baumann (1996), and it has been validated by means of experimental data from turbulent flows in forced, mixed and natural convection. The numerical results obtained by using the TMBF show that stratified flows and buoyancy effects in mixed convection are well predicted. They cannot be adequately calculated by means of the k-ε-σ_t model.

New model relationships for the buoyancy term $P_{eb} = 2nbg_i\Psi_i$ of the ε equation and for the dissipation term $e_{U_i'T'} = (n+k)\Psi_i$ of the turbulent heat flux equations ($\Psi_i = \overline{(\partial T'/\partial x_l)(\partial U_i'/\partial x_l)}$) were developed by means of an analytical method using the two-point correlation technique, Wörner et al. (1999). The models were calibrated using a Direct Numerical Simulation (DNS) data base, Wörner and Grötzbach (1997), for different buoyant flows in several fluids and introduced in the TMBF in order to extend the validity of the TMBF to very low Peclet number flows, see table 13. This extended model was already validated in natural convection for the case of a buoyant air flow along a vertical heated wall, Carteciano et al. (1999). The calculation with the new model relationships agrees very good with the measured values, Tsuji and Nagano (1988), of the mean velocity and temperature (see figures 30 and 31). The extended model represents an improvement of the old version of the TMBF for 2D natural convection flows in air.

Table 13: Earlier, Carteciano et al. (1997), and new modelling in TMBF for P_{eb} and $e_{U_i'T'}$.

Term	Old Modelling	New Modelling
P_{eb}	$\frac{e}{k}c_{e1}(P_k+G_k)(1+c_{e3}Ri_f)$	$-\frac{1}{2}nbg_i\frac{\partial^2\overline{U_i'T'}}{\partial x_i^2}+\frac{e}{k}\left(c_{e1}P_k+\left(\frac{\mathrm{Pr}}{R}\right)^{0,7}G_k\right)$
$e_{U_i'T'}$	$-\frac{1+\mathrm{Pr}}{2\sqrt{\mathrm{Pr}}\sqrt{R}}\left(\frac{e}{k}\right)\exp(-c_{T5}(\mathrm{Re}_t+Pe_t))\overline{U'_i\,T'}$	$\frac{n+k}{4}\frac{\partial^2\overline{U_i'T'}}{\partial x_i^2}-\frac{1}{2}\left(1+\frac{1}{\mathrm{Pr}}\right)\left(\frac{\mathrm{Pr}}{R}\right)^{0,7}\left(\frac{e}{k}\right)\overline{U'_i\,T'}$
$c_{\varepsilon1}$, $c_{\varepsilon3}$, c_{T5} empirical coefficients, g_i gravitational acceleration, G_k buoyancy production of k, P_k production of k, Pe_t turbulent Peclet-number, Pr molecular Prandtl-number, R turbulent time-scale ratio, Re_t turbulent Reynolds-number, Ri_f flux Richardson number, ν molecular viscosity, κ molecular heat diffusivity.		

The TMBF is potentially suitable for simulations of the turbulent momentum and heat transport in light liquid metals, because the Reynolds analogy is not assumed and new model relationships, which contain numerical functions depending on the molecular Prandtl-number, are introduced. However, it has to be investigated which terms may require further improvements or adaptations and the model has to be validated with fundamental experiments in liquid lead-bismuth in order to test the new model relationships which extend the range of the TMBF to low Peclet-numbers. The new coefficients, which are introduced by these relationships, must be tuned by using experimental and Direct Numerical Simulation data.

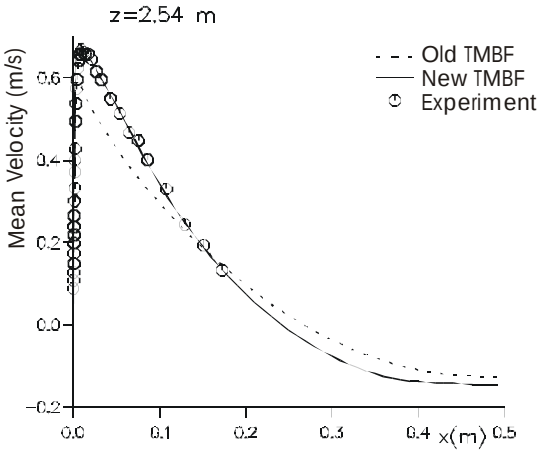

Figure 30: Radial profiles of mean velocity.

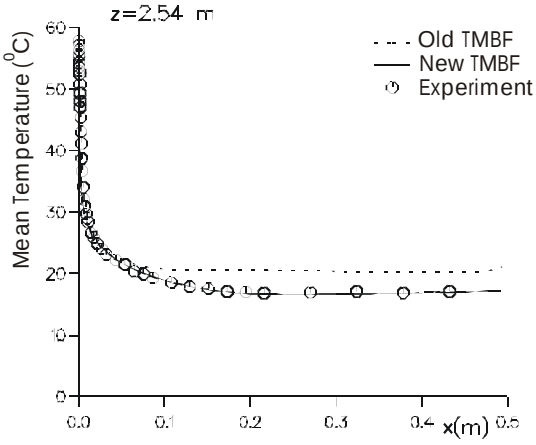

Figure 31: Radial profiles of mean temperature.

DNS of Turbulent Convection Flow:

Several years ago the existing DNS data base for light liquid metals like sodium with Prandtl numbers around 0.006 was extended with the TURBIT code for fluids with Prandtl numbers of around 0.02, Bunk and Wörner (1998). All those older DNS data do not reach sufficiently high Rayleigh numbers, so that turbulent heat transfer becomes dominant. E.g., in the Nusselt-Rayleigh-number domain the simulation results for the Nusselt number show, that all cases which could be run in the past were still in the conductive to turbulent convective heat transfer transition range and did not really reach the logarithmic convective range, figure 32. The reason is, that these simulations have much stronger requirements for spatial discretisations than simulations for fluids with Prandtl numbers around one. Meanwhile much faster and larger computer systems became available. Thus, it is now possible to extend the data base for the fluids which are here of interest to somewhat larger Rayleigh numbers.

The previous direct numerical simulations of Rayleigh-Bénard convection (RBC) were performed for mercury which has about the same molecular Prandtl number of 0.02 as lead-bismuth. The highest Rayleigh number considered was Ra = 50,000. This simulation - as well as the other ones at lower Rayleigh numbers - was performed with periodic boundary conditions in both horizontal directions to mimic an infinitely extended horizontal plane channel. The periodicity lengths $X_{1,2}$ used in both directions are eight. I.e., the horizontal size of the computational domain is eight times the distance between both horizontal walls. The horizontal channel extension has to be chosen large enough so that no large scale energy containing vortices are hindered or truncated by the finite size of the computational domain. For Rayleigh-Bénard convection in air it is known that with increasing Rayleigh number the

macroscopic length scale of the convective pattern is also increasing. For mercury, reliable experimental information about the Rayleigh number dependence of the macroscopic length scale is not available.

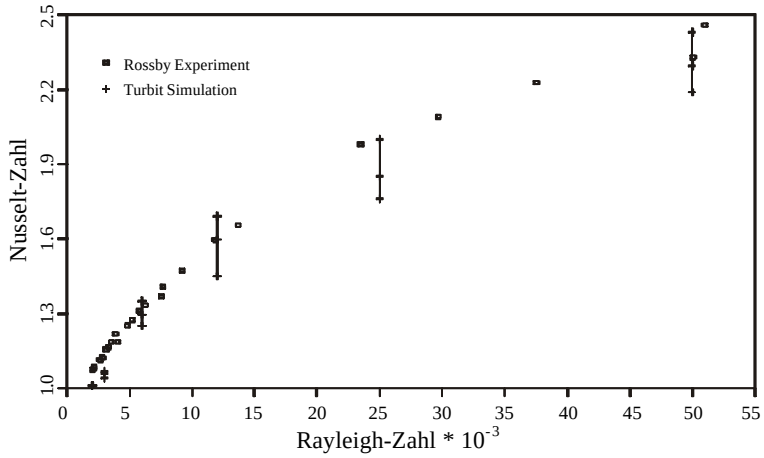

Figure 32: Nusselt numbers calculated from the existing DNS data base for mercury, Pr=0.02, compared to experimental results by Rossby (1969)

To support the definition of adequate periodicity lengths for a simulation with Ra = 100,000, here an additional simulation of RBC in mercury at Ra = 50,000 with periodicity lengths $X_{1,2}$ = 10.24 was performed. Although the size of the domain is increased by about 64% as compared to the simulation with $X_{1,2}$ = 8, the analysis of the results shows that the convection patterns as well as typical statistical data are unchanged. This is an indication that $X_{1,2}$ = 8 is sufficiently large.
Based on this finding, a simulation for Rayleigh-Bénard convection in mercury with Ra = 100,000 and $X_{1,2}$ = 8 was started on the VPP 300 supercomputer at Forschungszentrum Karlsruhe. The results of the final time level of the simulation with Ra = 50,000 and $X_{1,2}$ = 8 are used as initial data. These initial data were interpolated to the new finer grid which consists of 400x400x75 = 1.2x10^7 mesh cells. This was found to be really at the manageable limit of a single processor on the VPP 300 hardware. Nevertheless, a first inspection of the energy spectra showed that the grid may not be sufficiently fine to resolve the smallest scales in the velocity field. A continuation of the simulation run has been postponed, but will now be taken up again as the more powerful VPP 5000 hardware became available just recently. After some tests with the TURBIT code on this new hardware, the simulation will thus be continued on an even finer grid and the results will be used to test and improve models for closure terms in the heat transfer part of the TMBF.
The final validation of the new extended and adapted TMBF model will be performed using the detailed measurement from the heat transfer and turbulence experiments that will be performed in the technology loop of KALLA, see figure 9.

Conclusions:

The TMBF turbulence model in FLUTAN was extended and validated for mixed and buoyant convection of fluids with Prandtl numbers of around one. The required adaptation to heavy liquid metals needs further turbulence data which will come from direct numerical simulations and from detailed KALLA experiments. Starting from an already existing data base with direct numerical simulation data for Rayleigh-Bénard convection in heavy liquid metals at lower Rayleigh numbers, a new simulation was prepared and performed for a higher Rayleigh number. First evaluations of the results indicate, that this simulation has to be continued on a finer grid so that sufficiently reliable data are achieved to adapt the statistical turbulence models in FLUTAN for lead-bismuth.

5.2.3 Work Package WP3: Simulation Experiments for the Optimized Beam Window in Lead-Bismuth and Numerical Simulation

5.2.3.1 Numerical Simulations for the COULI Benchmark

Investigated Target Geometry:

In order to define an optimized target geometry, a reference geometry was specified for a first benchmark investigation in advance of experiments in a water loop at CEA Grenoble. The intention was to clarify whether the specified geometry is free of any areas with detached and recirculating flows, and to learn about the quality and reliability of the available turbulence models and CFD codes. Thus, calculations were also performed with the FLUTAN code, Willerding and Baumann (1996), for this COULI-benchmark. This benchmark uses an isothermal flow in an ADS target geometry which will later also be experimentally simulated in the KALLA experiments.

A target geometry was proposed for the benchmark calculations (figure 33). Two cases, one for a small (2x104) , and one for a realistically high Reynolds number (9x105) were given. The water temperature is 60°C. The funnel length must be set to $h_2 = 14\ D_f = 1.4286$ m ($D_f = 0.1$ m is the funnel diameter) in order to achieve a fully developed flow at the inlet of the connector.
The calculations with the computer code FLUTAN were performed with a 2D numerical grid. The mesh size was uniform ($\Delta x = \Delta z = 0.71$ mm) in the connector area. A coarser grid size was used in the vertical direction for the funnel ($\Delta z = 7.1$ mm) and for the riser ($\Delta z = 3.6$ mm). The total length of the geometry, which was simulated with 55,929 cells in cylindrical coordinates, was 2.176 m including funnel and riser.

Modelling Approach:

The standard k-ε turbulence model was used. The system of the momentum equations and turbulence equations was solved using iterative solvers, respectively CRESOR and SOR. A very low value for the convergence criterion parameter was chosen: $\varepsilon_3 = 10^{-7}$. The steady state is reached when the change of each velocity component from one time step to the next one divided by the maximum velocity magnitude in the entire field is less than ε_3. The calculations were performed with a first order upwind discretisation method of the convective terms for the momentum and turbulence quantities equations. A first order time discretisation was used with a time step width of $\Delta t = 0.1$s.

Numerical Results:

The numerical results for the high Reynolds number case are presented here. Similar results were obtained for the case with the lower Reynolds number. The calculated modulus of the velocity vector in the plotting plane, normalized by the inlet velocity into the funnel, is given in figure 34. The FLUTAN calculations simulate very low velocity values with a clear flow detachment at the inner wall downstream of the beam window.
Calculations with discretisation methods of second order like QUICK and LECUSSO for the momentum equations were likewise performed with the same numerical grid again for the higher Reynolds number. Using the QUICK method, a very low value of

the time step must be used, $\Delta t = 0.0002$. Otherwise, wrong results could be obtained. The comparison of the fields of the modulus of velocity between three calculations using first order Upwind, QUICK, and LECUSSO shows that the extension of the detached flow depends also on the discretisation scheme (figures 34 to 36). The size of the recirculation zones increases in going from first to second order schemes. However, a qualitative influence from the discretisation method on the occurrence and size of the recirculation zone can only be avoided when adequate iteration parameters are used. This means, all three fully converged calculations show a flow detachment at the inner wall.

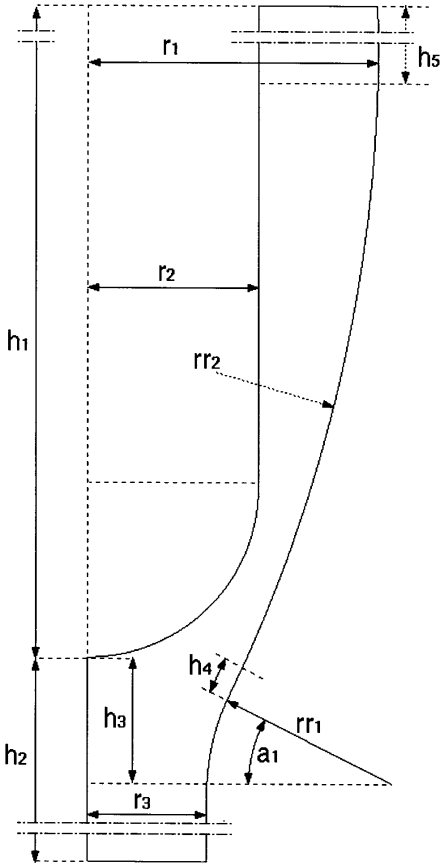

Figure 33: Target geometry for the COULI benchmark (the numbers in brackets can be deduced from the other dimensions).

Parameter	Full scale value	COULI (1/1.4)
h_1 (mm)	1000	714.29
h_2 (mm)	1000	714.29
h_3 (mm)	80	57.14
h_4 (mm)	10	7.14
h_5 (mm)	(638.93)	(456.38)
r_1 (mm)	170	121.43
r_2 (mm)	100	71.43
r_3 (mm)	70	50
rr_1 (mm)	134	95.71
a_1 (deg)	25	25
rr_2 (mm)	(888.22)	(634.4)

The reliability of this result is doubtful because the standard k-ε model uses universal wall functions to approximate the wall shear stresses, but wall functions are not valid in the surrounding of the stagnation point and in the detachment area. Turbulence models without universal wall functions must be used for this case. Calculations for the smaller Reynolds number with a k-ε model, which contains additional functions and extra terms in the transport equations for k and ε for the near wall area developed by Nagano, do not need wall functions, but require fine grids near walls. Such calculations were also performed with FLUTAN. The calculated field of the modulus of velocity shows a clear reduction of the size of the detachment area at the inner wall (figure 37). At the outer wall the area with small velocities increased, so that there may be a tendency to develop also a detached flow at the outer wall. However, this result is not representative for a reliable analysis because the numerical grid is near walls too course for this kind of turbulence models.

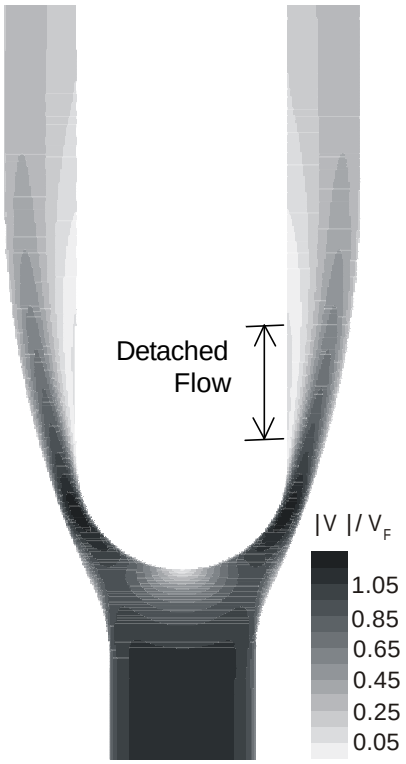

Figure 34: FLUTAN results. Field of the modulus of velocity for Re = $9x10^5$.

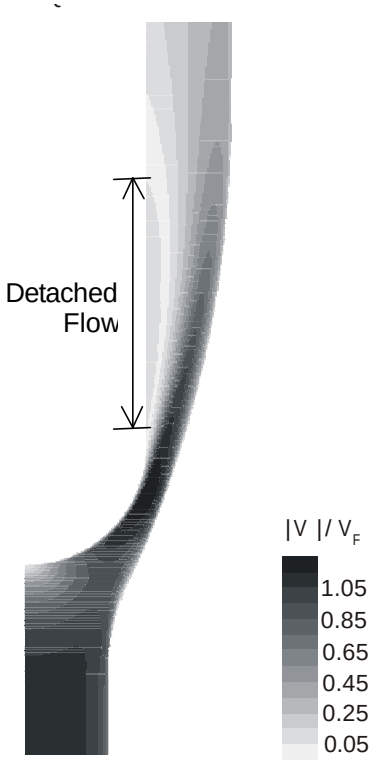

Figure 35: FLUTAN results. Field of the modulus of the velocity calculated with QUICK scheme, Re = $9x10^5$.

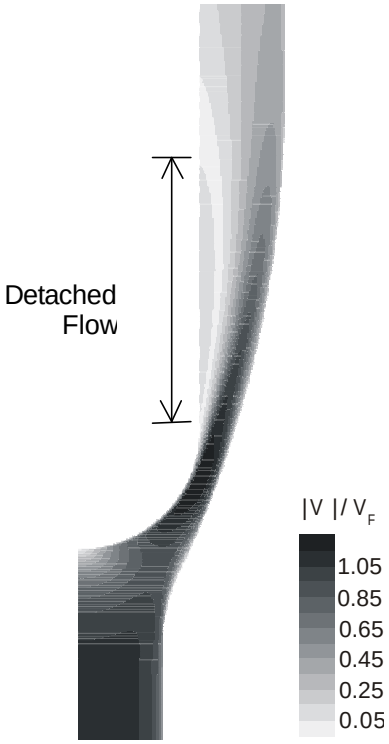

Figure 36: FLUTAN Results. Fields of the modulus of the velocity calculated with LECUSSO scheme, Re = $9x10^5$.

Figure 37: FLUTAN results with k-ε model for low Reynolds numbers. Field of the modulus of the velocity for Re = $2x10^4$.

The results from other codes presented at the first benchmark discussion showed in some cases the detached area not at the inner wall, but at the outer wall. E.g., Star-CD gave with a low Reynolds number model at the larger Reynolds number the detached area near the outer wall and for the smaller Reynolds number mainly near the inner wall and a small recirculation zone also near the outer wall, Komen and Koning (2000).

Conclusions:

The problem of evaluating the validity of current thermal- and fluiddynamical computer codes for problems, which are specific for a spallation target, was investigated by participation in a benchmark exercise. The status quo of available codes and turbulence models was analyzed for the critical flow around the beam window. All codes found some flow detachments downstream of the target window, but at different places and at different Reynolds numbers.
At the moment, no computer code participating in the COULI benchmark can reliably predict the location and the extension of the flow detachment at least with the used models. Therefore, already without heat transport a complex interaction turns out between physical models and numerics in the simulation of typical flows for ADS and the experiments to be performed in KALLA. As a consequence an extremely careful modeling is necessary. A final conclusion on the quality of these results, on the models to be selected for such flows, and on the reliability of the different computer codes engaged can only be basing on the experiments to come.

5.3 Sub-Project SP2: Investigation of Corrosion of Metals in Flowing Lead-Bismuth

5.3.1 Work Package WP1: Investigation of the Corrosion and Erosion of Structure and Window Materials in Flowing Lead-Bismuth

In 1999 this work package is not worked upon, cf. table 7.

5.3.2 Work Package WP2: Improvement of the Corrosion Resistivity using Surface Protection

5.3.2.1 Introduction

In the design of a spallation target one important issue is the corrosion of the structural components that are in contact with the liquid Pb-Bi. Lead-bismuth is highly corrosive in a too low or too high oxygen concentration environment. The rapid corrosion of the structural material must be reduced for economic and safety reasons. This is accomplished by either monitoring and maintaining a specific oxygen concentration within the liquid Pb-Bi (see Work-Package WP 3) or by forming a stable corrosion barrier on the surface of the steel. Thin alumina scales have the ability to reduce the corrosive attack, however cracks within the alumina layer form preferential paths for corrosion. Austenitic steel is one of the most likely candidate material for structural components. This chapter deals with the research and testing of suitable protection coatings on austenitic steel.
One of the preferred methods of coating structural steel is hot-dip aluminizing (HDA). The steel has to be immersed in an aluminium melt. It is possible to pump the liquid melt through the components, depending on their shape. As a result of the steel being immersed, an aluminium diffusion into the bulk can be observed. This diffusion forms an intermetallic layer on the surface. Depending on the dip time, the steel will possess a varying intermetallic layer thickness. The longer the steel is submersed in the aluminium melt the thicker the coating layers become. The steels which were heated at high temperature, regardless of whether annealing was performed, formed brittle phases in the over layer. The steels exposed to medium heat treatment temperatures exhibited a softer over layer with the thickness and the hardness of the intermetallic layer increasing with heat treatment temperature. When 10 wt.-% silicon was added to the aluminium melt, it was necessary to increase the immersion time to produce uniform surface coverage. With the silicon in the melt the thickness of the surface layers drastically decreased. Softer over layers, compared to samples without silicon, were developed after the heat treatment.

5.3.2.2 Experiments

In 1999 only orientation experiments in stagnant Pb-Bi were performed.
The chemical composition of the steel to be aluminized is shown in table 14. The specimens are from sheets of austenitic steel cut into 50 mm x 15 mm pieces, with a thickness of approximately 1 mm.

Table 14: Chemical composition of the steel 1.4571.

Standard number 1.4571									
DIN number X6CrNiMoTi17-12-2									
Analyse (%)									
C	Si	Mn	P	S	Cr	Mo	Ni	V	others
≈ 0.08	1.00	2.00	0.045	0.030	16.5-18.5	2.00-2.50	10.5-13.5	0	Ti>5% C≤0.08

Three different surface pre-treatments were completed on the samples: vibration grinding with stainless steel balls and needles, vibration grinding with ceramic pyramids, and sand blasting with fine glass particles. The samples with the different surface pre-treatments were examined in order to determine which pre-treatment would boast the best wetting ability. The surface wetting is extremely important, any unwetted area is the first to be attacked by corrosion. All three different surface pre-treatments displayed the same wetting ability. It was determined from inspection that the stainless steel vibration ground, and the sand blasted surface were too finely polished. Therefore further testing was carried out using ceramic vibration ground samples. Following the pre-treatment the sheets were placed in an ultrasonic propanol bath for 15 min to remove residual grease or dirt. The samples were transferred to a glove box where the hot-dip aluminizing could be completed in a controlled Ar-5%-H_2-environment.

Before a sample was dipped into the aluminium, a flux was used to remove any oxide layer which had formed on the surface of the melt. The composition of the flux was 51%KCl, 39%NaCl, and 10%Na_3AlF_6. The aluminium melt was maintained at a temperature of 700°C. This temperature has no influence on the structure of the austenitic steel, Glasbrenner et al. (1998). The majority of the specimens were exposed to the melt for 30 s, the exception being a series of samples dipped at specified times in order to understand the growth of the intermetallic layer with dip time. The samples were naturally cooled inside the glove box. Following the HDA process the coupons were subjected to varied heat treatments, table 15, to observe the transformation of the intermetallic layer.

Table 15: Heat treatment conditions.

Dipping Process	Heat Treatment	Annealing
700°C, 30 s	1050°C, 0.5 h	
700°C, 30 s	1050°C, 0.5 h	750°C, 2 h
700°C, 30 s	650°C, 2 h	
700°C, 30 s	600°C, 2 h	
700°C, 30 s	550°C, 2 h	
700°C, 30 s	500°C, 2 h	

The heat treatment was performed in an air environment. After the required time the specimens were removed and allowed to air cool. After the heat treatment metallographic cross sections were prepared for examination.
Analytical investigations were carried out using optical microscopy and SEM/EDS. The hardness of the specimen was measured using Vickers hardness testing. For additional samples a new aluminium melt was used. After the aluminium had reached the temperature of 700°C, silicon was added up to a concentration of 10 wt.-%. The specimen that were dipped for short periods of time, under 60 s, were slightly vibrated to increase the wetting ability.

5.3.2.3 Results

Aluminized Specimens:

In order to understand how the coating layers grow with immersion time, a series of tests were completed. Coupons were submerged in the aluminium melt for times ranging from 10 s to 400 s. Two layers were formed on the steel surface during the dipping process. The layer closest to the steel surface, the “intermetallic layer”, is composed of both iron and aluminium. The outer layer is composed of mainly aluminium. Figure 38 illustrates the growth of the intermetallic layer versus immersion time.

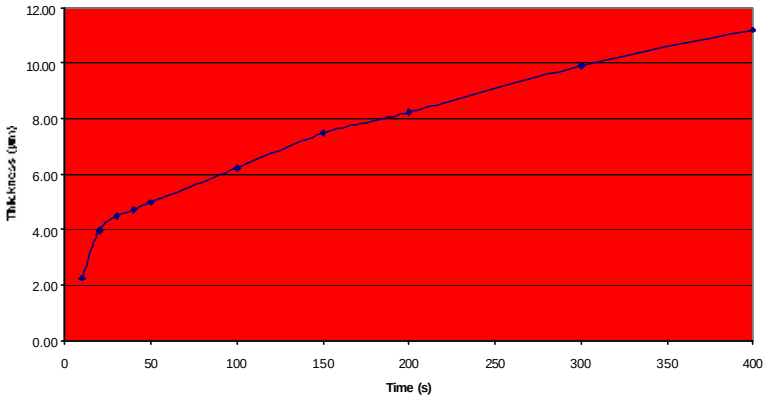

Figure 38: Thickness of the intermetallic layer after HDA.

It can be observed that the thickness of the intermetallic layer increases according to a square root function. This is because diffusion is the major contributor to the creation of the intermetallic layer, Stein-Fechner et al. (1997). The intermetallic layer was measured at five different points on two samples from each sample group. These ten data points were averaged giving an approximate intermetallic layer thickness for any sample. The aluminium over layer had a thickness of approximately 20 µm for the samples with the lower immersion times, increasing to about 50 µm for the specimen immersed for 400 s. Unwetted spots could be observed on both the 10 s and the 20 s samples.

The samples immersed for 30 s and longer offered a uniform intermetallic and aluminium layer on the surface of the steel, figure 39. The adhesion of the aluminium layers to the steel face appeared to be good.
Further testing was completed using the 30 s immersion time. It was important to maintain uniform wetting of the surface while maintaining a low dipping time. For the longer dipped specimens needle formations began to form on the surface. This was due to combined phases in the aluminium melt adhering to the sample surface. These combined phases are formed from the melt and the specimen. Parts of scale dissolve in the melt until saturation occurs, Stein-Fechner et al. (1997). Aluminium dissolves the elements from the austenitic steel. When the concentration of nickel, iron, or chromium is high; crystals precipitate in the melt. These crystals have a higher melting temperature than pure aluminium and pollute the aluminium melt. The iron enrichment of the melt is caused by the instability of the initial phases. Small imperfections can be observed on the steel face, the majority of these will be dirt from the environment, or titanium. Titanium is used in the formation of austenitic steels to stabilise the material.

Figure 39: HDA specimen, 700°C / 30 s.

SEM/EDS line analysis for the 700°C / 30 s sample illustrates the decreasing and increasing of iron and aluminium, respectively, when moving away from the original surface. Figure 40 shows a step decrease of iron from the original specimen to the intermetallic layer, and to the outer layer. The reverse is true of the aluminium. The nickel and chromium concentrations decrease away from the original surface. It can also be seen that the outer layer is composed almost entirely of aluminium.
The hardness of the intermetallic layer is approximately 450 HV 0.05. The hardness of the original austenitic steel is 200 HV 0.05.

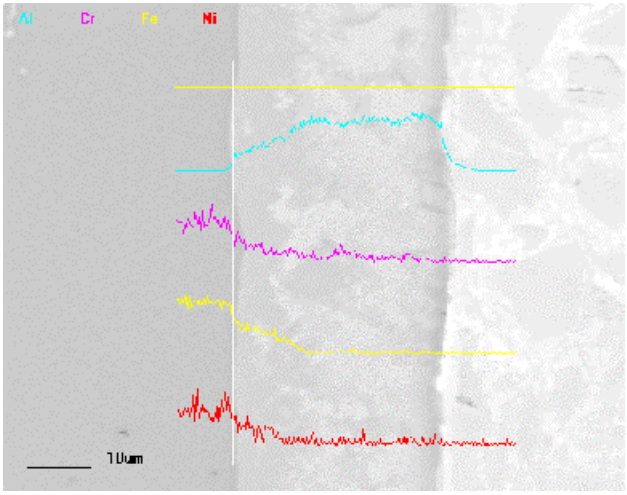

Figure 40: EDS line analysis, HDA 700°C / 30 s.

Aluminized and Subsequent Heat Treated Specimens:

The first heat treatment applied to the specimens was a temperature of 1050°C for a time of 0.5 h. The temperature and time chosen is a standard heat treatment for austenitic steel. Two distinct layers were observed after the heat treatment, figure 41).

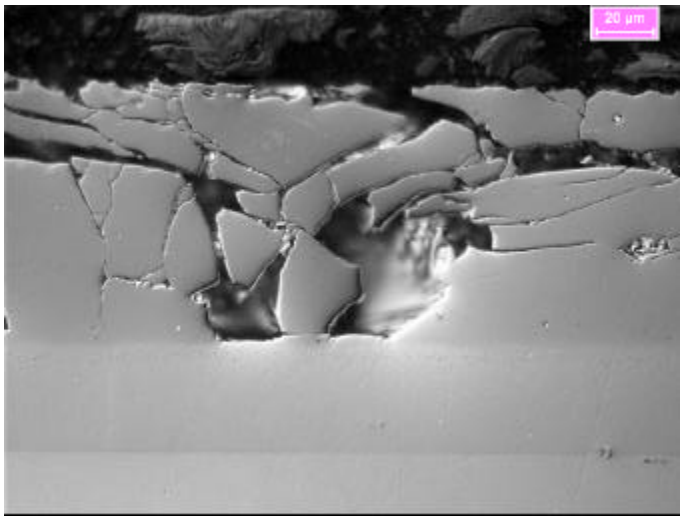

Figure 41: Heat treated at 1050°C for 0.5 h.

Figure 42 illustrates a brittle outer layer, and a consistent intermetallic layer. The outer layer is known to be brittle from the number of cracks observed. Vickers hardness testing was completed at various locations in order to develop an understanding of the hardness.

Figure 42: Vickers Hardness for 1050°C and 0.5hr

The hardness determined for the outer layer was approximately 780 HV 0.05, 400 HV 0.05 for the intermetallic layer, and 200 HV 0.05 for the original steel. When the outer layer is brittle, erosion could be a problem in the system. In order to reduce this brittleness the specimens heat treated for 0.5 h at 1050°C were annealed. The annealing process is completed to relieve the stresses in the outer layer. Annealing was completed at 750°C for 2 h. Vickers hardness was measured for the annealed specimen; 700 HV 0.05 for the outer layer, 350 HV 0.05 for the intermetallic layer, and 200 HV 0.05 for the base steel.
SEM/EDS was completed for the annealed sample, figure 43. The two vertical lines in figure 43 mark the intermetallic boundaries. Chromium content remains uniform throughout the intermetallic layer, but then the concentration steps down in the outer layer. The iron content displays a slightly decreasing concentration slope with no drastic change. The aluminium content displays a gradual increase through the intermetallic layer, this slope is caused by diffusion. A sharp peak of nickel can be observed at the boundary of the outer and intermetallic phase.

This sharp peak was confirmed when image analysis was completed on the sample, figure 44. The specimen displays a nickel rich boundary separating the outer and the intermetallic layer.
The hardness of the outer layer was still quite high, 700 HV 0.05. The heat treatment following the dip was altered. A series of samples were heat treated in temperatures ranging from 500-650°C for 2 h. The hardness of the outer layer of these samples was approximately 200 HV 0.05. This is much softer than the high temperature heat treated samples.
The thickness of the intermetallic layer also varies with the heat treatment temperature, figure 45. Prior to heat treatment the thickness of the layer was approximately 4.5 µm.

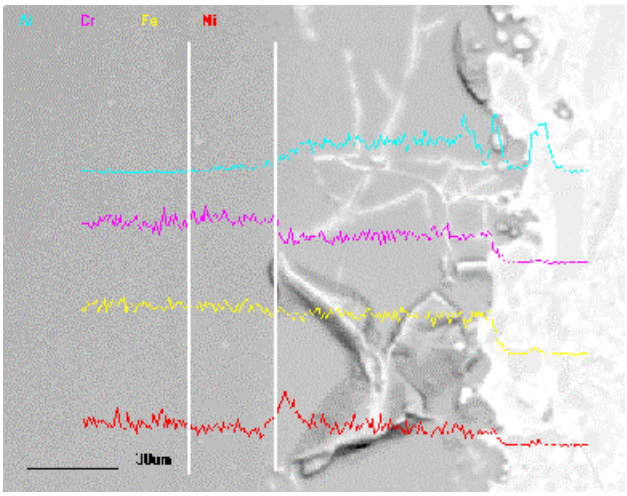

Figure 43: EDS line analysis,
HT 1050°C / 0.5 h,
annealed 750°C / 2h.

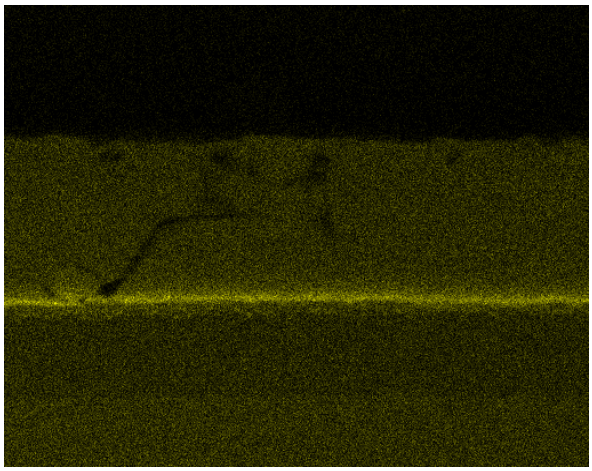

Figure 44: High nickel concentration
at boundary.

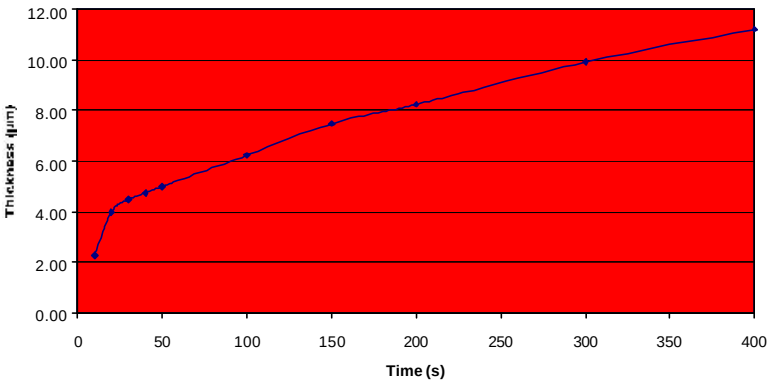

Figure 45: Thickness of the
intermetallic layer
after heat treatment.

The intermetallic layer thickness increases in an exponential manner. The exponential increase is caused by the enhanced diffusion of iron and aluminium at higher heat treatment temperatures, Glasbrenner et al. (1997). The sample heat treated at 500°C displays very little change from the after dipping stage, figure 46. When viewed closely, small pores can be seen in the outer layer of the sample heat treated at 500°C for 2 h. These pores are formed during the heat treatment and are approximately 1 µm in diameter. They are caused by the different diffusion rates of iron and aluminium, known as the Kirkendall effect, Konys et al. (1998). The inward diffusion of aluminium is faster than the outward diffusion of iron. Pore formation is a time and temperature dependent process, Glasbrenner and Wedemeyer (1998).

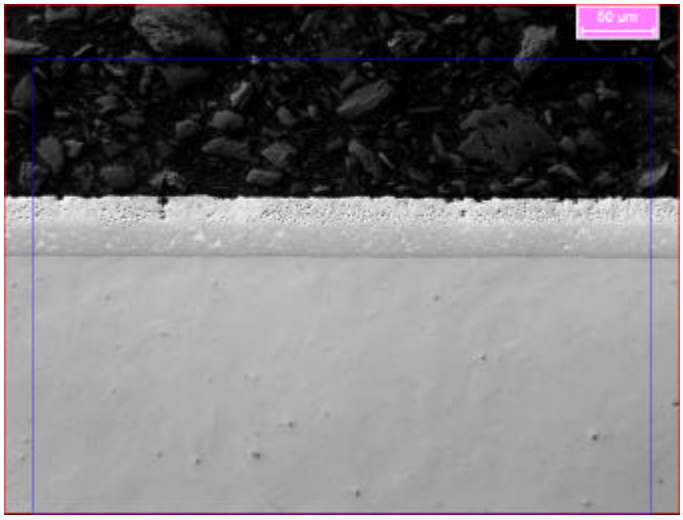

Figure 46: Heat treated sample, 500°C / 2 h.

Aluminized with 10 wt.-% Silicon:

Silicon was added to the melt mixture in order to reduce the hardness after heat treatment and to decrease the intermetallic layer size. It is known that silicon will minimize the coating layer thickness and form a silicon rich dividing layer, Konys et al. (1998), Glasbrenner et al. (1996). The disadvantage of silicon is that it forms very brittle phases which make forming of the material difficult. In industry it has been observed that for ferritic steel the wetting ability of the surface is increased with the addition of silicon in the coating melt. A series of samples were dipped at 700°C for 30 s in a melt containing 10 wt.-% silicon, when examined visually, it was observed that there were many unwetted areas. Specimens were then immersed for 3, 5, 10, and 20 minutes. All of the samples dipped for the longer times were uniformly covered. The intermetallic layer thickness before heat treatment increases in a square root function as well, figure 47.

All of the samples exhibit crystal formation in the outer aluminium layer, figure 48. These are crystals of pure silicon. They appear as long sharp needles organized in a random manner.

From the samples that were immersed in the melt for 30 s some specimens were chosen for heat treatment. These specimens displayed small unwetted areas. After the heat treatment was complete hardness measurements were taken on the intermetallic layer, approximately 450 HV 0.05. The aluminium outer layer became practically non-existent after the heat treatment, figure 49.

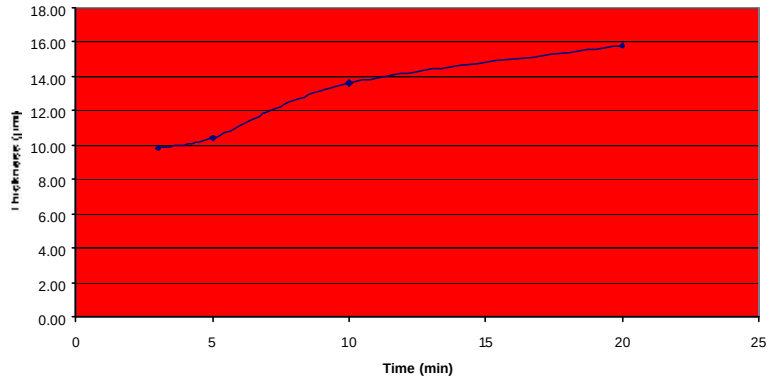

Figure 47: Intermetallic thickness with 10 wt.-% Silicon versus time.

Figure 48: HDA sample, 700°C / 10 min.

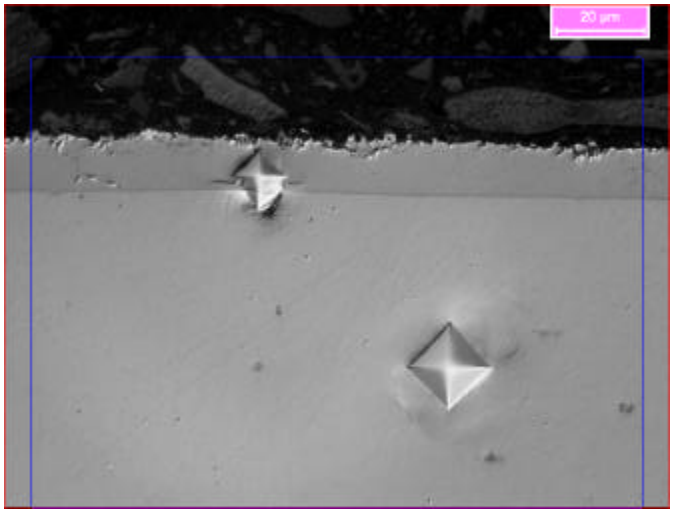

Figure 49: 10wt.% Silicon in Aluminium melt, HT 550°C 2 h.

The outer layer is barely visible in this photo of the specimen and it is obvious that the coating layer is quite small, approximately 10 µm. The adhesion to the face of the steel appears to be quite good. The coating thickness is uniform along the surface of the sample. Observing the outer edge of the specimen many jagged points can be seen.

After the heat treatment silicon, iron, and aluminium form crystals which can be very brittle. Pure silicon particles also remain in the coating layer, figure 50.

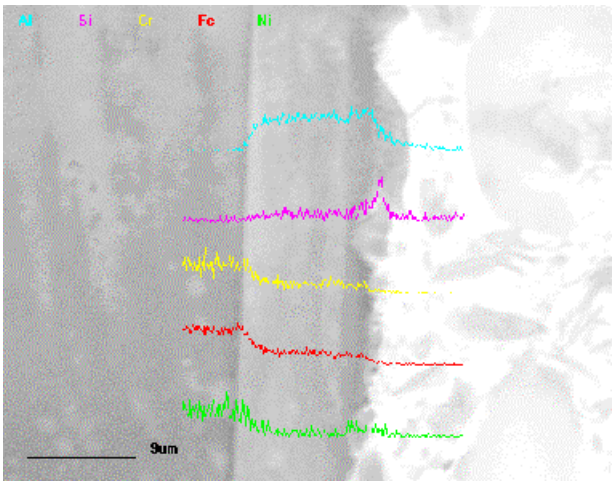

Figure 50: EDS line analysis for specimen with 10 wt.-% silicon, HT 550°C / 2 h.

It is known that this silicon peak is due to a particle in the surface and not a silicon rich layer from the image analysis graphs. The iron, chromium, and nickel display a uniform concentration through the coating layer. There is a small aluminium rich area at the outer edge of the sample. If the scale in the bottom left corner is analyzed, the size of the coating layer can be seen to be small. The layer size has decreased drastically from the specimens dipped in pure aluminium.

5.3.2.4 Conclusions

It has been shown that the hot-dip aluminizing method is acceptable for coating of austenitic steels. If a dipping time of 30 s was performed, a uniform surface layer formed on the steel face was found and there was no sign of unwetted areas. The intermetallic layer formed on the surface of the steel after hot-dipping increased in size as the immersion time increased. The increase forms a square root function, because the formation is controlled by diffusion.
After silicon was added to the melt the thickness of the coating was reduced. The coating after heat treatment was approximately 10 µm thick. The hardness of the intermetallic layer was measured as 450 HV 0.05, compared to about 780 HV 0.05 without any silicon in the melt.
For the future, additional testing and research should be carried out to further study the effect of silicon in the melt. Heat treatments should be performed on the specimens which have been dipped for longer times to observe the effects. Analysis of the melts should be completed to verify the 10 wt.-% silicon concentration.

5.3.3 Work Package WP3: Surface Modification using the Pulsed Electron Beam Facility (GESA)

Pulsed electron beam treatment of thin surface layers was done using the pulsed electron beam facility GESA. The very fine grained structure of the rapid solidified melt layer is a suitable basis for the formation of protective oxide scales with good adhesion, Müller et al. (1998). The micrograph of the cross section perpendicular to the surface structure of a treated OPTIFER specimen is presented in figure 51. After etching no structural details are visible in the solidified melt region on top of the coarse grained base material.

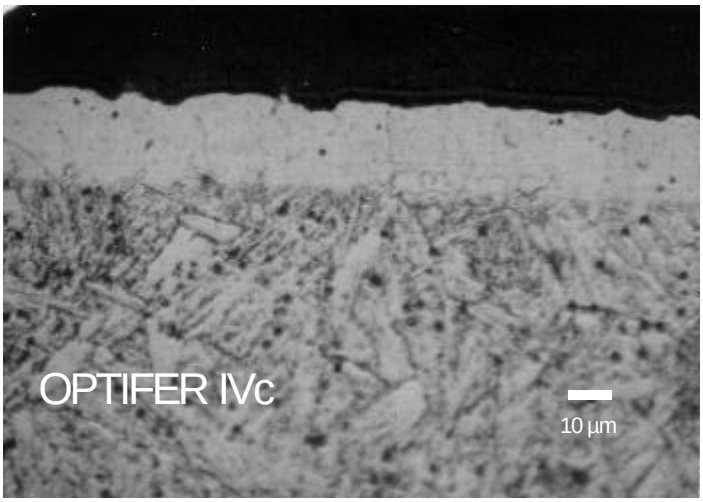

Figure 51: Micrograph of the cross section of OPTIFER after GESA treatment. The bright region on top is the molten layer.

The treatment of the steel specimen employed for the corrosion tests in liquid lead consist of alloying Al into a surface layer of 15 µm depth. For this purpose, a 18 µm Al-foil is placed on the steel surface. It melts and mixes with the molten steel surface layer. A great part of the Al evaporates during this process, but the remainder, about 25%, is alloyed into the steel. The Al-concentration profile perpendicular to the surface after different treatment steps are shown in figure 52.

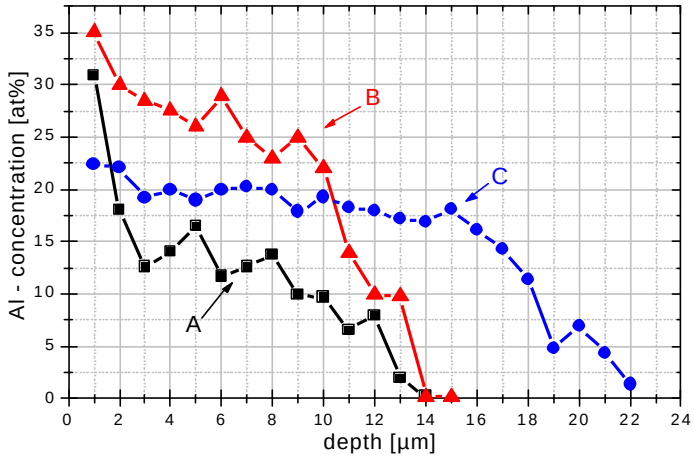

Figure 52: Aluminum (Al) concentration profile after surface alloying of OPTIFER IVc.
A: 1 pulse with 18 µm Al foil,
B: 2 pulses, each one with 18 µm Al foil,
C: 2 pulses, first with, second without 18 µm Al foil.

They are obtained by analysis of the cross section with an ECON 3,4 O detector attached to the SEM (Scanning electron microscope) AMR 1000 (Leitz, Wetzlar). The EDAX DX-4 eDX ZAF system was used for the calculation of the concentrations by employing the standardless method. The analysis shows, that Al penetrates into the steel within the molten surface layer. Profile A is obtained with an 18 µm Al-foil by applying just one electron pulse and profile B with a second pulse after replacing the Al-foil. When an additional pulse is applied to the surface with a B-profile without

replacing the Al-foil, profile C is obtained, which is almost constant up to a depth of 15 µm. The concentration profiles are not typical for a diffusion process, but for a distribution by turbulences in the melt.
The structure of the alloyed surface layer is shown in figure 53. The SEM of the etched cross section reveals a laminar structure with varying Al concentrations parallel to the surface. Regions with higher Al concentrations are stronger attacked by the etching agent. The variations in Al concentration can also be seen from the profiles in figure 52.

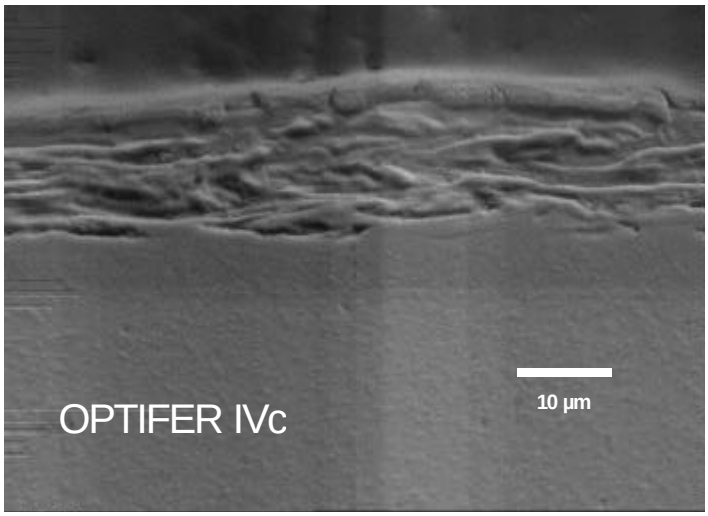

Figure 53: SEM of cross section of Al alloyed (1pulse) OPTIFER IVc after etching.

Concentrations of Al after one pulse scatter from 9.5 to 35 at% in the elevations and cavities, respectively. At some places a swivel of those profiles can be observed which hints again to mixing by convection and not by diffusion.
The structure of the Al alloyed layer is also examined by X-ray diffractometry with CuK_α (λ = 154.06 pm) irradiation. For comparison the pattern of original and GESA treated OPTIFER IVc without alloying of Al is also drawn in figure 54. By GESA treatment the α-Fe10Cr peaks shift slightly to the right because of stresses created by the rapid solidification. If Al is alloyed those peaks shift again to the left by solution of Al in α-Fe10Cr. This shift corresponds to a solution of about 16 at% of Al. Furthermore peaks of FeAl appear. The 2 peaks with question marks could not be identified. It results that the major part of Al is dissolved in α-Fe10Cr only a small amount precipitates in the FeAl phase. Those phase regions are in the nanometer size range and cannot be resolved in the cross section.

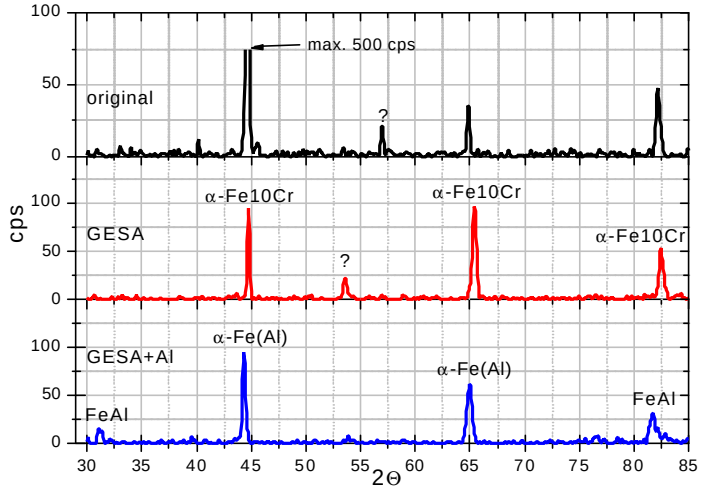

Figure 54: X-ray diffraction patterns of OPTIFER in the original state, after GESA treatment and after surface alloying of Al.

5.4 Sub-Project SP3: Oxygen Measurement and Oxygen Control in Lead-Bismuth

5.4.1 Work Package WP1: Oxygen measurement in flowing lead-bismuth

5.4.1.1 Introduction

In literature, corrosion problems with steel being in contact with lead alloys are well known: Severe intergranular attack was observed for AISI 316 steel. Corrosion effects in the 100 µm range occurred in Fe-Cr steels between 575°C and 750°C after 3250 h of exposure. The highest solubility in lead is that of Ni for which the phase diagram of Massalski (1990) shows 2at.-% at 550°C.
One way to reduce corrosion of metals in liquid Pb or PbBi would be the use of metals with very low solubility, e.g. tungsten or molybdenum. Another way is to form a stable oxide layer on the steel surface. Theoretical thermodynamic investigations of Al-Fe alloys in Pb-Li by Kleykamp and Glasbrenner (1997) showed the possibility that a self-healing of the alumina scale can take place if the kinetics of the process is fast enough. Gromov et al (1995) and Markov (1997) stabilized the oxide layer by maintaining an oxygen concentration of 10^{-6} at.-% in liquid Pb or Pb-Bi with an oxygen control system.
The concentration of oxygen in lead which is necessary for the protective oxide scale formation on steel structures, can be controlled by an atmosphere with a definite oxygen partial pressure that determines the chemical potential of oxygen in the liquid metal. To prevent PbO precipitation and to support Fe_3O_4 formation the following conditions for the oxygen potential must be established:

$$2\Delta G^0_{PbO} > RT \ln p_{O_2} > 0.5\Delta G^0_{Fe_3O_4} \quad . \tag{3}$$

The standard values ΔG^0 of the Gibbs energies are well known for all relevant oxides and with these values the equilibrium oxygen partial pressure region that retains the stable conditions can be calculated. The oxygen partial pressure as a function of the H_2/H_20 ratio can be calculated as follows:

$$p_{O_2} = \frac{p^2_{H_2O}}{p^2_{H_2}} exp \frac{2DG^0_{H_2O}}{RT} \quad . \tag{4}$$

If we choose a H_2/H_2O ratio of 0.4 we will attain $Po_2 \approx 10^{-25}$ bar at 550°C and $Po_2 \approx 10^{-29}$ bar at 400°C. At both temperatures we still form iron oxide and no PbO in the case of stagnant Pb. If we consider a liquid metal loop, there will be no equilibration across the temperature region via the H_2/H_2O ratio but through the oxygen dissolved in Pb (Pb-Bi). In this case we have to consider the variation of the oxygen potential for a constant oxygen concentration throughout the temperature region between 400°C and 500°C.
The oxygen activity a_0 of the oxygen in lead or lead-bismuth in equilibrium with an oxygen partial pressure p_{O2} can be calculated as follows:

$$a_o = g_o c_o = \frac{c_o}{c_{o,s}} = \left(\frac{p_{o_2}}{p_{o_2,s}} \right)^{\frac{1}{2}} \quad . \tag{5}$$

The suffix “s“ indicates the values that correspond to saturation conditions at which the activity a_o becomes unity.
To control the oxygen level in the liquid metal, an oxygen sensitive sensor is necessary to be incorporated into the oxygen control unit. Usually electrochemical based oxygen meters are used to fulfill this demand.
Electrochemical oxygen meters used for the measurement of oxygen potentials in liquid metals have been developed over a long period of time for many liquid metal applications, e.g. Na, K, Pb-17Li, Borgstedt (1984), Borgstedt et al. (1994). Inherent problems associated with these meters were breakage of the ceramic electrolyte tube, non-theoretical response to oxygen activity and design related failures. For use of oxygen meters in Pb and/or Pb-Bi, only rarely published data from Russian groups are available, Orlov (1998).
Within this project, the activities are focussed on the development of oxygen meters for the use in lead-bismuth. This includes the selection of appropriate reference systems, the estimation of deviations from theoretical behavior and testing of the long-term stability.

5.4.1.2 Theoretical Background

An electrochemical oxygen meter with a solid electrolyte measures the EMF (Electro Motive Force) of the following concentration cell:

$$Po_2\text{“ // solid electrolyte // } Po_2\text{‘} \qquad (6)$$

Where Po_2“ and Po_2‘ are the oxygen partial pressures of the reference electrode and of the corresponding liquid metal. The EMF is given by the Nernst equation:

$$E = \frac{R\,T}{4\,F}\,ln\frac{p''_{2}}{p'_{2}} \quad . \qquad (7)$$

For fixing the oxygen potential of the reference side, pure oxygen or air as gas electrodes or metal oxide buffers such as In/In_2O_3, Sn/SnO_2 or Cu/Cu_2O can be used. The oxygen potentials can be calculated using tabulated data of the Gibbs Energy of Formation. Therefore, the desired Po_2‘ can be estimated from the measured EMF value, for specific temperatures.

5.4.1.3 Experiment

Platinum/Air Reference Electrode:

Using data from Ullmann et.al. [8], the following relationship between the EMF and Po_2‘ was calculated:

$$E = -0.03369\ T - 0.021526\ T\ \ln(p_{O2}\text{‘}) \quad , \qquad (8)$$

With
$$T\ ln\ p_{O_2}' = \frac{2\,\Delta G^{0}_{PbO}}{R} \qquad (9)$$

and
$$\Delta G°_{PbO} = -436850 + 197.99\ T \quad , \quad \text{in [J/mol } O_2\text{]} \qquad (10)$$

the EMK for oxygen saturated solution of Pb or Pb-Bi (if only PbO is assumed as precipitating oxide) is as follows:

$$E\ (mV) = 1131.06 - 0.5463\ T \quad , \quad \text{in [K]} \quad . \qquad (11)$$

For unsaturated solutions of oxygen, one has to take into account the solubility of oxygen in Pb-Bi. With the data of Orlov (1998) and the relationship

$$a = \frac{c_0}{c_{0s}} \quad , \tag{12}$$

where c_0 is the oxygen concentration and c_{0s} the saturation concentration in the liquid metal, one can calculate the dependency of the EMF on the oxygen concentration in Pb-Bi

$$E\ (mV) = 794.11 - 0.03102\ T - 0.043\ T\ \ln(c_{0Pb\text{-}Bi}) \quad . \cdot \tag{13}$$

Here, $c_{0Pb\text{-}Bi}$ is in wppm oxygen.

In/In_2O_3 Reference Electrode:

Corresponding to the chemical reaction:

$$2In + \frac{3}{2}O_2 \Leftrightarrow In_2O_3 \tag{14}$$

the oxygen potential P_{O2}" can be derived as follows:

$$RT \ln Po_2'' = \frac{2}{3}\Delta G^\circ_{In2O3} \tag{15}$$

With $\Delta G^\circ_{In2O3} = -618365 + 216.3T$ in [J/mol O_2] (16)

and the Nernst equation (7), it is possible to calculate the EMF for oxygen saturated Pb-Bi as:

$$E\ (V) = 0.4703 - 4.744 \cdot 10^{-5} T(K) \tag{17}$$

For unsaturated solutions of oxygen, the EMF can be calculated corresponding to the Pt/air system by using the solubilities from Orlov (1998):

$$E\ (V) = 0.13309 + 4.6823 \cdot 10^{-4}\ T - 4.308 \cdot 10^{-5}\ T\ \ln co_{Pb\text{-}Bi} \tag{18}$$

$co_{Pb\text{-}Bi}$ is in wppm oxygen.

Oxygen Meter Design:

The design of the oxygen meter is given in figure 55.
The meter was connected to the test capsules with a Conoseal flange. Regardless of the type of reference electrode, O^{2-} ions are moving through the ceramic solid electrolyte towards the liquid metal side where the oxygen ions will be discharged. Afterwards, the 2 electrons are transported through the connecting wires back to the reference side where oxygen atoms are ionized into the O^{2-} state. This principle is shown on the left side of figure 55. The EMF was measured by means of a Keithley high impedance volt meter, whereas the data were stored on a PC. All oxygen meters were built and prepared for testing in an inert Argon glove box.

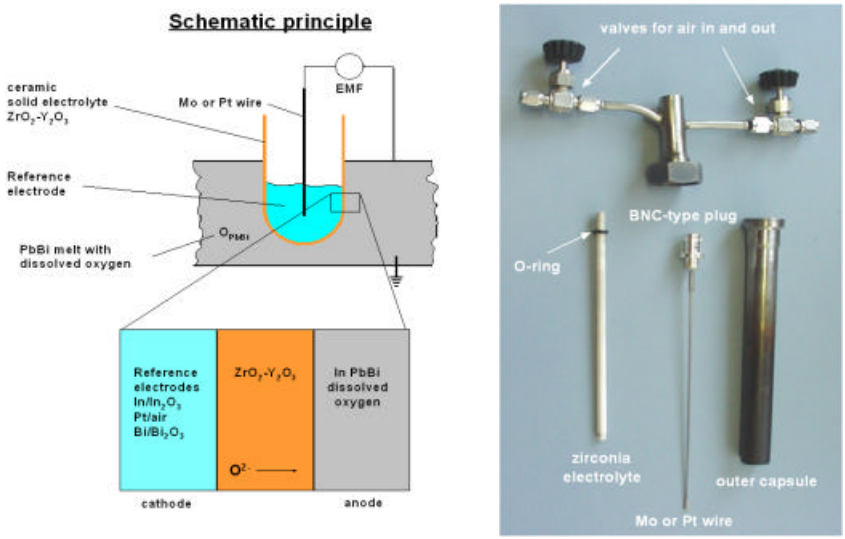

Figure 55: Schematic principle and disassembled parts of the oxygen meter.

5.4.1.4 Results

A series of oxygen meters with both type of reference electrodes were built and tested in different "qualities" of Pb-Bi, concerning the oxygen content. All measurements were compared with theoretical calculations. Figures 56 and 57 represent the dependency of the EMF on temperature and oxygen concentration of the Pb-Bi for Pt/air and In/In_2O_3 as reference systems respectively.
It can be clearly seen in figure 56 that for oxygen saturated Pb-Bi, the EMF lies at around 0.7 V for temperatures between 500°C and 550°C. At lower temperatures down to about 400°C, the EMF rises up to 0.8 V with a negative temperature coefficient. The dashed lines show the dependency of the EMF for unsaturated solutions of oxygen in Pb-Bi, corresponding to the respective oxygen concentrations in wppm.
Both red lines indicate the readings of 2 oxygen meters in two different Pb-Bi "qualities", regarding the oxygen concentrations. Oxygen meter 1, which was tested in oxygen saturated Pb-Bi, showed nearly theoretical behavior of the EMF versus temperature, with the same negative slope down to 400°C. The oxygen meter 2, tested in very "pure" Pb-Bi, revealed the expected dependency of the EMF as a function of temperature for unsaturated solutions, regardless the "real" oxygen concentration in wppm. The slope of the temperature curve is linear down to about 400°C with the same positive slope as predicted for unsaturated oxygen solutions in Pb-Bi.
Figure 57 shows the theoretical dependency of the EMF of an oxygen meter with In/In_2O_3 as reference system. In comparison to Pt/air, the EMF values are slightly different. An oxygen saturated solution of Pb-Bi shows voltages in the range of ca. 0.45 V at around 550°C, whereas an oxygen concentration of 10^{-6} wppm results in about 1 V for In/In_2O_3 and about 1.15 V for Pt/air.
The colored curves represent EMF readings for specific cooling rates of 1, 2 and larger than 2 K/min. It is obvious that the time to reach equilibrium has a significant influence on the oxygen eter output. Furthermore, compared to Pt/air reference system, the oxygen meters with In/In_2O_3 show a distinct drop in the EMF readings below about 520°C. The reason for that behavior is not yet clear and needs more detailed investigations.

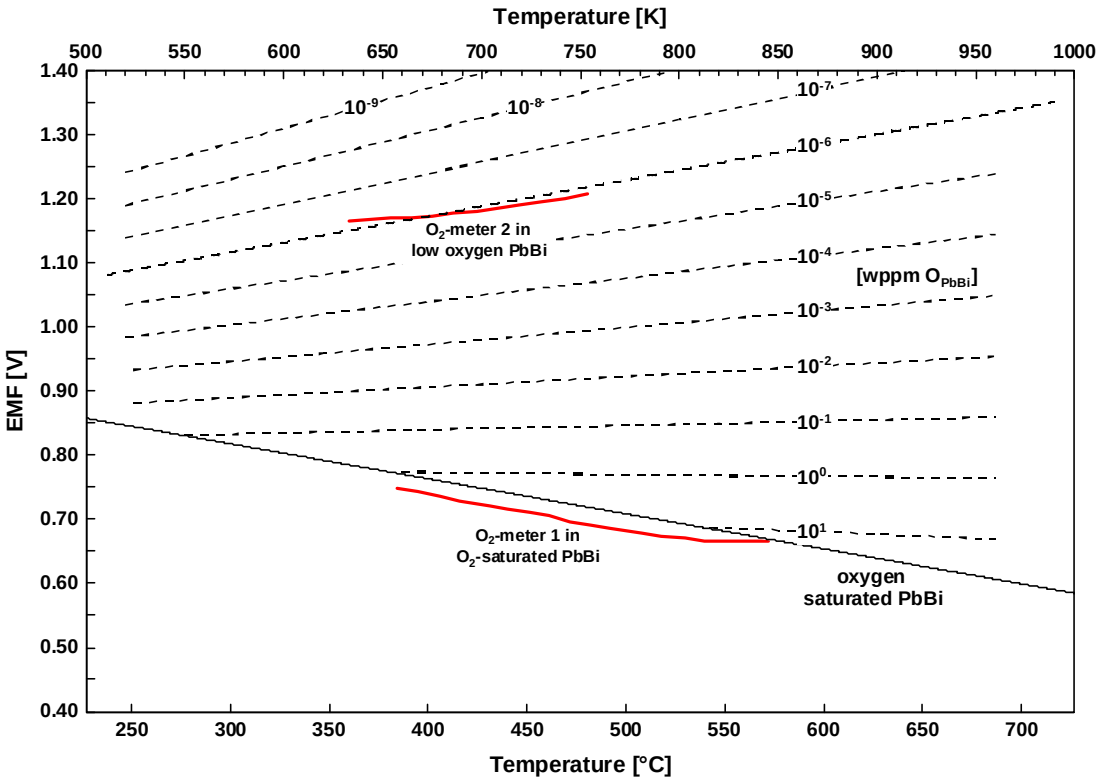

Figure 56: EMF of oxygen meter in Pb-Bi with Pt/air reference system.

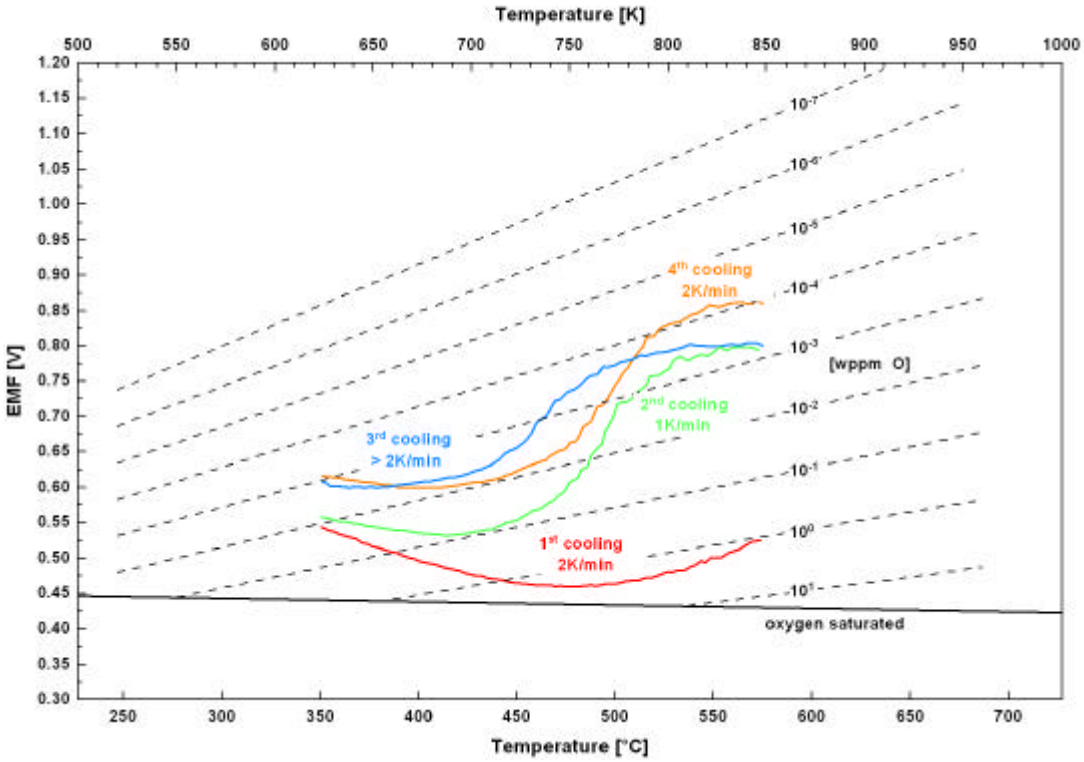

Figure 57: EMF of oxygen meter in Pb-Bi with In/In_2O_3 reference system.

5.4.1.5 Conclusions

It has been shown that zirconia based solid electrolyte oxygen meters have the potential to measure the oxygen activity of liquid lead-bismuth. The theoretical calculations have indicated that the EMF values to be detected lie in a range of 0.5 to 1.5 V, depending on the oxygen concentration in the Pb-Bi. The Pt/air reference system has shown, that it is working very stable in oxygen saturated as well as in very “pure“ Pb-Bi. The In/In_2O_3 reference system is because of its much lower oxygen partial pressure, more complicated from the design point of view. The first results indicated, that, regardless of principal differences to Pt/air, this kind of oxygen meters can be developed, too.
The next investigations have to be focussed on the estimation of long-term stability of the oxygen sensors, reliability, reproducibility and the limitations in use. This includes operational temperatures and oxygen concentrations of the Pb-Bi.

5.4.2 Work Package WP2: Oxygen control in flowing lead-bismuth

5.4.2.1 Introduction

Using a heavy liquid metal such as Pb-Bi or Pb as a coolant in an ADS system results in serious corrosion problems with the structural materials, cf. Chapter 5.4.1. Steel and Pb-Bi or Pb are not compatible. Since all the solubilities vary with temperature, transport processes will take place which live from the enhanced solubility of steel components at high temperatures and precipitation of the corrosion products at low temperatures. A temperature difference of 150 K is typical for Pb-Bi cooling loops. Having high flow velocities in the range of m/s and long in pile times even small solubilities can lead to heavy corrosion effects.
One possibility to slow down corrosion of metals in liquid Pb-Bi is the application of metals with no or very low solubility in Pb-Bi, e.g. Mo and W with a solubility below 0.005 wt% at 1200°C. Another possibility is to protect the metal surface by an oxide layer that has the ability to slow down the dissolution of the protected metal components to tolerable values, Markov (1997), Orlov (1998). With the latter possibility oxygen is added to the liquid Pb-Bi in a concentration at which a protective oxide layer is formed on the surface of the metal, however, no PbO is precipitated in the liquid Pb-Bi.
An overview on the corrosion behavior of 2 different steels in a loop with liquid lead at 550°C as a function of oxygen concentration after 3000 h of exposure is presented in figure 58, Markov (1997). At oxygen concentrations below 10^{-7} at% in lead corrosion is determined by solution of alloy components in steel. It increases strongly with decreasing oxygen content. Above 10^{-6} at% oxygen corrosion is caused by oxidation of the surface that on the other hand protects the steel from dissolution of alloying components. No clear statement about the corrosion behavior can be given for the transition zone between 10^{-6} and 10^{-7} at% oxygen, in which dissolution as well as oxidation could be possible.

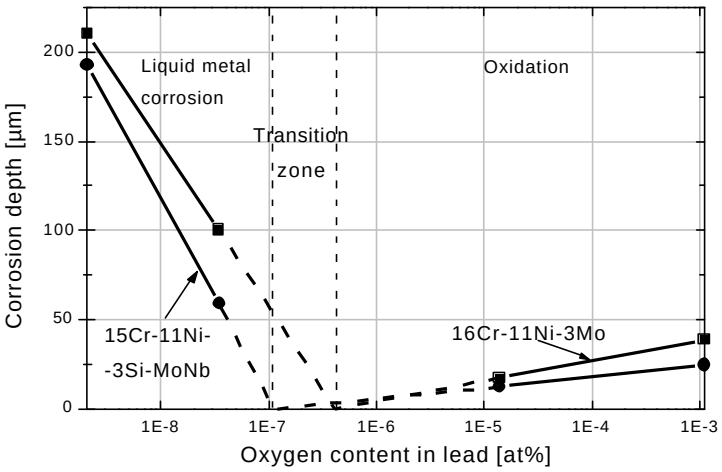

Figure 58: Corrosion behaviour of steels in flowing Pb after 3000 h at 550°C, Markov (1997).

From this discussion it becomes obvious that it is necessary to measure and control the oxygen concentration exactly to keep the conditions of the liquid lead in a range of low corrosion effects. After a certain time period, oxygen in Pb or Pb-Bi will be depleted by oxide formation on the surface of the structure steel and thus the conditions will shift to the region with low oxygen concentration and hence strong corrosion effects, if there would be no oxygen control.

5.4.2.2 Working conditions for a Pb-Bi test loop

The concentration of oxygen in lead that is necessary for the protective oxide scale formation on steel structures, may be controlled by solid electrolyte cells that measure and feed oxygen into the liquid lead or lead-bismuth. Such cells are sophisticated and require a special know-how to build them. Another possibility is control by an atmosphere with a definite oxygen partial pressure that determines the chemical potential of oxygen within the liquid metal bath. To prevent PbO precipitation and to support Fe_3O_4 formation the following conditions must be established:

$$2\ DG^{0}_{PbO} > m_{O_2} = RT\ lnP_{O_2} > 1.5\ DG^{0}_{Fe_2O_3} \quad . \tag{19}$$

The standard values ΔG^0 of the Gibbs energies are known for the oxides in question and with these values the equilibrium oxygen partial pressure region that retains the stable conditions can be determined. The easiest way to do this is to draw a diagram (figure 59) that contains oxygen potentials as a function of temperature of the relevant oxides PbO, NiO, Fe_3O_4 and Cr_2O_3 and the lines for constant oxygen partial pressures and constant H_2/H_2O ratios as a function of temperature. The latter will be used to control the oxygen potential as follows:

$$P_{O_2} = \frac{P^2_{H_2O}}{P^2_{O_2}} \exp \frac{2\ \Delta G^0_{H_2O}}{RT} \quad . \tag{20}$$

Figure 59 demonstrates in which region the stable conditions exist and how they can be established. The ordinate shows the chemical potential of oxygen, the abscissa the temperature. Dashed lines in the diagram represent the isobars of the oxygen partial pressure and the lines of constant H_2/H_2O ratios in the gas atmosphere above the oxidizing species or above the liquid lead that dissolved oxygen, respectively. The important region in the diagram is the one between the lines of the oxygen potential for PbO and Fe_3O_4 in the temperature regime of 400 to 550°C.
For working conditions with reduced corrosion we have to select a field of oxygen partial pressures, the lines of which would not cross the PbO- and Fe_3O_4-lines within the temperature regime of 400 to 550°C. Lines of constant H_2/H_2O ratios within the boarders of this field show the ratios that must be established to maintain the appropriate oxygen partial pressures.
If we chose a H_2/H_2O ratio of 0.4 we will attain $Po_2 \approx 10^{-25}$ at 550°C and $Po_2 \approx 10^{-29}$ at 400°C. At both temperatures we still form iron oxide and no PbO in the case of stagnant Pb. If we consider a liquid metal loop, there will be no equilibration across the temperature region via the H_2/H_2O ratio but through the oxygen dissolved in Pb (Pb/Bi). In this case we have to consider the variation of the oxygen potential for a constant oxygen concentration in throughout the considered temperature region between 400 and 500°C.
For the calculation of the oxygen concentration c_0 in equilibrium with an oxygen partial pressure p_{O_2} we need to know the activity coefficient γ_0 that we get from the following relation for the oxygen activity in lead a_o:

$$a_o = g_o c_o = \frac{c_o}{c_{o,s}} = \left(\frac{p_{o_2}}{p_{o_2,s}} \right)^{\frac{1}{2}} \quad . \tag{21}$$

The suffix (s) indicates the values that correspond to saturation conditions at which the activity becomes unity.

With saturation values for the oxygen concentration in lead of 410^{-2} at% at 550°C and $7.5 \cdot 10^{-3}$ at% at 400°C (Massalski (1990)) equilibrium oxygen concentrations in the range 400 to 550°C were calculated and drawn in figure 59. The solid vertical lines at 400 and 550°C mark the operating range for a lead cooled loop and the dashed lines at 300 and 450°C the one for a lead - bismuth coolant. The lines of constant oxygen concentrations indicate safe regions with 10^{-3} to 10^{-5} at% oxygen for the high temperature Pb - loop and 10^{-4} to 10^{-6} at% for the low temperature Pb-Bi loop. Activity coefficients for Pb and Pb-Bi do not differ much in the region above about 50 at% of Pb. Therefore, the values calculated here for Pb can be extrapolated for Pb - Bi as an approximation.

Figure 59 also shows the advantage of controlling the oxygen partial pressure by the H_2/H_2O ratio. It would not be possible with an oxygen partial pressure of 10^{-25} bar to replace oxygen that was used for oxidation of the surface of the specimen in lead. However with a H_2/H_2O ratio of 0.4 it is easy to replace the oxygen. With a gas flow of 200 cm^3/min it is possible to provide 10 cm^3 O_2/min which corresponds to about 1000 cm^2 Cr_2O_3-oxide layer of 1µm thickness. With this gas flow delivery of the amount necessary for solution of 10^{-6} at% oxygen in 1000 cm^3 Pb would take about one second. Therefore, the controlling step is only the uptake of oxygen from the gas phase. Thus, not only small and medium loops could be managed by controlling them via the H_2/H_2O ratio in the gas phase if one can deliver the available oxygen through the surface to the lead, e.g. by bubbling.

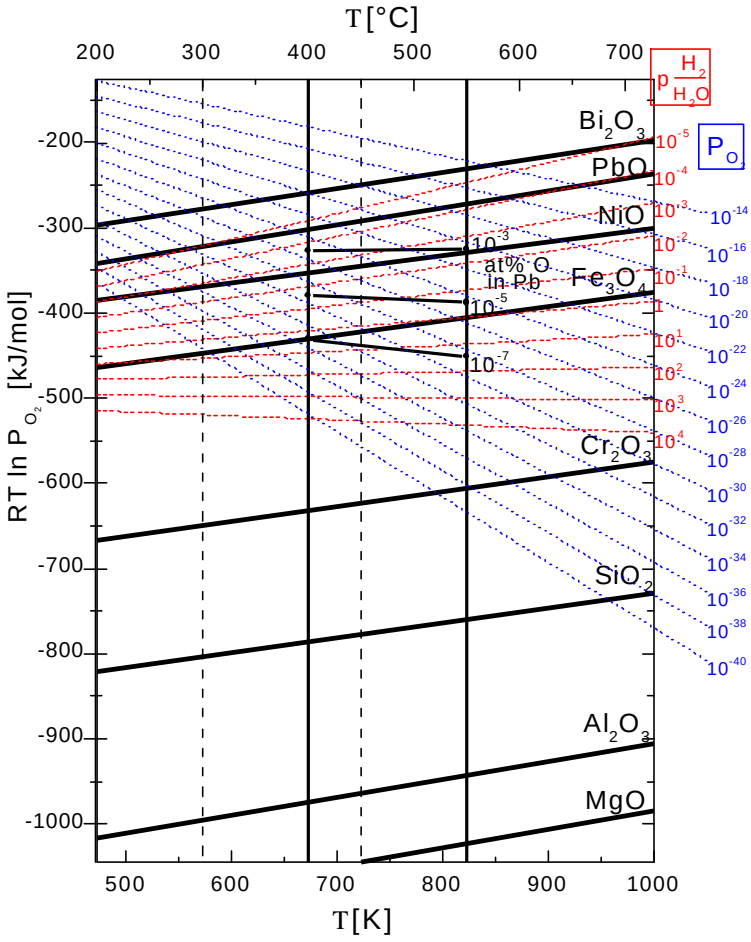

Figure 59: Oxygen potential-diagram with PbO, Fe_3O_4 and other oxides of interest containing lines of constant oxygen partial pressures and H_2/H_2O ratios. Loop temperature regions are marked for Pb by solid, and Pb-Bi by dashed vertical lines. Lines of constant oxygen concentration are drawn in the Pb loop region for 10^{-7}, 10^{-5} and 10^{-3} at%., Müller and Schumacher (1999).

5.4.2.3 Corrosion test stand, gas-phase oxygen control and results

A corrosion test stand was installed in which the oxygen potential of liquid Pb is controlled via the gas phase as described above, figure 60. The reactor is a Quartz tube inside an oven that is controlled at 550°C. A mixture of Ar and Ar/5%H_2 allows to adjust the hydrogen concentration in the gas. The water vapor is added by passing the gas through water of 7.4°C. In the actual experiment the gas mixture is chosen thus that the H_2/H_2O ratio is 0.4. Looking at figure 59 one can see that these conditions guarantee the formation of iron oxide and correspond to an oxygen partial pressure of about 10^{-24} at 550°C. Moisture sensors and an oxygen detector allow to determine the oxygen potential of the gas by 2 different methods.

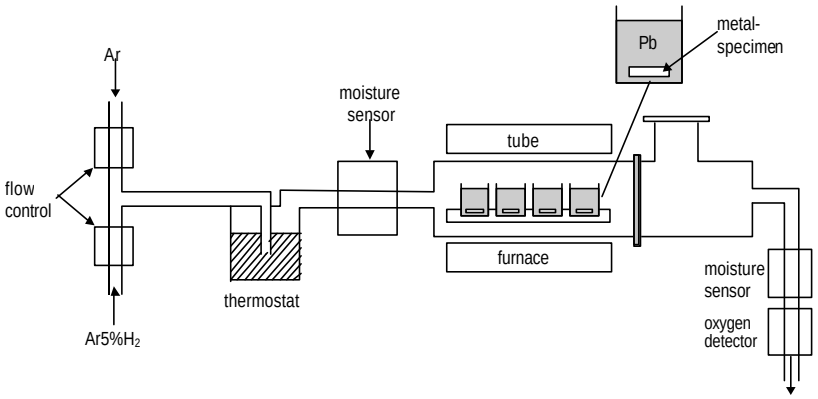

Figure 60:
Scheme of the corrosion test stand with stagnant liquid lead, Müller and Schumacher (1999).

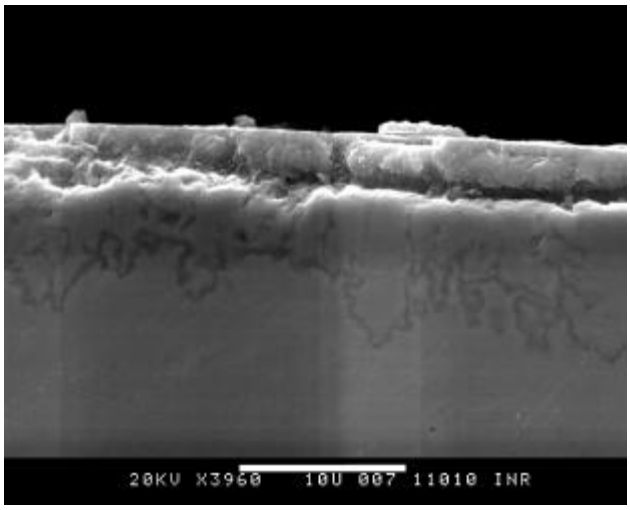

Figure 61:
Cross section of OPTIFER IVc steel after 1000 h in liquid lead at 550°C, oxygen control by H_2/H_20 ratio of 0.4.

Up to now corrosion tests run 1000 h with several steel specimens. As an example the cross section perpendicular to the surface of an OPTIFER steel specimen is shown in figure 61. The surface of this specimen was treated by a pulsed electron beam with the GESA installation (Müller and Schumacher (1999)) to improve the corrosion behavior. The scanning electron micrograph shows a dense oxide scale of about 3-4 µm thickness on top and an oxygen penetration zone below the steel surface.
In the oxygen control test stand KOCOS (Kinetics of Oxygen COntrol Systems, Lefhalm et al. (2000)), which is set up within the KArlsruhe Lead Laboratory KALLA, investigations of the kinetics of the oxygen control process via the gas phase are performed. The test stand basically consists of a crucible which is filled with 688 g of liquid Pb-Bi and heated from the side (temperature 430°C). Within the Pb-Bi a natural

circulation flow establishes which results in a good mixing of the fluid. The gas-phase oxygen control system applied is similar to the system described in figure 60.
Up to now two important characteristics of the gas-phase oxygen control system have been demonstrated: first, the time scale in which the thermodynamic equilibrum for this setup establishes is found to be about 1.5 hours when changing the H_2/H_2O ratio up to one dimension at a constant total gas flow rate of 8 l/h, figure 62. The free surface of the liquid metal to the gas atmosphere is 47 cm². The thermodynamic equilibrium is observed over more than 60 hours and can be supposed to be stable. This rather short time scale shows that the limiting process is the solution of oxygen from the gas phase into the liquid metal or vice versa, probably allowing a good temperature following behaviour of such an oxygen control system in an ADS.

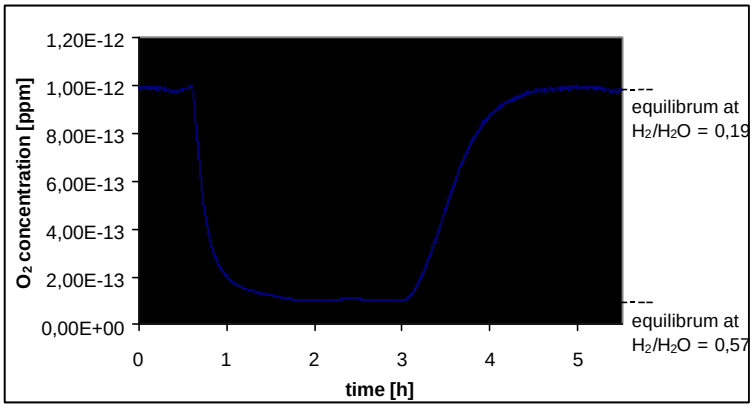

Figure 62:
Oxygen concentration as a function of time for different H_2/H_2O ratios.

Second, experiments are performed that demonstrate the reversibility of the process. The oxygen concentration in figure 62 can be perfectly re-established after 1.5 hours when setting back to the old boundary conditions. However, a good mixing of the fluid within the bulk and along the free surface to the gas phase, e.g. by natural circulation, has to be ensured.

5.4.2.4 Summary

Heavy liquid metal loops with Pb-Bi that are of interest for a spallation target are only feasible if the problem of steel corrosion by liquid Pb-Bi at the relevant temperatures can be solved. It is known that an oxide scale at the surface of steel can act as a protective barrier for the solution of steel components in the liquid metal. The conditions are described under which an iron oxide scale is formed on the steel surface, but not PbO that would precipitate at the lowest temperature of a loop and could eventually block the liquid metal flow. These conditions are maintained in the temperature region of 400°C - 550°C by an oxygen concentration in liquid Pb-Bi or Pb that is in equilibrium with a gas phase which contains hydrogen and water vapor with a H_2/H_2O-ratio of 0.4. Corrosion experiments in stagnant lead at 550°C were carried out that show protective oxide formation on steel after 1000 h under those conditions.
The applied gas-phase oxygen control system will be used for oxygen control in the loops of the KArlsruhe Lead LAboratory KALLA, cf. chapter 5.1.

6. OVERALL CONCLUSIONS AND PERSPECTIVES

The objective of the HGF Project is to provide the scientific-technical basis which allows the conception and the design of a spallation target. The application of a spallation target is in the fields of, first, spallation neutron source for material investigations and, second, transmutation of highly radioactive waste.

The HGF Strategy Fund Project is divided into three sub-projects

- SP1: Thermalhydraulic investigations,
- SP2: Material specific investigations,
- SP3: Oxygen control.

Each sub-project consists of several work packages. All the work packages that were due to start in 1999, delivered successful results. As the HGF Project was approved by the HGF Council dated July 09, 1999 and as the funding was granted by BMBF dated October 18, 1999, Forschungszentrum Karlsruhe could employ most of the staff for this project after this date. This resulted in a general delay of some tasks. However, the general time table of the project can be fulfilled.

The major results are:

- KALLA:
  The laboratory is in the design and construction phase. Commissioning will be in 2000. However, small-scale test sections for corrosion tests in stagnant Pb-Bi and for testing of the oxygen control system were taken in operation.
- SP1: Thermalhydraulic investigations
  Experimental (HYTAS test facility) and numerical (CFX and FIDAP) results for a beam window with water as model fluid were performed. Good agreement between measurement and calculation is achieved. The detailed design of a beam window in Pb-Bi can be done.
  The fundamental heat transfer experiment in Pb-Bi was prepared (geometry, measurement technique, heater).
  The TMBF turbulence model in FLUTAN was extended and validated for mixed and buoyant convection of fluids with Prandtl numbers of around one. The model was partly adapted to heavy liquid metal flow.
  The numerical analysis of the critical flow around the beam window with Pb-Bi as fluid was started by participation in a numerical benchmark.
- SP2: Material specific investigations
  The hot-dip aluminizing method was demonstrated to be acceptable for the coating of austenitic steels. The effect on hardness by adding silicon to the melt is described.
  The GESA test facility is operating and prepared to treat specimens by surface restructuring and surface aluminum alloying that will be exposed in KALLA.
- SP3: Oxygen control
  It could be demonstrated that zirconia based solid electrolyte oxygen meters have the potential to measure the oxygen activity of liquid lead-bismuth.
  The fundamentals of a gas-phase oxygen control system were developped and demonstrated in a small-scale test section. A protective oxide scale could be formed on the specimens.

7. Literature

G. Bauer, M. Salvatores, G. Heusener, 1999
The MEGAPIE Initiative – Executive Outline and Status as per November 1999, Paul Scherrer Institut, Würenlingen Switzerland

W. Baumann, L. Carteciano, D. Weinberg, 1997
Thermal propagation effects in a vertical turbulent flow behind a jet block - A benchmark exercise. Journal of Hydraulics Research, 1997, Vol. 35, pp. 843-864

G. Benamati, C. Latge, J.U. Knebel, 2000
Technologies for Lead Alloys, TECLA Project within the 5th Europ. Framework Prog., Ref.No. FIS5-1999-00308

BMBF, 1998
Wissenschaftlich-Technische Zusammenarbeit, Abkommen „Korrosionsverhalten von Strukturmaterialien“, Projekt-Nummer RUS-372-98

H.U. Borgstedt, 1984
Sauerstoff in flüssigen Alkalimetallen, Fachtagung Gase in Metallen, Deutsche Gesellschaft für Metallkunde e.V. (DGM), March 28-30, Darmstadt, pp. 117-130

H.U. Borgstedt, Z. Peric, P. Muralidaran , 1994
The application of solid electrolyte oxygen meters in liquid metals used in fission and fusion reactor concepts, Nat. Symp. on Electrochemistry in Nucl. Techn., January 5-7, Kalpakkam, Indien, pp. I.1-I.1.1

C.D. Bowman, E.D. Arthur, P.W. Lisowski, G.P. Lawrence, R.J. Jensen, J.L. Anderson, B. Blind, M. Cappiello, J.W. Davidson, T.R. England, L.N. Engel, R.C. Haight, H.G. Hughes III, J.R. Ireland, R.A. Krakowski, R.J. LaBauve, B.C. Letellier, R.T. Perry, G.J. Russell, K.P. Staudhammer, G. Versamis, W.B. Wilson, 1992
Nuclear Energy Generation And Waste Transmutation Using an Accelerator-Driven Intense Thermal Neutron Source, Nuclear Instruments and Methods in Physics Research A320, pp. 336-367

M. Bunk, M. Wörner, 1998
Direkte numerische Simulation turbulenter Rayleigh-Bénard-Konvektion in Quecksilber. FZKA 5915, Forschungszentrum Karlsruhe, April 1998

S. Buono, J.U. Knebel, S. Monti, F. Piacentini, P. Turroni, 1999
Working Group on Heavy Liquid Metal Thermal-Hydraulics, Minutes of the meeting, April 12-13, 1999, ENEA Brasimone, Italy

F. Carminati, R. Klapisch, J.P. Revol, Ch. Roche, J.A. Rubio, C. Rubbia, 1993
An Energy Amplifier For Cleaner and Inexhaustible Nuclear Energy Production Driven by a Particle Beam Accelerator, CERN/AT/93-47 (ET)

M.W. Cappiello, (1999)
The Fluidized Bed Spallation Target, Proc. Third Int. Top. Meeting on Nuclear Applications of Accelerator Technology AccApp’99, Long Beach, CA, November 14-18, pp. 53-58

L.N. Carteciano, D. Weinberg, U. Müller, 1997
Development and Analysis of a turbulence Model for Buoyant Flows. Proc. of the 4th World Conf. on Experimental Heat Transfer, Fluid Mechanics and Thermodynamics, Bruxelles, Belgium, June 2-6, Vol. 3, S. 1339-46. Pisa Edition ETS

L. N. Carteciano, M. Wörner, G. Grötzbach, 1999
Erweiterte Turbulenzmodelle für technische Anwendungen von FLUTAN auf Naturkonvektion. Jahrestagung Kerntechnik 1999, Karlsruhe, 18.-20. Mai, pp. 129–133

X. Cheng, J.U. Knebel, F. Hofmann, 1999
Thermalhydraulic Design of an ADS with Three Spallation Targets, Proc. of the ADTTA'99 Conference, Prague, June 7-11

CFX International Services (Harwell Lab.), 1995
CFX 4.1, Flow Solver User Guide, AEA Technology plc, Oxfordshire

Evaluierungskommission, 2000
Nukleare Sicherheits- und Endlagerforschung in Deutschland, Bericht der vom BMWi berufenen Arbeitsgruppe (Evaluierungskommission)

Fluid Dynamics International (1993)
FIDAP 7.0, User Manual

H. Glasbrenner, J. Konys, G. Reimann, K. Stein, O. Wedemeyer, 1996
The formation of aluminide coatings on MANET stainless steel as tritium permeation barrier by using a new test facility, Fusion Technology 1996, Vol. 2, pp. 1423

H. Glasbrenner, J. Konys, K. Stein-Fechner, O. Wedemeyer, 1998
Comparison of microstructure and formation of intermetallic phases on F82H-mod. and MANET II, Journal of Nuclear Materials 258, pp. 1173-1177

H. Glasbrenner, E. Nold, Z. Voss, 1997
The influence of alloying elements on the hot dip aluminizing process and on subsequent high temperature oxidation, Journal of Nuclear Materials 249, pp. 39-45

H. Glasbrenner, O. Wedemeyer, 1998
Comparison of hot dip aluminised F82H-mod. steel after different subsequent heat treatments, Journal of Nuclear Materials 257, pp. 274-281

B.F. Gromov, Yu.I. Orlov, P.N. Martynov, K.D. Ivanov, V.A. Gulevski, 1995
Physical-chemical principles of lead-bismuth coolant technology, in: Liquid Metal Systems, Edited by H. U. Borgstedt and G. Frees, Plenum Press, pp. 339-343

G. Heusener, 1999
Transmutation, ein neuer Weg der Entsorgung?, VDI Berichte Nr. 1493, pp. 187-201

G. Heusener, 2000
Transmutation – ein alternativer Weg der Entsorgung?, Vortrag Informationskreis Kernenergie, Bonn, 21.03.2000

G. Heusener, M. Salvatores, 1998
Use of heavy liquid metal: A perspective for critical/subcritical fast neutron concepts, HLMC'98, 5-9 October, Obninsk, Russia

M. Ishii, I. Kataoka, 1984
Scaling Laws for Thermal-Hydraulic Systems Under Single Phase and Two-Phase Natural Circulation, Nucl. Engrg. Des. 81, pp. 411-425

J.-U. Klügel, R. Gilli, J. Vigfusson, 1999
Ergebnisse einer ersten sicherheitstechnischen Beurteilung des Konzeptes eines bleigekühlten Energy Amplifiers aus behördlicher Sicht, atw 44, Heft 11, pp. 664-669

J.U. Knebel, 1993
Experimentelle Untersuchungen in turbulenten Auftriebsstrahlen in Natrium, Dissertation, Univ. Karlsruhe, KfK 5175, Kernforschungszentrum Karlsruhe

J.U. Knebel, 1999
Innovative Technology to Reduce Radiotoxicity, HGF Strategy Fund Project 99/16, funded by Bundesministerium für Bildung und Forschung (BMBF), Förderkennzeichen 01SF9926/3

J.U. Knebel, X. Cheng, C.H.M. Broeders, 1999
The FZK Three-Beam Concept for an ADS, Jahrestagung Kerntechnik, Karlsruhe, pp. 639-643

J.U. Knebel, L. Krebs, U. Müller, B.P. Axcell, 1998
Experimental Investigation of a confined Heated sSdium Jet in a Co-Flow, J. Fluid Mech, vol. 368, pp. 51-79

E.M.J. Komen, H. Koning, 2000
Pre-Test CFD analyses of the COULI experiment. Project 20014, February 25, 2000, NRG Petten

J. Konys, K. Stein-Fechner, O. Wedemeyer, 1998
Comparison of microstructure and formation of intermetallic phases on F82H-mod. and MANET II; H. Glasbrenner, Journal of Nuclear Materials 258, pp. 1173-1177

H. Kleykamp, H. Glasbrenner, 1997
Thermodynamic properties of solid aluminium-iron alloys, Z. Metallkd., 88, pp. 230-235

C.-H. Lefhalm, M. Daubner, J.U. Knebel, 1998
MEMESS V5: Das Modular Erweiterbare Messwerte Erfassungs- und Steuerungssystem, Forschungszentrum Karlsruhe, Wissenschaftliche Berichte FZKA 6122

C.H. Lefhalm, K.J. Mack, J.U. Knebel, 2000
Investigations into ADS at FZK within the HGF-Strategy Fund Project 99/16: Reduction of Radiotoxicity, Jahrestagung Kerntechnik 2000 Bonn, pp. 567-572

V. Markov, 1997
Corrosion of structural materials in Pb-Bi and Pb, Seminar on the Concept of Lead-Cooled fast Reactor, Cadarache, September 22-23

W. Maschek, D. Thiem, G. Heusener, 1999
Safety assessment of a reactor core dedicated to burn minor actinides, Proc. of the Jahrestagung Kerntechnik'99, Karlsruhe, pp.635-638

T.B. Massalski, 1990
Binary Phase Diagrams; Editor, ASM Int.

G. Müller, 2000
Korrosionsverhalten von Stählen in flüssigem Blei nach Behandlung mit hochenergetischen gepulsten Elektronenstrahlen, Dissertation Universität Karlsruhe und Forschungszentrum Karlsruhe, Wissenschaftliche Berichte FZKA 6422

G. Müller, G. Schumacher, 1999
Application of GESA for Improvement of Corrosion Resistance of Steel in Liquid Lead., in “Physics of Intense Light Ion Beams, Production of High Energy Density in Matter, and Pulsed Power Applications.”, Edt. H.-J. Bluhm, Wissenschaftliche Berichte FZKA 6205, pp. 123-127

G. Müller, G. Schumacher, D. Strauß, 1998
Oxide scale growth on MCrAlY coatings after pulsed electron beam treatment, Surface and Coating Technology, Vol. 43, pp. 108-109

G. Müller, G. Schumacher, D. Strauß, V. Engelko, A. Andreev and V. Kavaljov, 1996
Modification of material surfaces by the pulsed electron beam facility GESA, K. Jungwirth [Hrsg.], Beams 96: Proc. Of the 11th Intern. Conf. On High-power Particle Beams, praha, CR, June 10-14, Vol. 2 pp. 809-812

Y. Orlov, 1998
Stages of Development of Lead-Bismuth as a Coolant for Nuclear Reactors in Russia, Presentation at Forschungszentrum Karlsruhe, IATF, July 7

Paul Scherrer Institute, 1997
PSI Annual Report 1997 on: Solid State Research at Large Facilities, Annex IIIA, Paul Scherrer Institute (PSI) Switzerland

I. Platnieks, G.S. Bauer, O. Lielausis, Y. Takeda, 1998
Measurements of Heat Transfer at the Beam Window in a Mockup Target for SINQ using mercury, 14th Meeting of the Intern. Collaboration on Adv. Neutron Sources, Starved Rock Lodge, Utica, Ill., USA, June 14-19

Projekt Nukleare Sicherheitsforschung, 1999
Projekt Nukleare Sicherheitsforschung Jahresbericht 1998, B. Mühl (Hrsg.), Forschungszentrum Karlsruhe, Wissenschaftliche Berichte FZKA 6300

Projekt Nukleare Sicherheitsforschung, 2000
Projekt Nukleare Sicherheitsforschung Jahresbericht 1999, B. Mühl (Hrsg.), Forschungszentrum Karlsruhe, Wissenschaftliche Berichte FZKA 6480

H.T. Rossby, 1969
A study of Bénard convection with and without rotation. J. Fluid Mech. 36, 309-335

C. Rubbia, Rubio, J.A., Buono, S., Carminati, F., Fiétier, F., Galvez, J., Gelès, C., Kadi, Y., Klapisch, R., Mandrillon, P., Revol, J.P., Roche, Ch., 1995
Conceptual design of a fast neutron operated high power energy emplifier, CERN/AT/95-44(ET)

SNS Project Office, (2000)
Spallation Neutron Source (SNS), Oak Ridge National Laboratory, http: //www.sns.gov/brochures/newSNSBrochure.pdf

K. Stein-Fechner, J. Konys, O. Wedemeyer, 1997
Investigations on the transformation behavior of the intermetallic phase $(Fe,Cr)_2Al_5$ formed on Manet II steel by aluminizing, Journal of Nuclear Materials 249, pp. 33-38

Y. Takeda, H. Kikura, 1997
Measurement of Liquid Metal Flow in a SINQ Target Geometry, in: PSI Annual Report 1997 Annex IIIA, pp. 20-21

T. Takizuka, K. Tsujimoto, T. Sasa, H. Takano, K. Hirota, Y. Kamishima, 1998
Heavy liquid-metal cooling option of JAERI accelerator-driven transmutation systems, HLMC’98, Vol.1, pp.143-155, October 5-9, Obninsk, Russia

Technical Working Group, 1998
Interim Report of the TWG on ADS, Issued by the three parties (France/Italy/Spain) TWG on ADS chaired by C. Rubbia, October 12

Technical Working Group, 1999
Overview of the Ongoing Activities in Europe and Recommendations of the TWG on ADS, Issued by the Enlarged TWG on ADS chaired by C. Rubbia, September 6

T. Tsuji, Y. Nagano, 1988
Turbulence measurements in a natural convection boundary layer along a vertical flat plate, Int. J. Heat Mass Transfer, 10, pp. 2101-2111

H. Ullmann, K. Teske, T. Reetz, 1973
Die Entwicklung elektrochemischer Meßverfahren für die Kontrolle schädlicher Verunreinigungen in Natriumkreisläufen, Kernenergie, 16, pp. 291-297

United States Department of Energy, 1999
A Roadmap for Developing Accelerator Transmutation of Waste (ATW) Technology, A Report to Congress, DOE/RW-0519, October 1999

Verband der Technischen Überwachungs-Vereine, VdTÜV (1986)
Werkstoffe für Druckbehälter, AD-Merkblatt W 0, Ausgabe Juni 1986

Verband der Technischen Überwachungs-Vereine, VdTÜV (1996)
Herstellung und Prüfung von Druckbehältern, AD-Merkblatt HP 0, Ausgabe Dezember 1996

H. Wider, 1998
Safety of acclerator-driven nuclear waste burners, Proc. of the Jahrestagung Kerntechnik'98, München, pp.217-220

G. Willerding, W. Baumann, 1996
FLUTAN 2.0 Input Specifications, Forschungszentrum Karlsruhe, Wissenschaftliche Berichte FZKA 5712, Mai 1996

M. Wörner, G. Grötzbach, 1997
DNS database of turbulent natural convection in horizontal fluid layers. World Wide Web-site http:// www.fzk.de/irs/turbit

M. Wörner, Q.-Y. Ye, G. Grötzbach, 1999
Consistent modelling of fluctuating temperature-gradient-velocity-gradient correlations for natural convection. "Engineering Turbulence Modelling and Experiments 4", Eds.: W. Rodi, D. Laurence, Elsevier Science B. V., pp. 165-174

8. Appendix

Table 16: Physical properties of water, sodium, lead and lead-bismuth.

physical properties	unit	wasser H_2O T=25°C	sodium Na T=300°C	lead Pb T=600°C	lead-bismuth $Pb^{45}Bi^{55}$ T=400°C
density ρ	kg/m³	997	880	10330	10570
dyn. viscosity μ	Pa s 10^{-6}	891	345	1550	3360
kin. viscosity ν	m² / s 10^{-6}	0.89	0.392	0.15	0.32
spec. Heat capacity c_p	kJ / kg / K	4.18	1.3	0.15	0.146
thermal conductivity λ	W / m / K	0.609	76.6	16.4	10.9
molekular diffusivity Γ	m² / s 10^{-6}	0.146	66.7	10.6	7.1
volumetric expansion coefficient β	1 / K 10^{-4}	2.57	2.69	1.39	1.2
mol. Prandtl number Pr	1	6.13	0.00587	0.014	0.045
melting temperature T_m	°C	0	98	328	125
boiling temperature T_b	°C	100	880	1743	1670